



APPENDICES

BOLTED END-PLATE JOINTS FOR CRANE BRACKETS AND BEAM-TO-BEAM CONNECTIONS

PhD Dissertation

KATULA, Levente

Budapest University of Technology and Economics

Supervisors:

DUNAI, László PhD

Professor

Budapest University of Technology and Economics, Hungary

PASTERNAK, Hartmut PhD

Professor

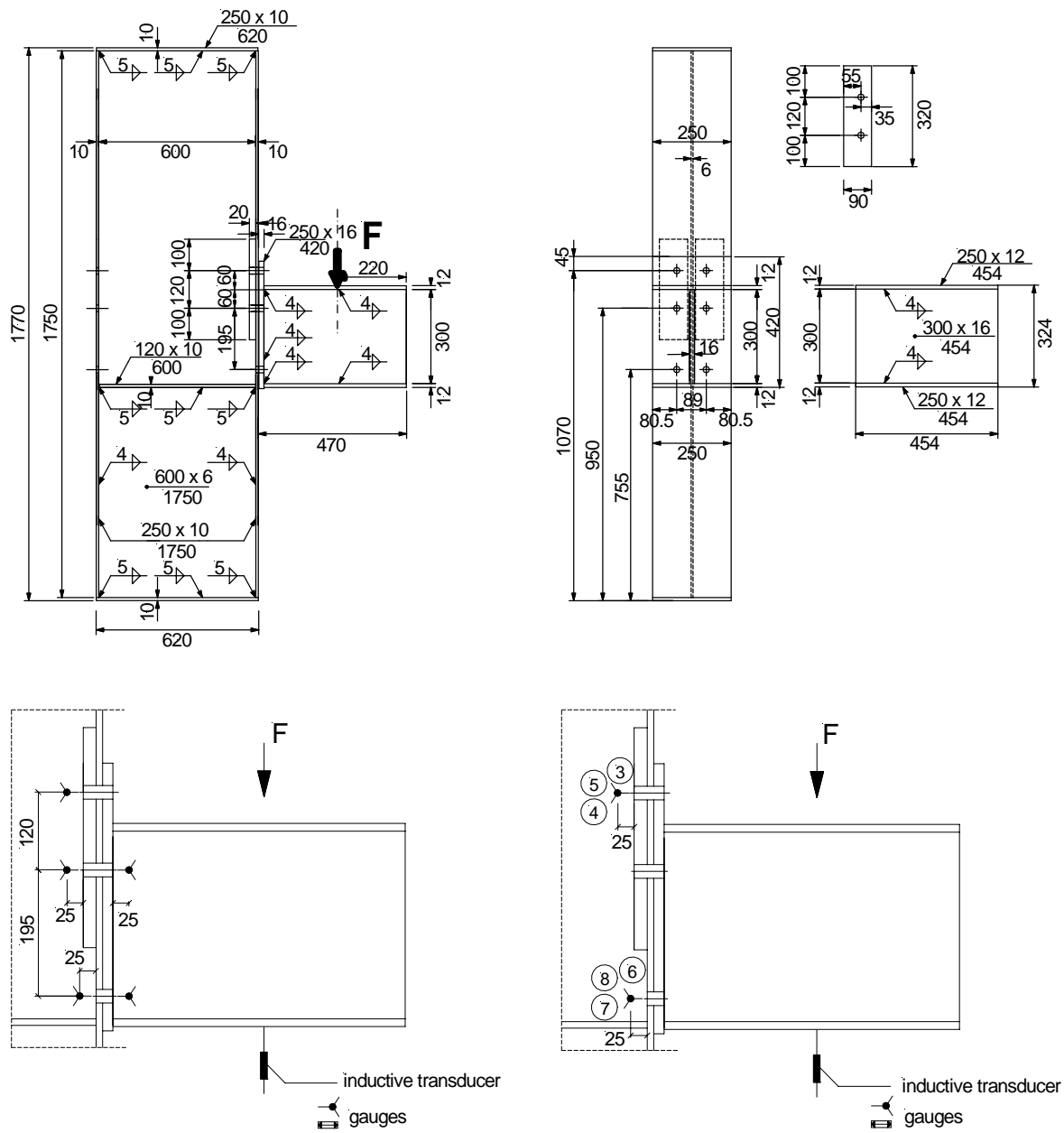
Brandenburg Technical University of Cottbus, Germany

Budapest, 2007.

Contents

	Page
<i>Appendix A:</i> Geometry of the test specimens	p. 13.
<i>Appendix B:</i> Material tests	p. 16.
<i>Appendix C:</i> Pre-tensioning of the bolts	p. 2.
<i>Appendix D:</i> Measuring the end-plate surface	p. 22.
<i>Appendix E:</i> Load cell calibrations	p. 6.
<i>Appendix F:</i> Summary of the Eurocode 3 model	p. 14.
<i>Appendix G:</i> Classification of cross-section according to EN 1993-1-1	p. 9.
<i>Appendix H:</i> Design moment calculations example according to EN 1993-1-8	p. 8.

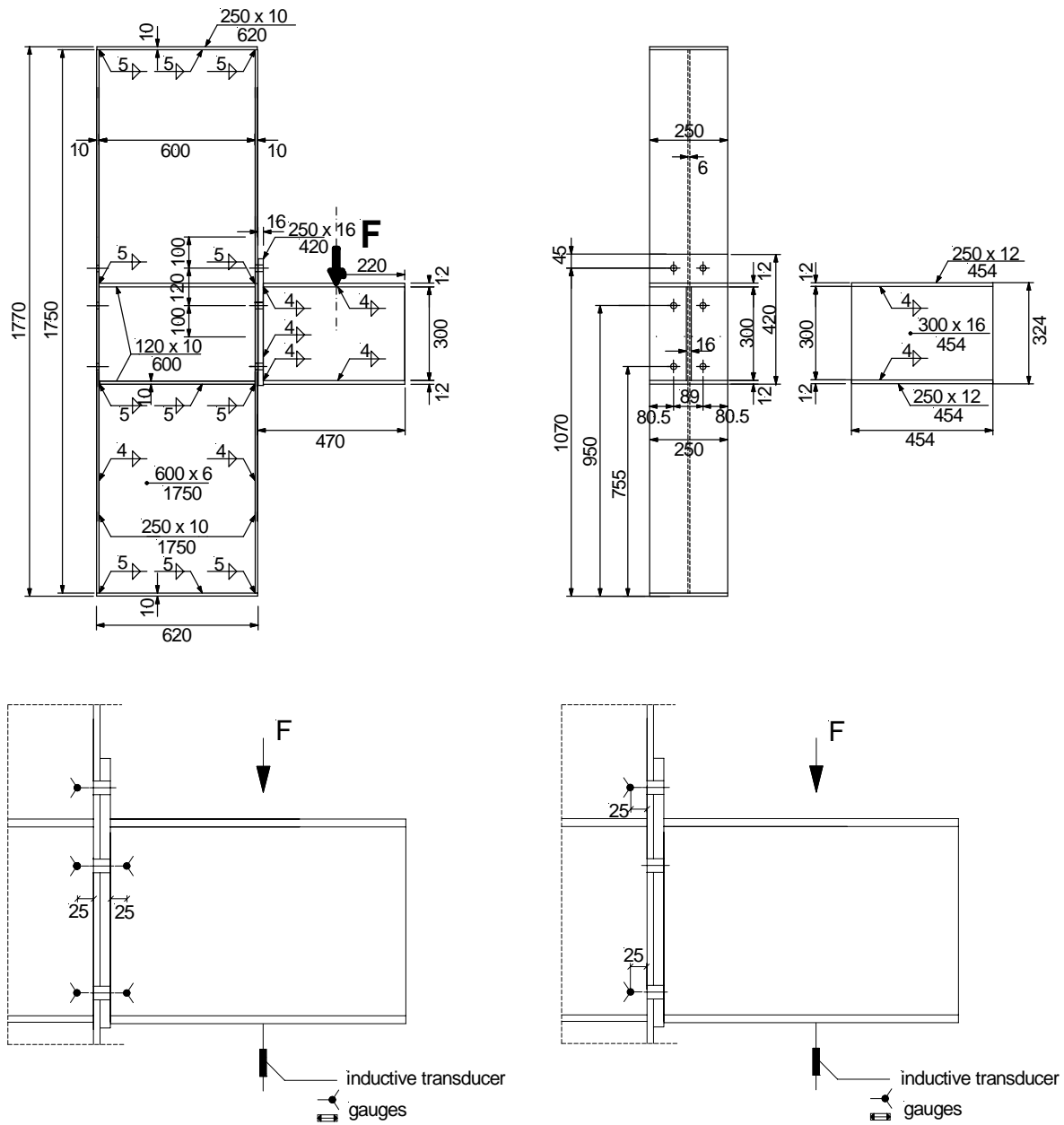
Geometry of the test specimens



Location of the gauges under static loading

Location of the gauges under fatigue loading

Fig. A1 Test specimen Z1.



Location of the gauges under static loading

Location of the gauges under fatigue loading

Fig. A2 Test specimen Z2.

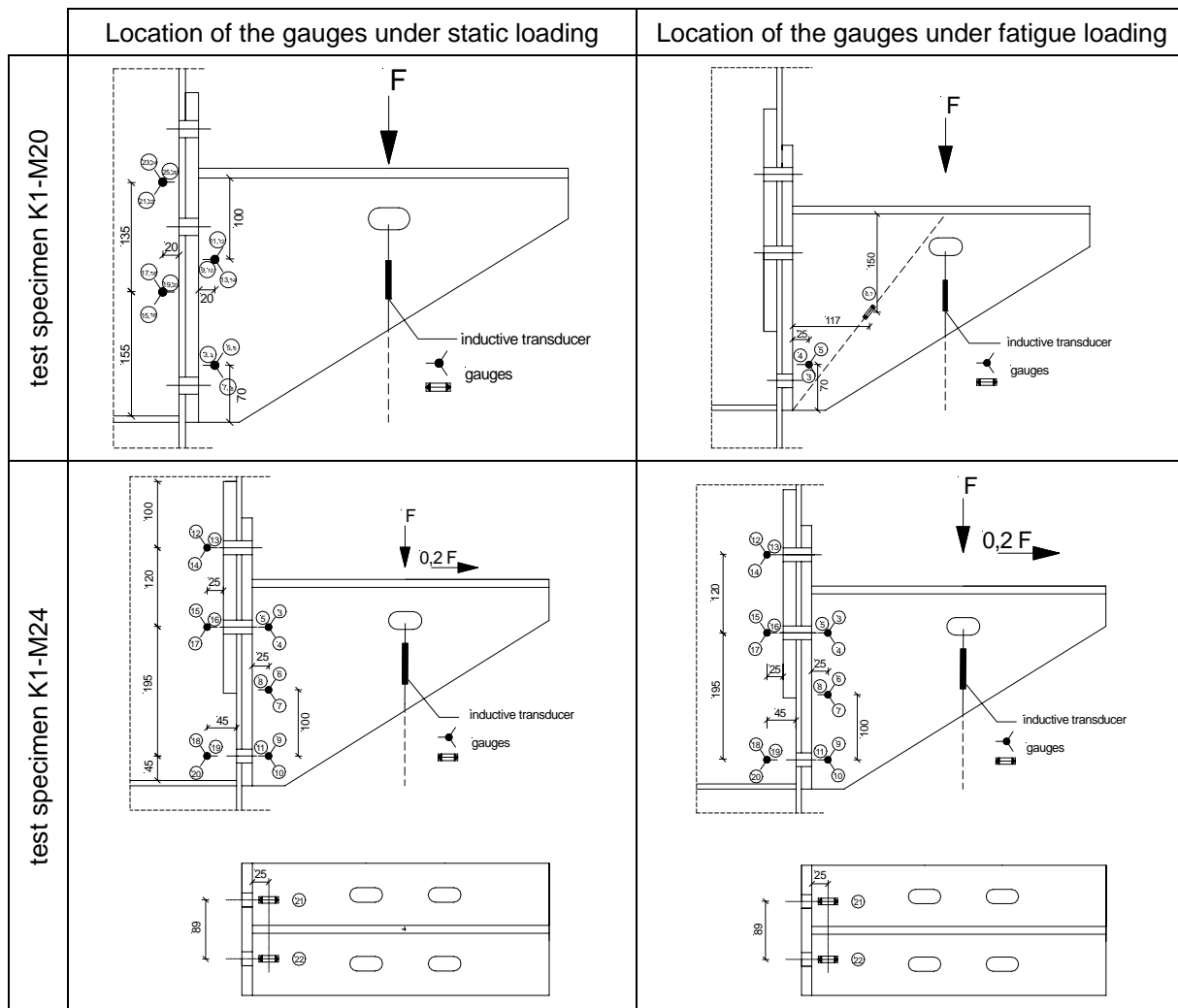
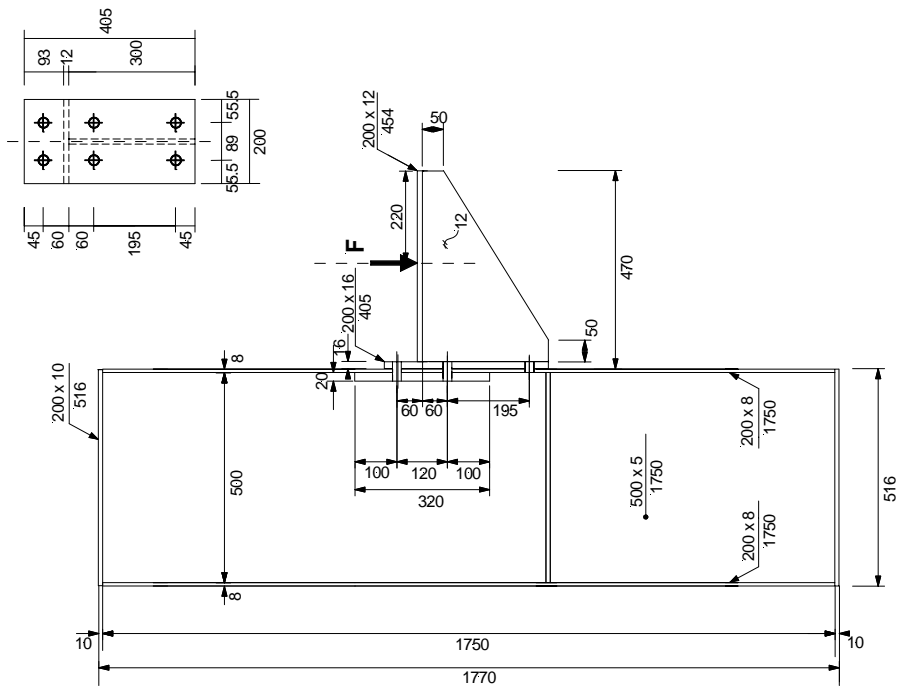


Fig. A3 Test specimen K1.

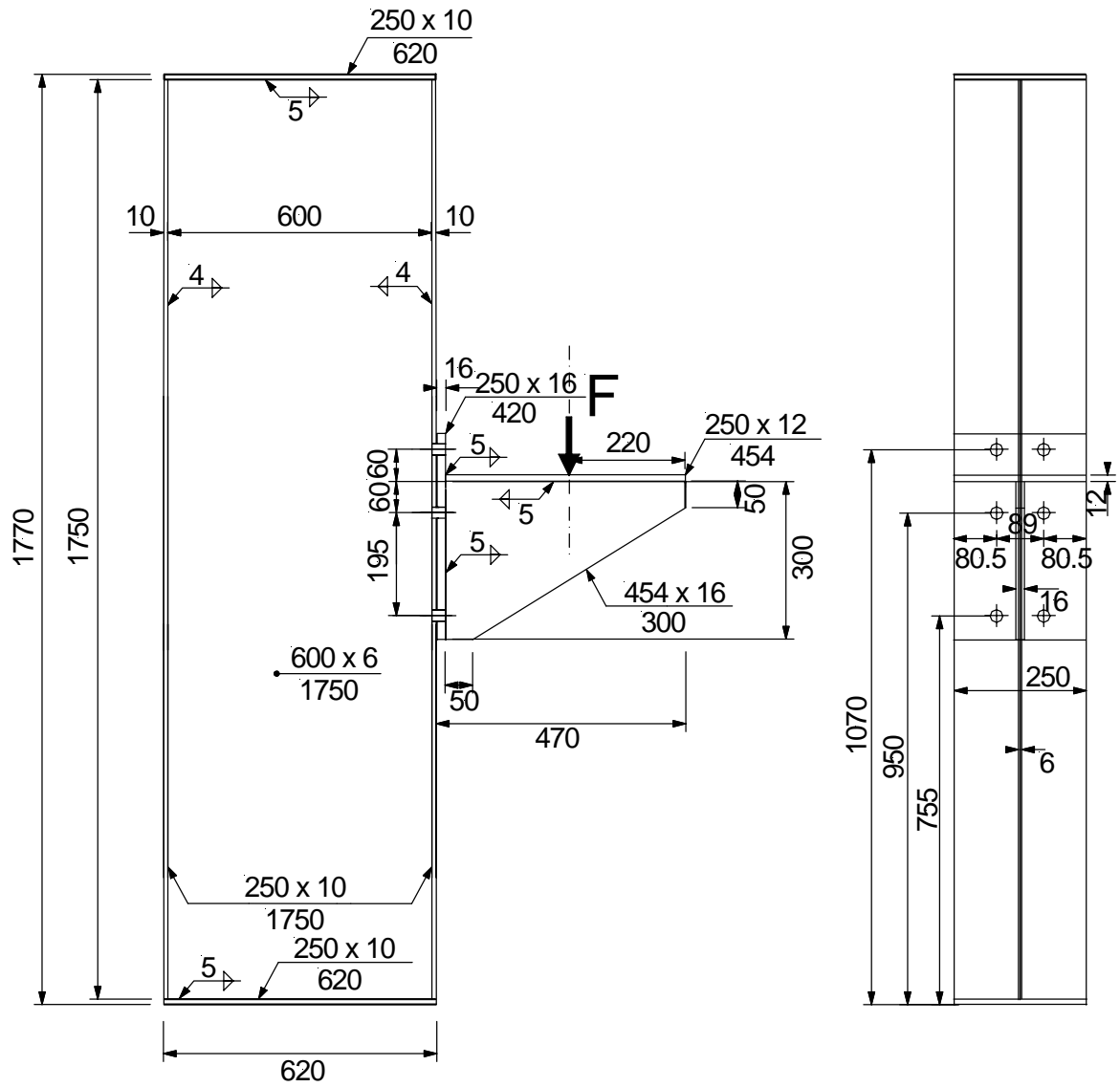
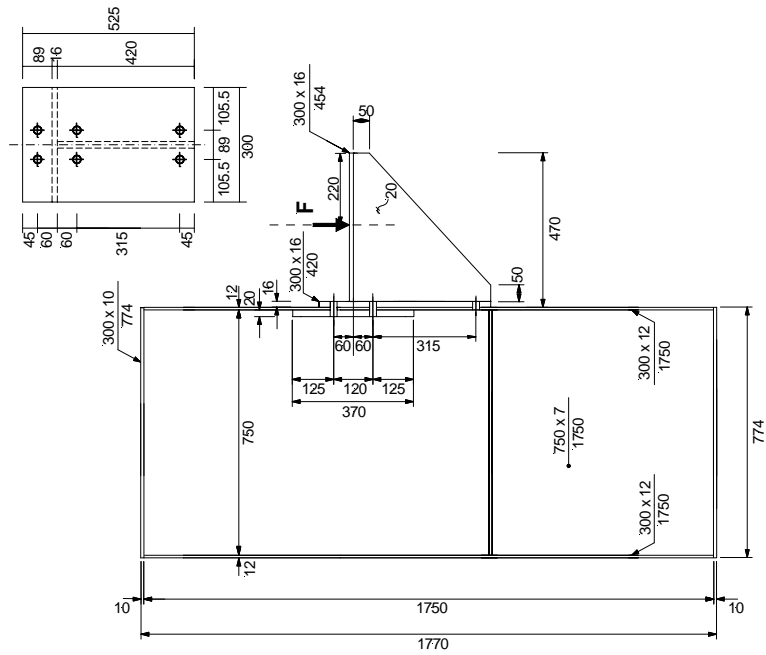


Fig. A5 Test specimen K2_z.



	Location of the gauges under static loading	Location of the gauges under fatigue loading
test specimen K3-M20	no test	
test specimen K3-M24		

Fig. A6 Test specimen K3.

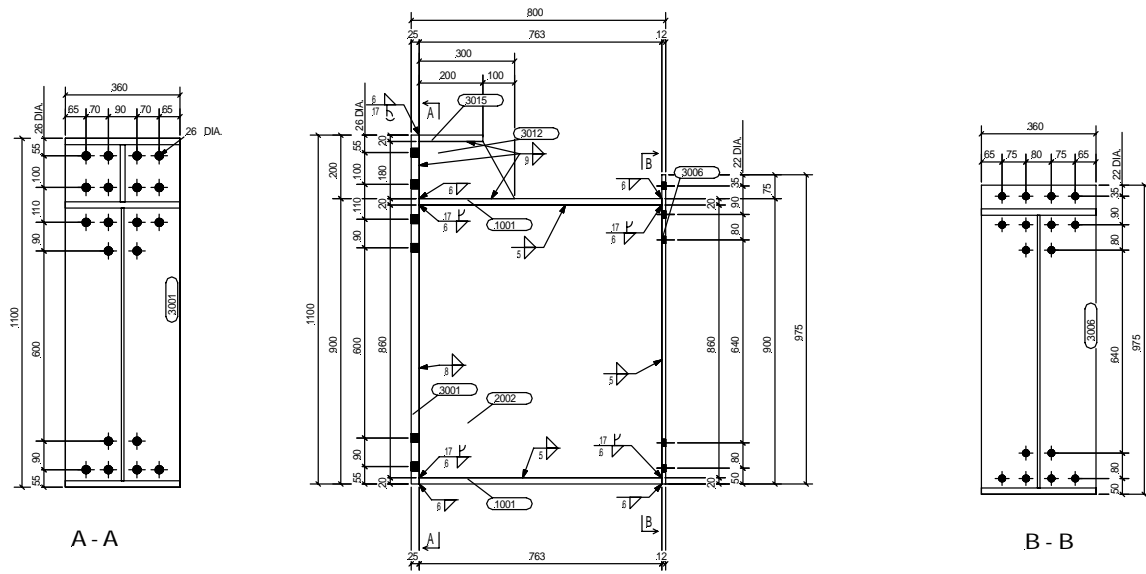


Fig. A9 Test specimen TB4.

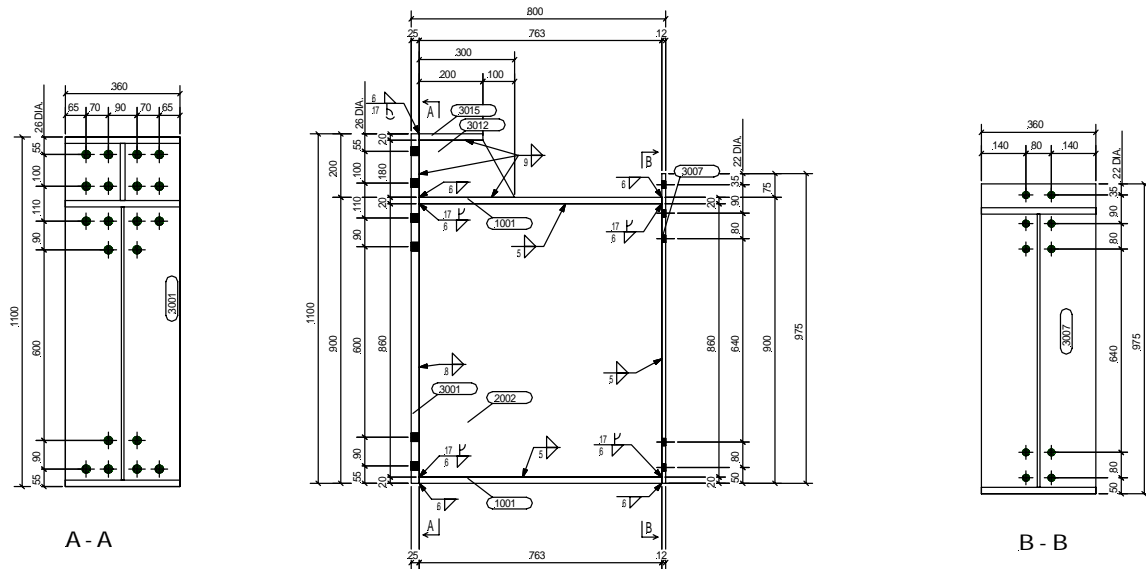


Fig. A10 Test specimen TB5.

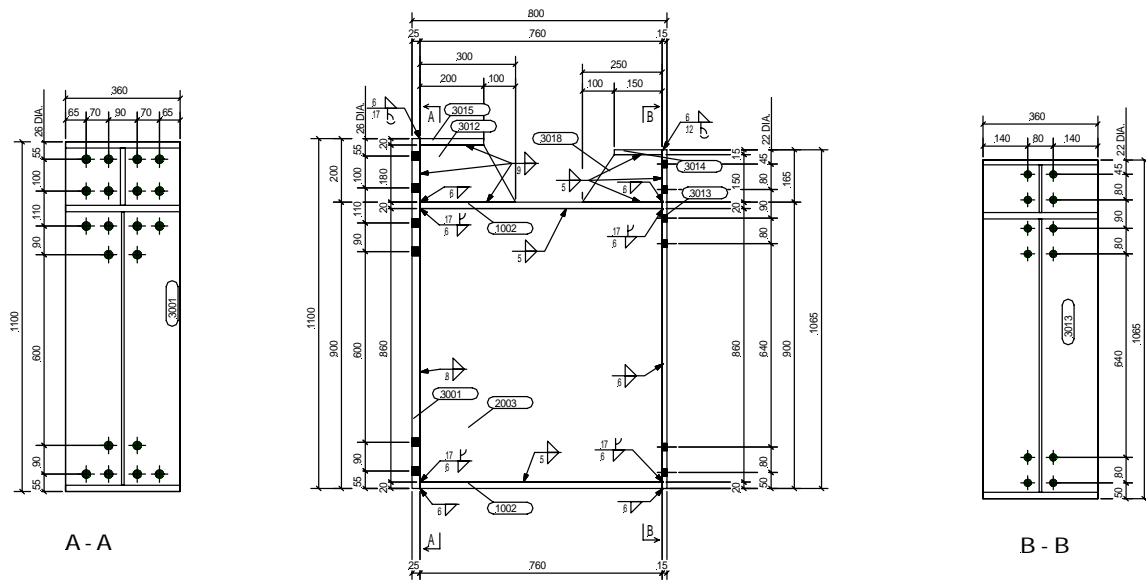


Fig. A11 Test specimen TB6.

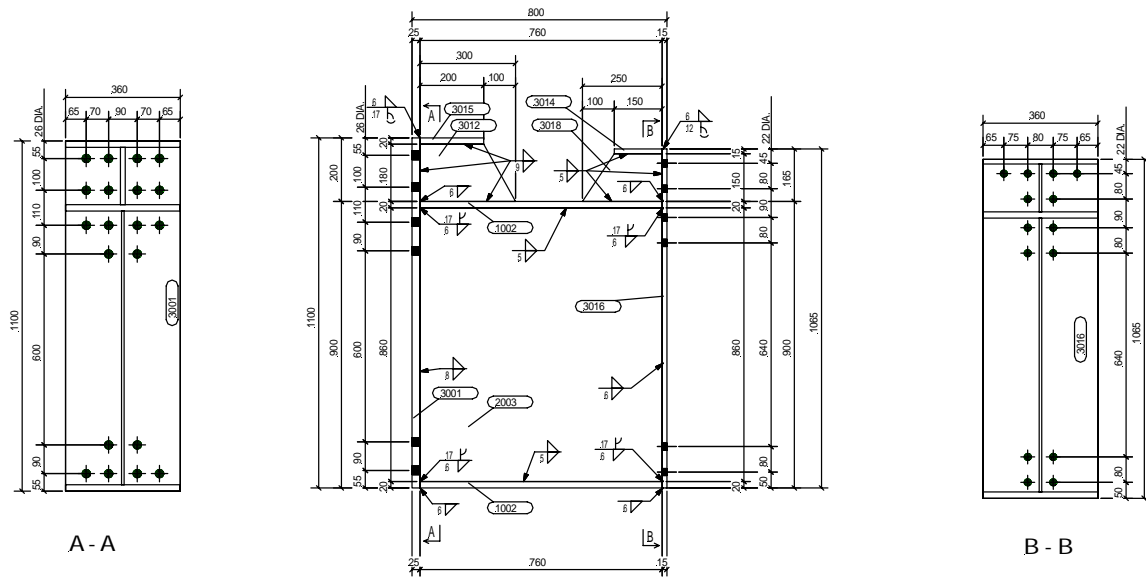


Fig. A12 Test specimen TB7.

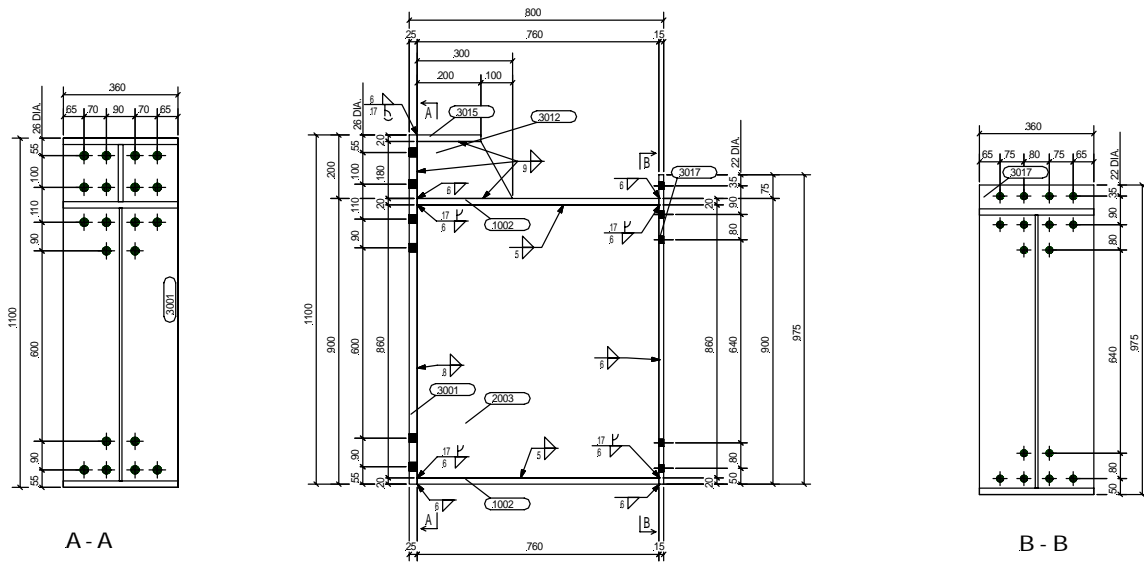


Fig. A13 Test specimen TB8.

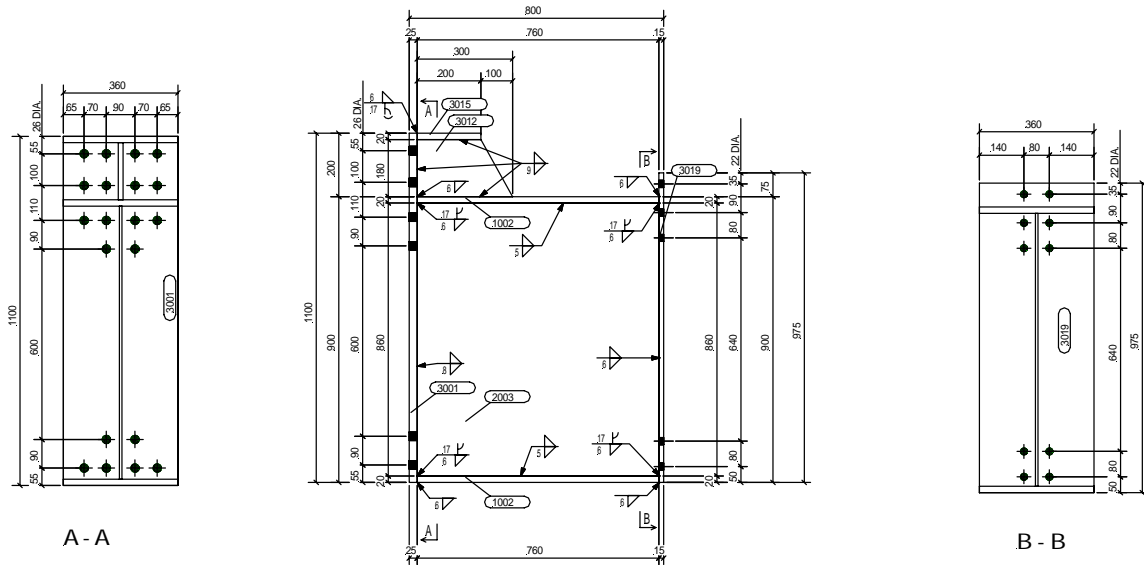


Fig. A14 Test specimen TB9.

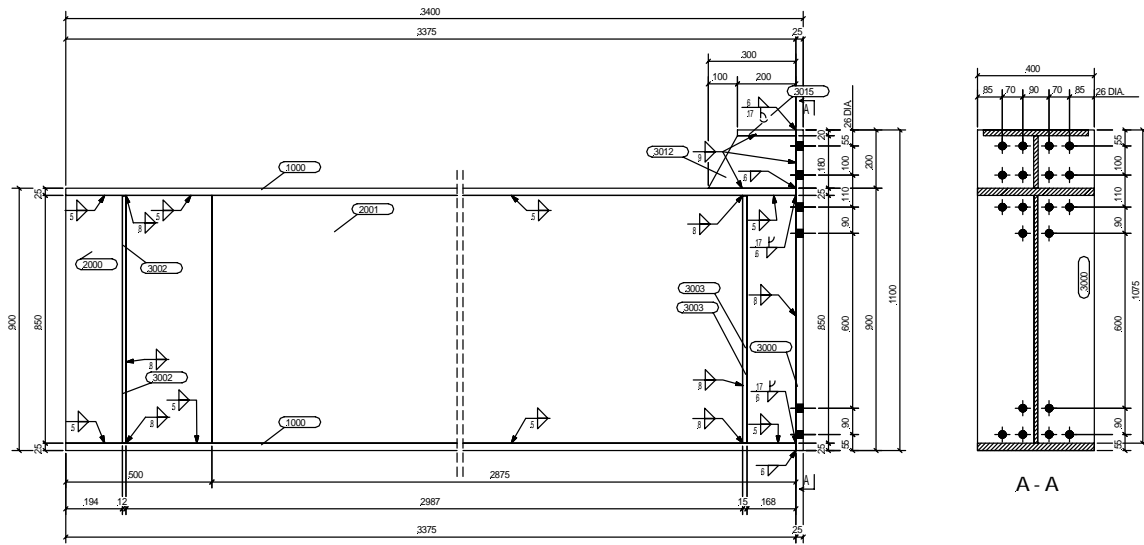


Fig. A19 Test specimen TB1, fixed beam.

Material tests

Test on crane brackets

The steel grade of the specimens was S355. To verify this material test specimens were prepared. Table B1 shows the locations where the specimens were cut out and the measured main material properties.

The material properties of the tension tests were accomplished according to the standard EN 10002-1.

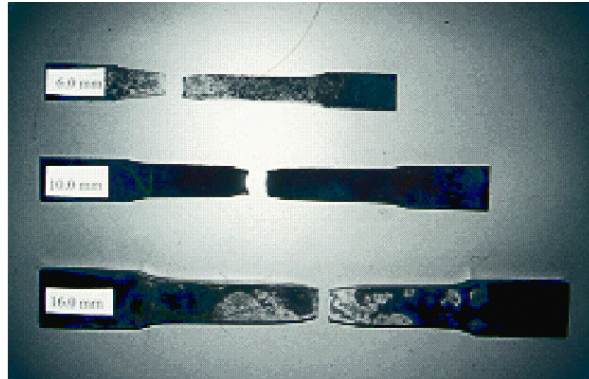


Fig. B1 Material test of test specimen Z1.

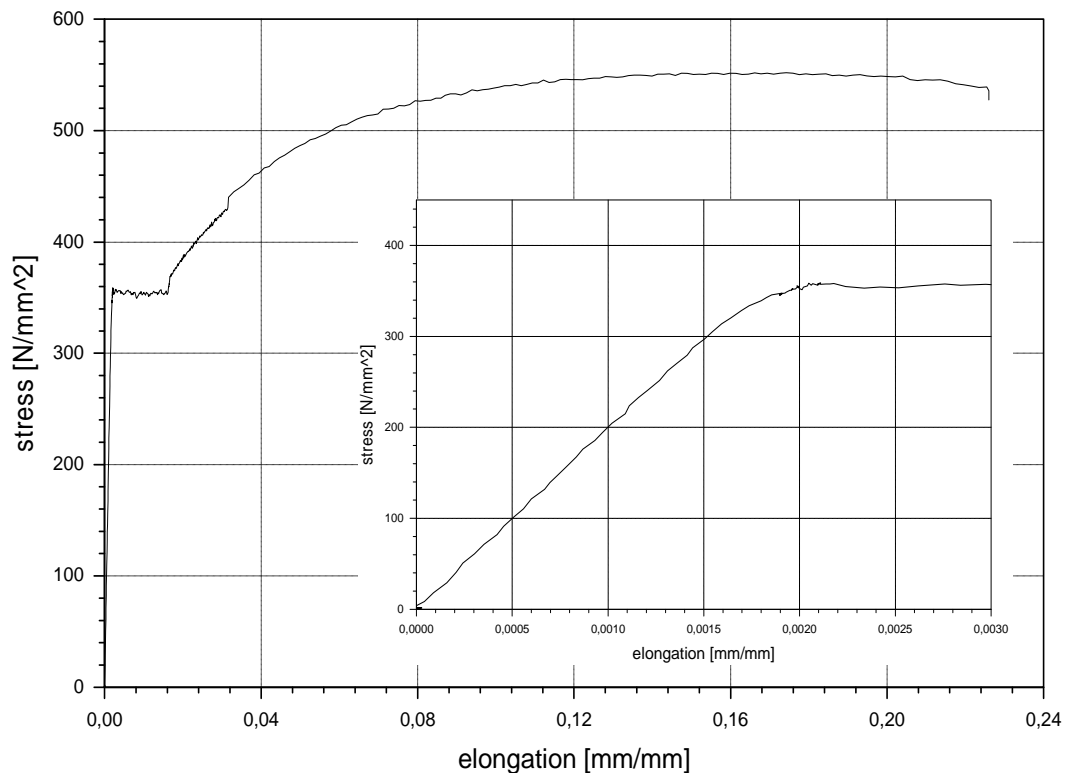


Fig. B2 Material test of the test specimen K2 with M20 bolts, bracket web.

As an example, Figure B2 shows the determination of the yield point and Young's modulus.

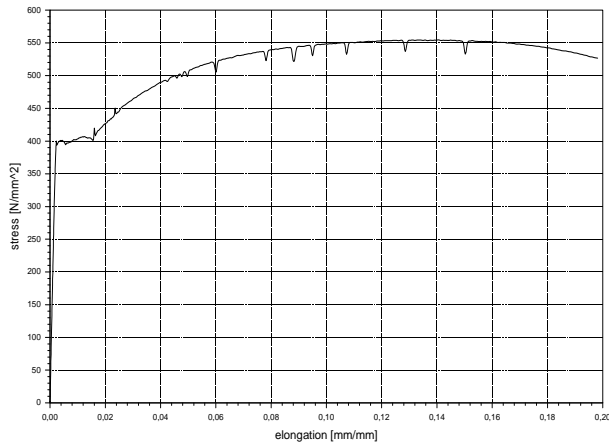


Fig. B3 Stress-elongation diagram of test specimen K1 with M20 bolts, column web.

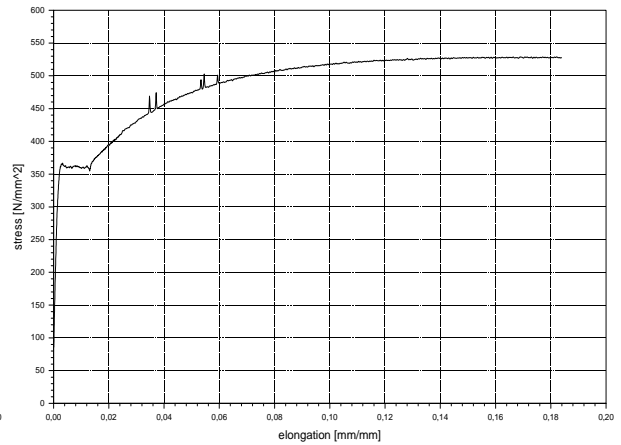


Fig. B4 Stress-elongation diagram of test specimen K1 with M20 bolts, column flange.

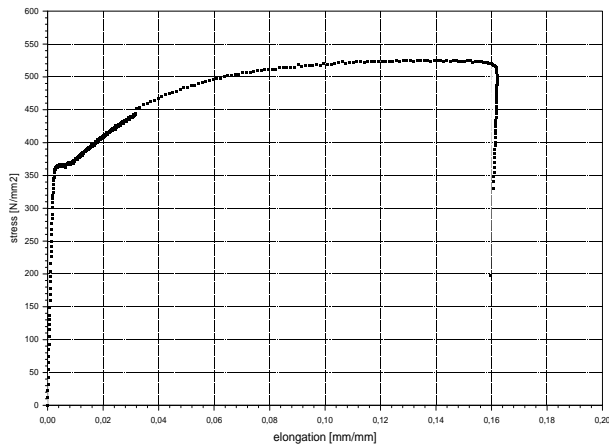


Fig. B5 Stress-elongation diagram of test specimen K1 with M20 bolts, bracket web.

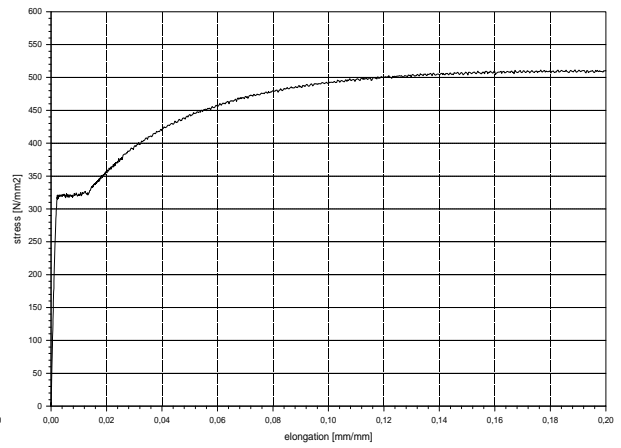


Fig. B6 Stress-elongation diagram of test specimen K1 with M20 bolts, bracket flange.

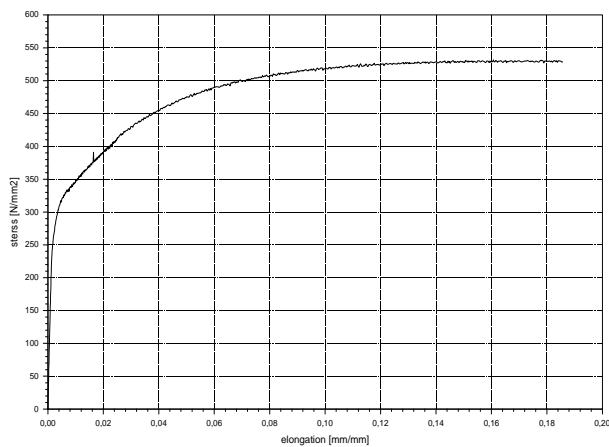


Fig. B7 Stress-elongation diagram of test specimen K1 with M20 bolts, end-plate.

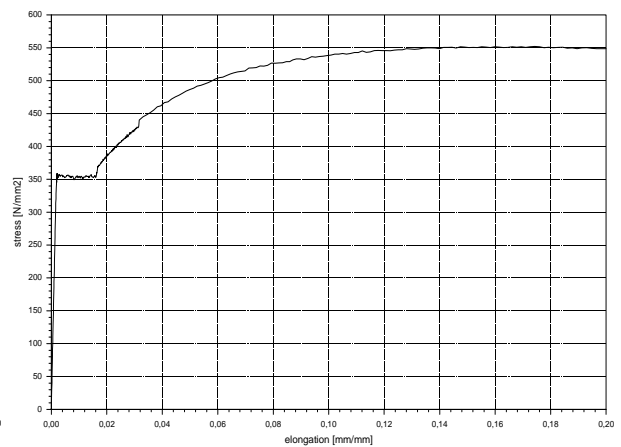


Fig. B8 Stress-elongation diagram of test specimen K2 with M20 bolts, bracket web.

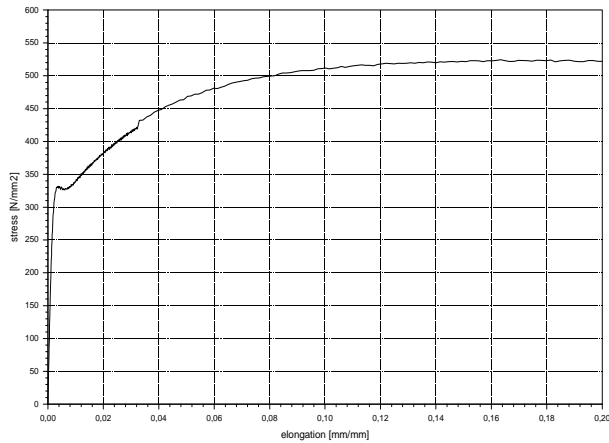


Fig. B9 Stress-elongation diagram of test specimen K2 with M20 bolts, bracket flange.

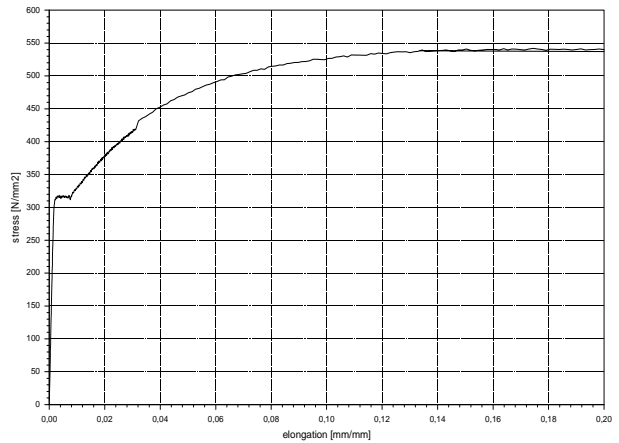


Fig. B10 Stress-elongation diagram of test specimen K2 with M20 bolts, end-plate.

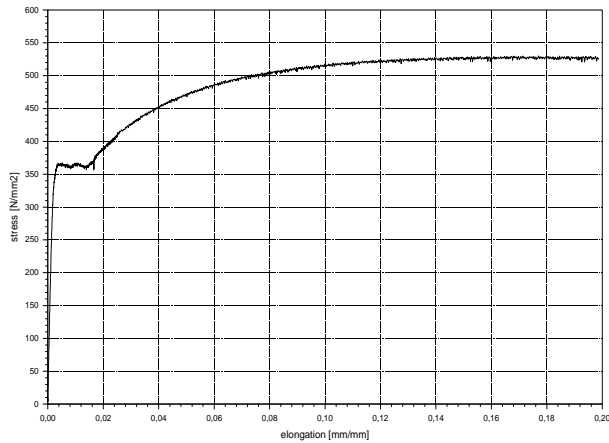


Fig. B11 Stress-elongation diagram of test specimen K3 with M20 bolts, column web.

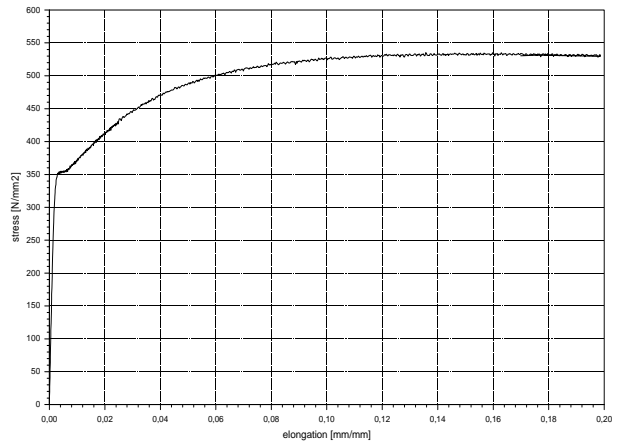


Fig. B12 Stress-elongation diagram of test specimen K3 with M20 bolts, column flange.

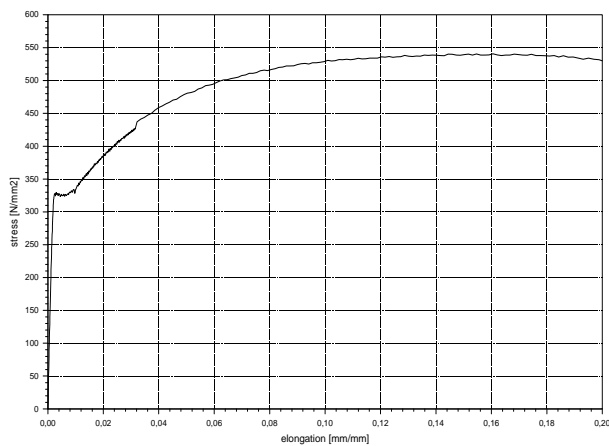


Fig. B13 Stress-elongation diagram of test specimen K3 with M20 bolts, bracket web.

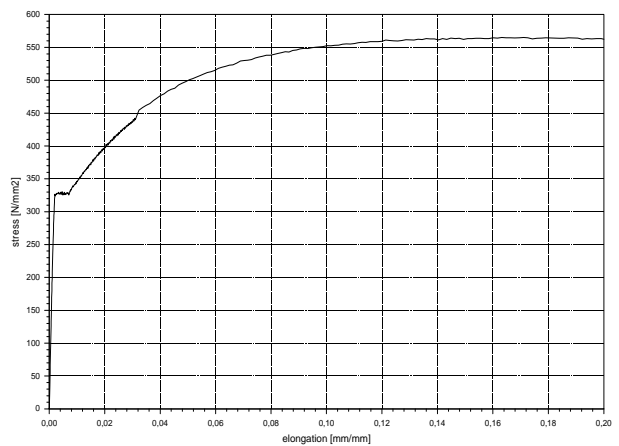


Fig. B14 Stress-elongation diagram of test specimen K3 with M20 bolts, bracket flange.

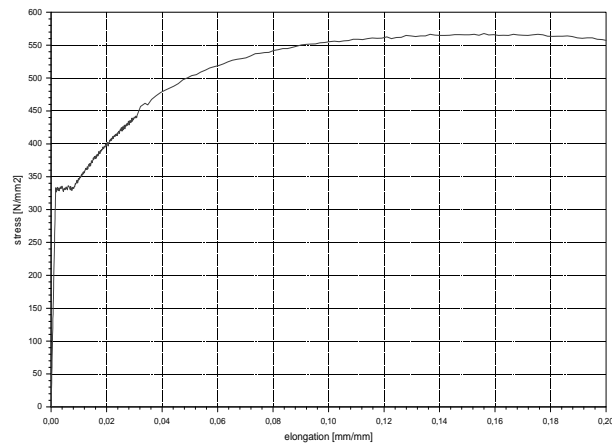


Fig. B15 Stress-elongation diagram of test specimen K3 with M20 bolts, end-plate.

Table B1 Actual material properties.

specimen	plate	thickness [mm]	yield point [N/mm ²]	tensile strength [N/mm ²]	Young modulus E [N/mm ²]
Z1 Z2	column web	6	309	466	209,271
	column flange	10	372	527	209,150
	bracket web	16	334	483	208,334
	bracket flange	12	317	487	206,897
K1-M20	column web	5	396	555	199,500
	column flange	8	369	528	186,670
	bracket web	12	365	524	191,500
	bracket flange	12	322	511	184,500
	end-plate	16	332	529	201,000
K1-M24	column web	5	387	537	203,818
	column flange	8	467	612	208,545
	bracket web	12	327	504	206,213
	bracket flange	12	317	501	197,711
K2-M20	bracket web	16	358	552	200,500
	bracket flange	12	332	523	194,500
	end-plate	16	317	541	202,500
K2-M24	column web	6	315	537	207,737
	column flange	10	375	556	207,029
	bracket web	16	337	535	206,143
	bracket flange	12	317	501	197,711
K3-M20	column web	7	366	526	210,000
	column flange	12	351	532	202,000
	bracket web	20	327	542	196,500
	bracket flange	16	327	559	202,500
	end-plate	16	333	567	202,500
K3-M24	column web	7	319	507	208,312
	column flange	12	352	536	202,059
	bracket web	20	447	571	212,144
	bracket flange	16	343	528	203,182
Z1, Z2, K1-M24, K2-M24, K3-M24	end-plate	16	349	541	208,367

*Tests on beam-to-beam joints**Series I*

Altogether test specimens were cut from six end-plates, and these specimens were subjected to the material tests. Figures B16-B19 show the process.



Fig. B16 Marked end-plate.



Fig. B17 Cutting of the test specimen.



Fig. B18 Cut surface.



Fig. B19 End-plate after cutting the test specimen.

Four specimens were cut out, as the follows: The 12 mm thick test specimens were cut out from the specimen TB2, the 15 mm thick test specimen from item TB6 and the 15 mm thick test specimen from TB10.



Fig. B20 Parallel-side milling of the test specimens.



Fig. B21 Raw test specimens.



Fig. B22 Milling of the specimens.



Fig.. B23 The complete specimens.

The test specimens were milled in the Laboratory for Testing of Structures of the Department of Structural Engineering. The material tests were carried out also in the same laboratory.



Fig. B24 The tensile testing machine.



Fig. B25 Test specimen failure 1.



Fig. B26 Test specimen failure 2.



Fig. B27 Test specimens after the test.

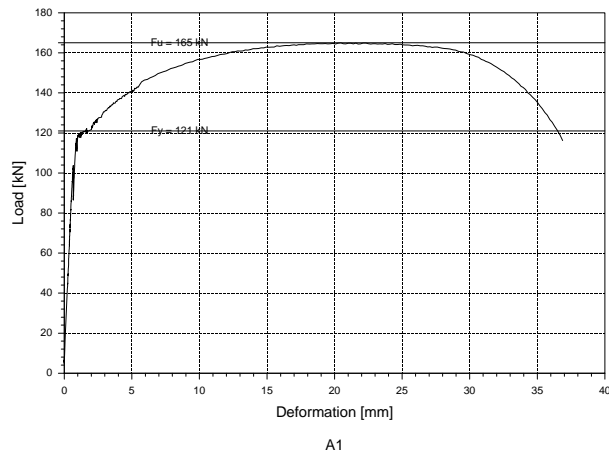


Fig. B28 Load-deformation diagram, specimen A1 ($t_{ep} = 12$ mm).

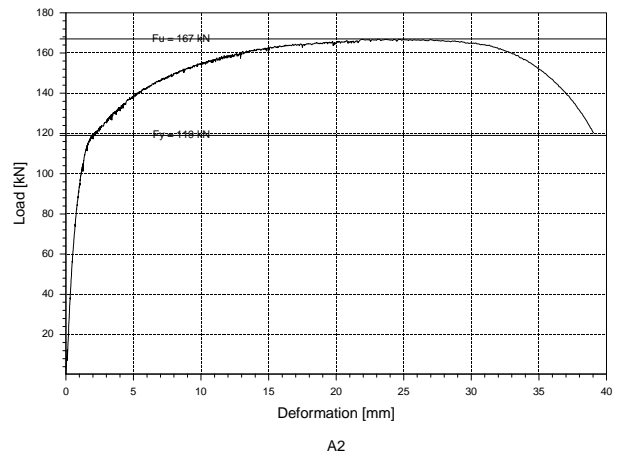


Fig. B29 Load-deformation diagram, specimen A2 ($t_{ep} = 12$ mm).

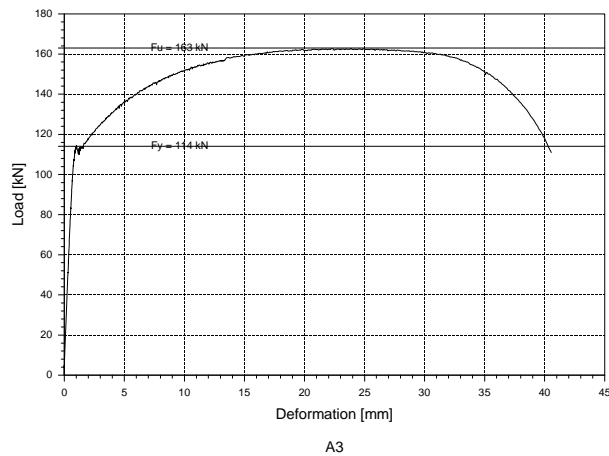


Fig. B30 Load-deformation diagram, specimen A3 ($t_{ep} = 12$ mm).

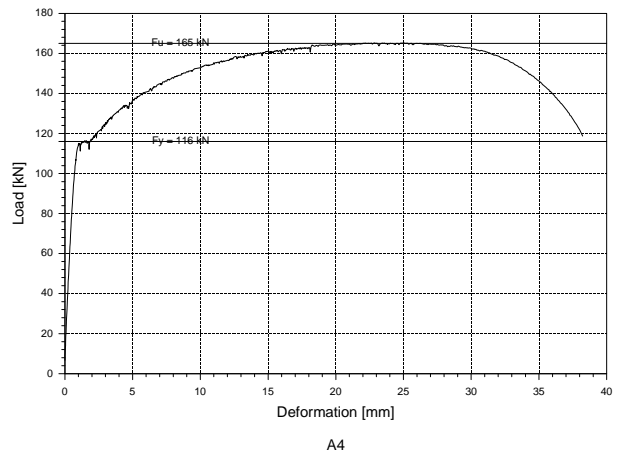


Fig. B31 Load-deformation diagram, specimen A4 ($t_{ep} = 12$ mm).

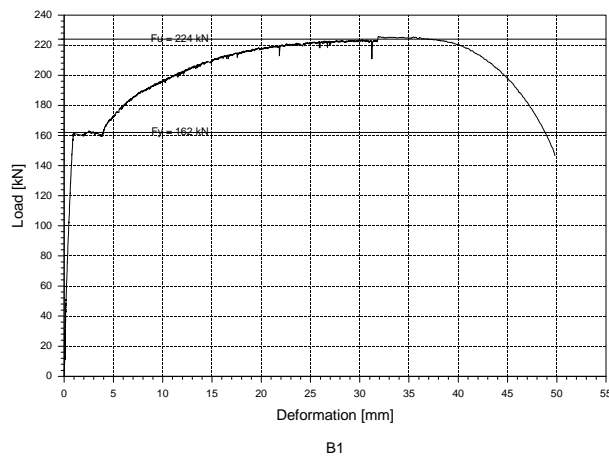


Fig. B32 Load-deformation diagram, specimen B1 ($t_{ep} = 15$ mm).

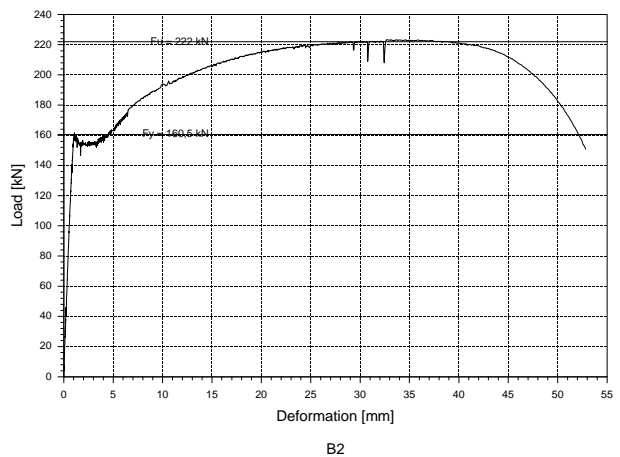
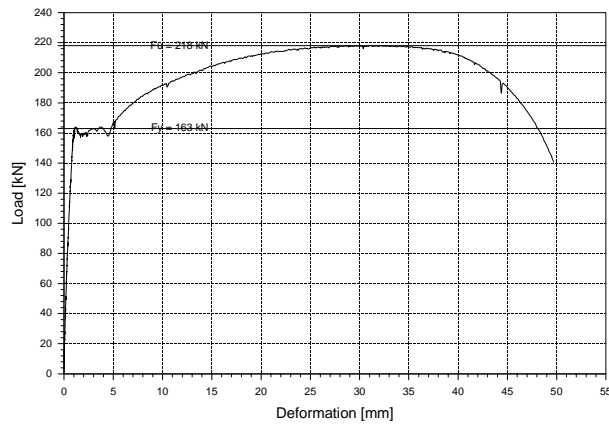
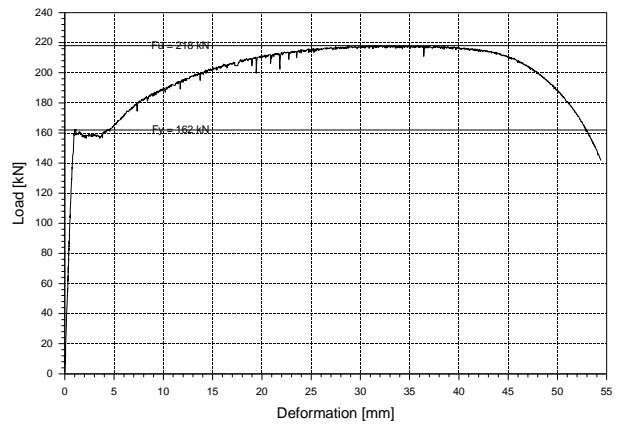


Fig. B33 Load-deformation diagram, specimen B2 ($t_{ep} = 15$ mm).



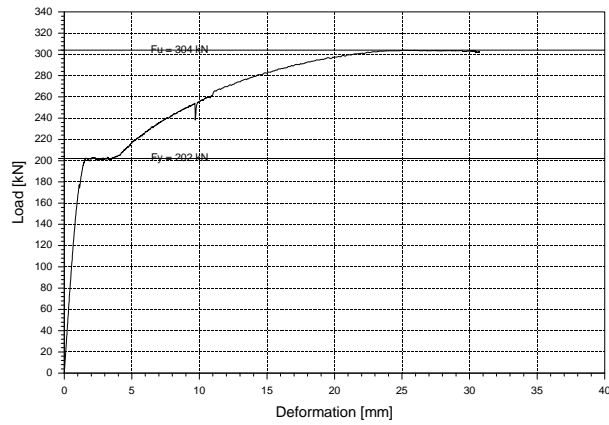
B3

Fig. B34 Load-deformation diagram, specimen B3 ($t_{ep} = 15$ mm).



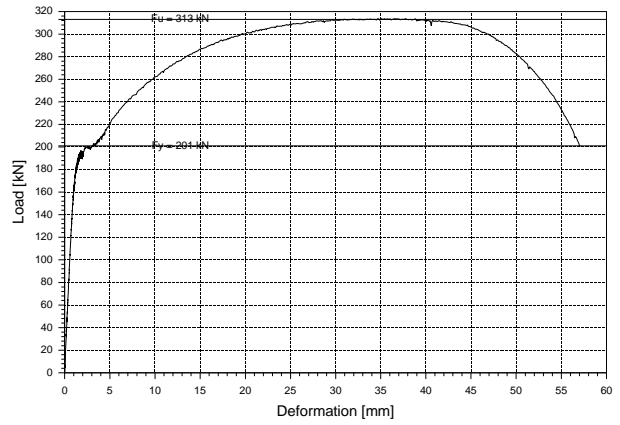
B4

Fig. B35 Load-deformation diagram, specimen B4 ($t_{ep} = 15$ mm).



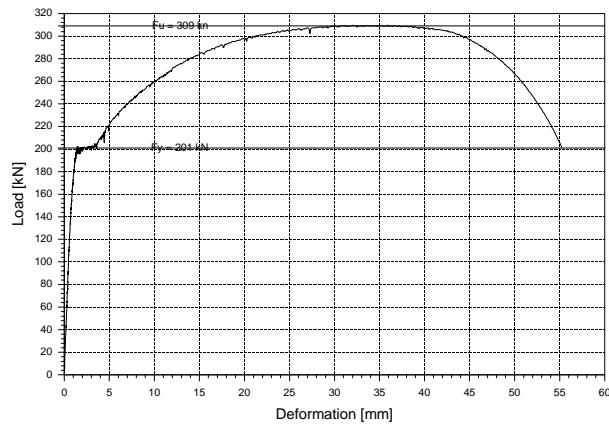
C1

Fig. B36 Load-deformation diagram, specimen C1 ($t_{ep} = 20$ mm).



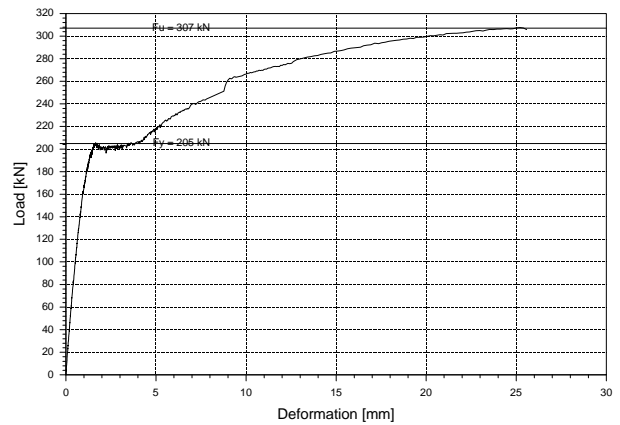
C2

Fig. B37 Load-deformation diagram, specimen C2 ($t_{ep} = 20$ mm).



C3

Fig. B38 Load-deformation diagram, specimen C3 ($t_{ep} = 20$ mm).



C4

Fig. B39 Load-deformation diagram, specimen C4 ($t_{ep} = 20$ mm).

Table B2 Measured geometrical and material properties.

specimen	nominal cross-section [mm]		measured cross-section [mm]		a x b [mm ²]	base length [mm]	base length after test [mm]	elongation	yield point [N/mm ²]	tensile strength [N/mm ²]
	a*	b*	a	b	A	L ₀		%	f _y	f _u
A1	12	26	11.6	25.4	294.6	100	130	30	411	560
A2			11.6	26.0	301.6		131	31	394	554
A3			11.6	25.7	298.1		134	34	382	547
A4			11.6	26.1	302.8		130	30	383	545
B1	15	30	15.1	29.8	450.0	120	160	33	360	498
B2			15.1	30.0	453.0		162	35	354	490
B3			14.8	30.0	444.0		161	34	367	491
B4			14.8	30.0	444.0		165	37	367	491
C1	20	30	20.1	29.7	597.0	140	-	-	338	509
C2			20.4	30.0	612.0		187	33	328	511
C3			20.3	29.9	607.0		186	33	331	509
C4			20.3	30.1	611.0		-	-	335	502

Table B3 shows the measured main material properties.

Table B3 Material properties.

plate thickness t _{ep} [mm]		test 1		test 2		test 3		test 4		average	
		f _y	f _u								
		[N/mm ²]									
12		411	560	394	554	382	547	383	545	393	552
15		360	498	354	490	367	491	367	491	362	493
20		338	509	328	511	331	509	335	502	333	508

Series II

In total specimens were cut from three end-plates, and these specimens were subjected to the material tests.



Fig. B40 Marked end-plates.



Fig. B41 Cutting of the specimen.



Fig. B42 Cut surface.



Fig. B43 End-plate after cut out of the specimen.

From each end-plate thickness (16 mm; 20 mm; 24 mm) four specimens were cut. The 16 mm thick specimens were cut from specimen D, the 20 mm thick specimens from test specimen E, and the 24 mm thick specimens from test specimen F.



Fig. B44 Parallel-side milling of the specimens.



Fig. B45 Raw test specimens.



Fig. B46 Milling of the specimens.



Fig. B47 Completed test specimens.

The specimens were prepared and the material tests carried out in the laboratory of the BME, Department of Structural Engineering.



Fig. B48 Test specimen failure 1 (B3).



Fig. B49 Test specimen failure 2 (B3).



Fig. B50 Test specimens after the test.

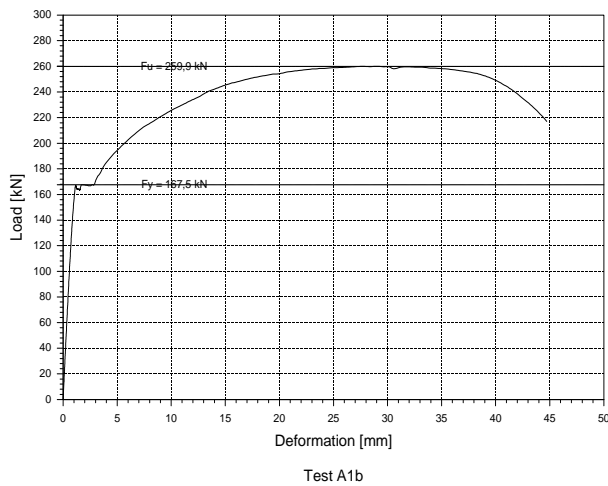


Fig. B51 Load-deformation diagram, specimen A1b ($t_{ep} = 16$ mm).

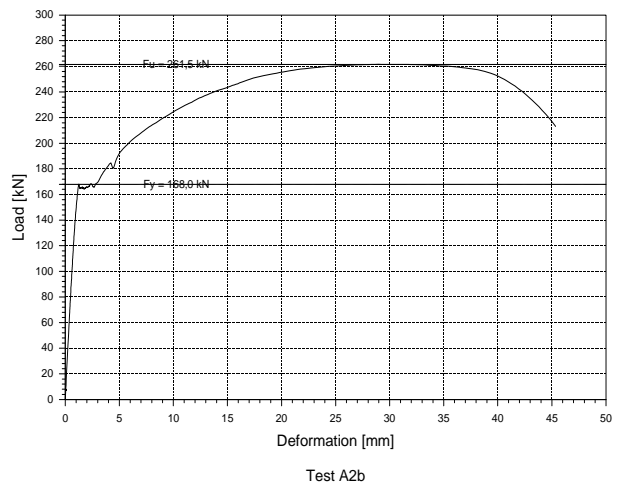


Fig. B52 Load-deformation diagram, specimen A2b ($t_{ep} = 16$ mm).

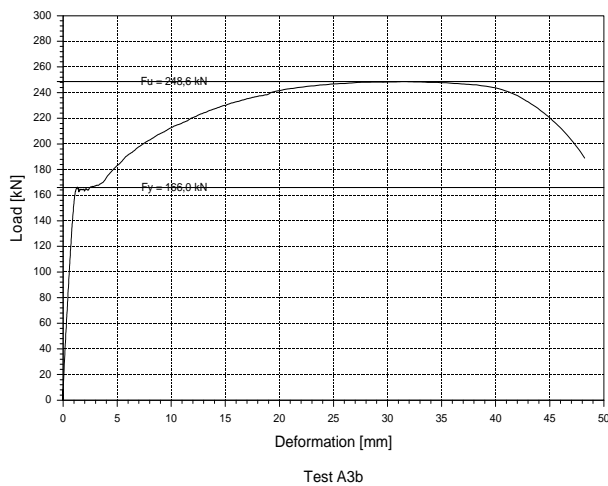


Fig. B53 Load-deformation diagram, specimen A3b ($t_{ep} = 16$ mm).

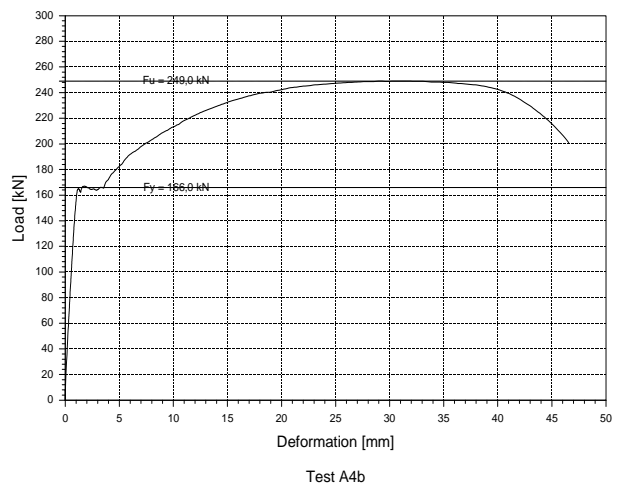


Fig. B54 Load-deformation diagram, specimen A4b ($t_{ep} = 16$ mm).

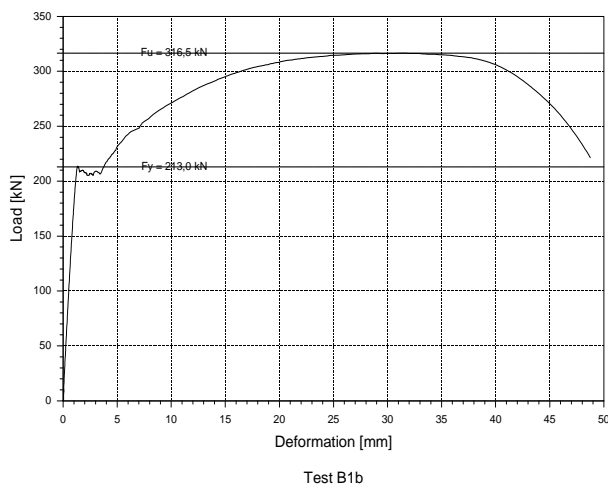


Fig. B55 Load-deformation diagram, specimen B1b ($t_{ep} = 20$ mm).

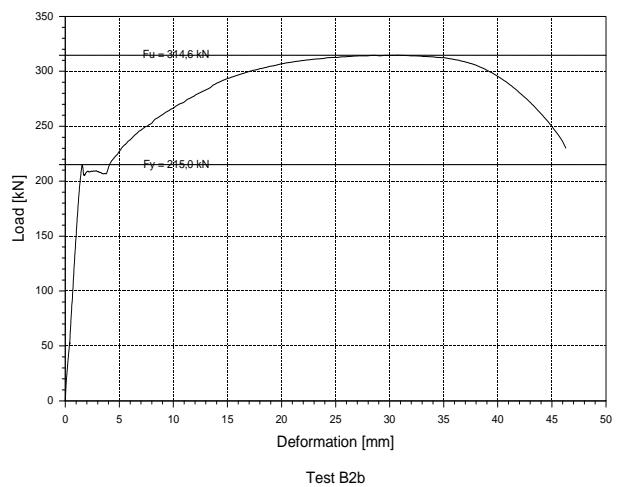


Fig. B56 Load-deformation diagram, specimen B2b ($t_{ep} = 20$ mm).

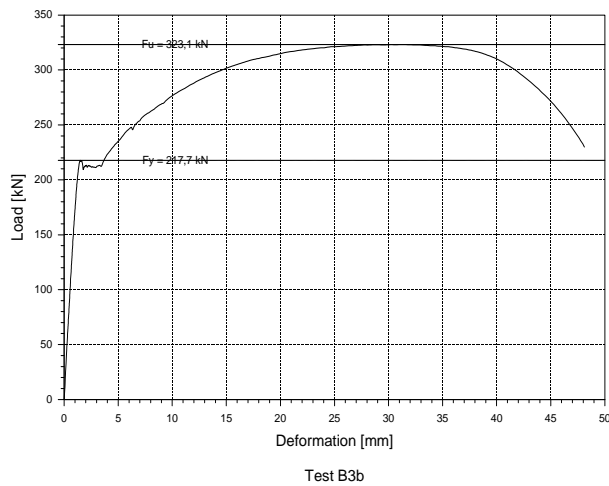


Fig. B57 Load-deformation diagram, specimen B3b ($t_{ep} = 20$ mm).

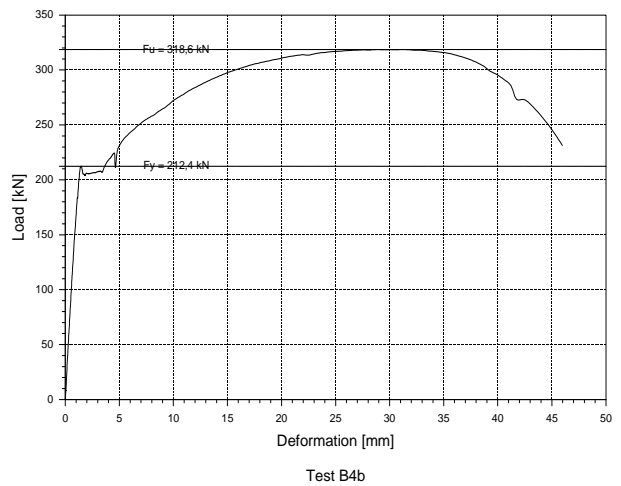


Fig. B58 Load-deformation diagram, specimen B4b ($t_{ep} = 20$ mm).

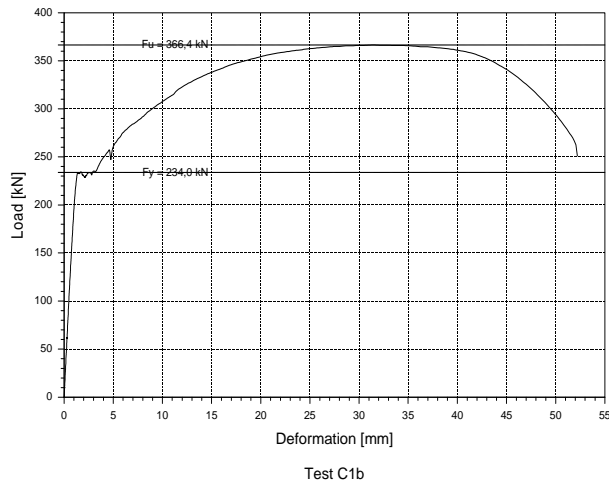


Fig. B59 Load-deformation diagram, specimen C1b ($t_{ep} = 24$ mm).

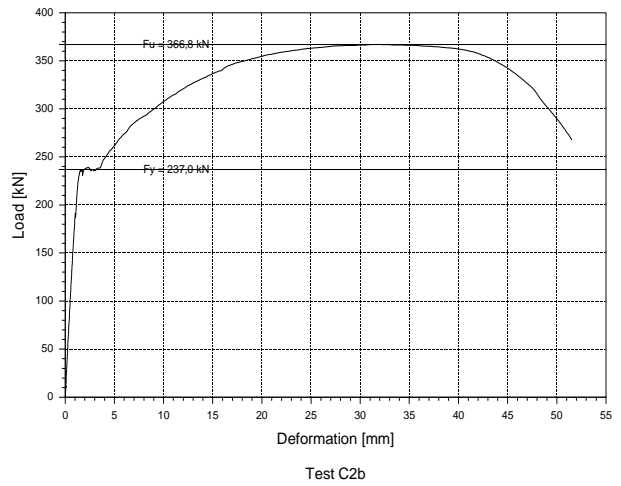


Fig. B60 Load-deformation diagram, specimen C2b ($t_{ep} = 24$ mm).

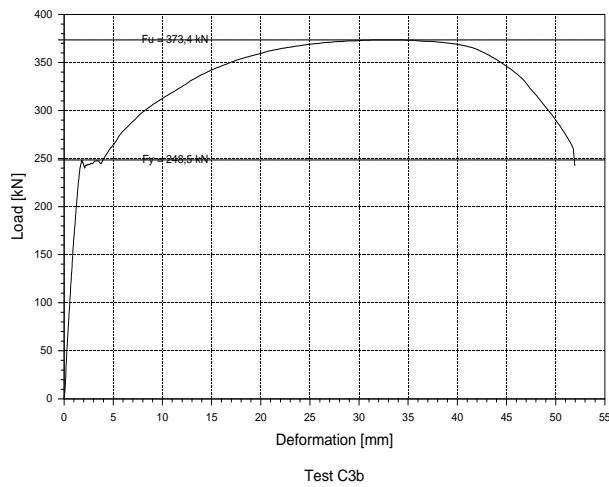


Fig. B61 Load-deformation diagram, specimen C3b ($t_{ep} = 24$ mm).

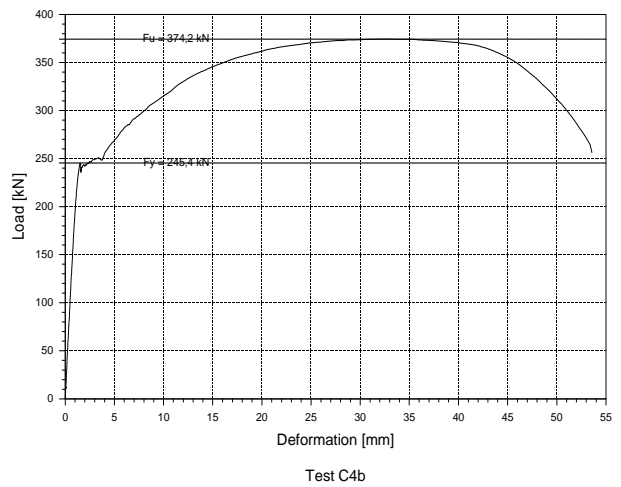


Fig. B62 Load-deformation diagram, specimen C4b ($t_{ep} = 24$ mm).

Table B4 Measured geometrical and material properties.

specimen	nominal cross-section [mm]		measured cross-section [mm]		a* x b* [mm ²]	base length [mm]	base length after test [mm]	elongation [%]	yield point [N/mm ²]	tensile strength [N/mm ²]
	a	b	a*	b*	A*	L ₀	L* ₀	-	f _y	f _u
A1b	16	30	15.5	29.7	460.3	120	156	30	363.9	564.6
A2b			15.5	29.8	461.9		156	30	363.7	566.1
A3b			15.5	29.8	461.9		158	32	359.4	538.2
A4b			15.5	29.9	463.5		157	31	358.1	537.2
B1b	20	30	19.2	29.7	570.2	140	180	29	373.6	555.1
B2b			19.3	29.6	571.3		178	27	376.3	550.6
B3b			19.5	29.8	581.1		180	29	374.6	556.0
B4b			19.5	29.7	579.2		179	28	366.7	550.1
C1b	24	30	23.4	29.5	690.3	155	202	30	338.9	530.8
C2b			23.2	29.6	686.7		200	29	345.1	534.1
C3b			23.5	29.5	693.3		201	30	358.4	538.6
C4b			23.5	29.6	695.6		201	30	352.8	537.9

Table B5 shows the measured main material properties.

Table B5 Material properties.

plate thickness t _{ep} [mm]		test 1		test 2		test 3		test 4		average	
		f _y [N/mm ²]	f _u [N/mm ²]	f _y [N/mm ²]	f _u [N/mm ²]	f _y [N/mm ²]	f _u [N/mm ²]	f _y [N/mm ²]	f _u [N/mm ²]	f _y [N/mm ²]	f _u [N/mm ²]
16		363.9	564.6	363.7	566.1	359.4	538.2	358.1	537.2	361.3	551.5
20		373.6	555.1	376.3	550.6	374.6	556.0	366.7	550.1	372.8	553.0
24		338.9	530.8	345.1	534.1	358.4	538.6	352.8	537.9	348.8	535.4

Test on bolts

Altogether twelve bolts were subjected to tensile tests as part of the material tests, six from bolt grade 8.8 and six from 10.9. The material tests were performed in the laboratory of the BME, Department of Structural Engineering with the ZD 100 RENEW testing machine, which has a maximum load capacity of 1,000 kN.

Figures B63 and B64 show the tested bolts before and after test.



a.) bolts before test



b.) bolts after test

Fig. B63 Bolt grade 10.9.



a.) bolts before test



b.) bolts after test

Fig. B64 Bolt grade 8.8

Figure B65 shows the testing machine, and Figure B66 presents an example of a bolt after failure.



Fig. B65 The testing machine ZD 100.



Fig. B66 Bolt failure.

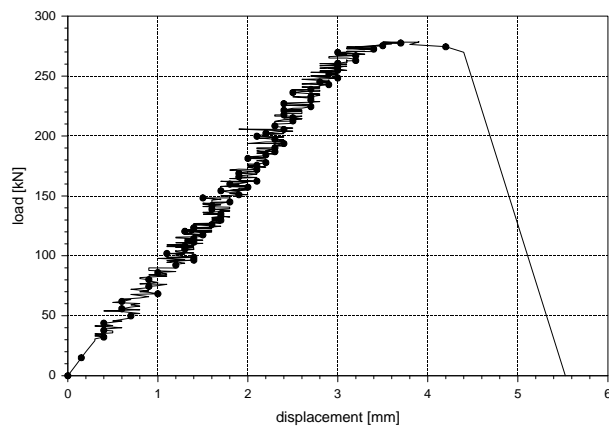


Fig. B67 Load-deflection diagram, bolt Ba6.

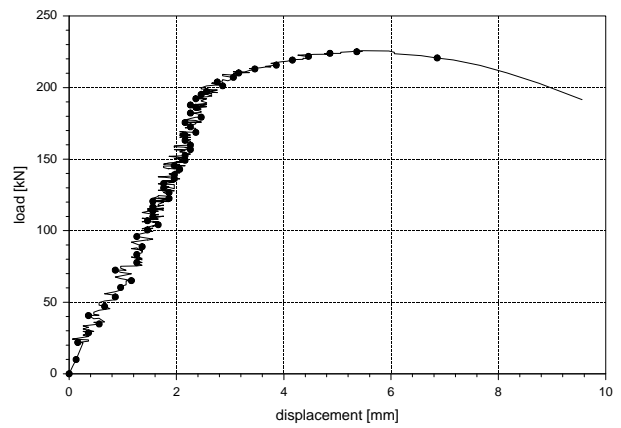


Fig. B68 Load-deflection diagram, bolt Bb1.

Figures B67 and B68 present load-displacement curves measured during the material tests.

Table B6 shows the measured maximal bolt resistances.

Table B6 Results of the material test.

bolt	measured tension load capacity in kN						average
	B1	B2	B3	B4	B5	B5	[kN]
10.9	273.5	265.4	265.2	277.3	272.7	278.7	272.1
8.8	225.8	223.3	224.4	222.8	223.9	226.0	224.4

Pre-tensioning of the bolts

Test series I

Table C1 Measured preloads in the bolts.

bolt position	test series I name of the specimen											
	TB2	TB3	TB4	TB5	TB6	TB7	TB8	TB9	TB10	TB11	TB12	TB13
A [kN]	48.3	60.6	-	-	30.1	40.5	-	-	38.9	46.1	-	-
AA [kN]	-	67.1	-	-	-	78.9	-	-	-	43.2	-	-
A2 [kN]	43.3	47.9	-	-	51.1	53.2	-	-	29.9	43.0	-	-
AA2 [kN]	-	64.6	-	-	-	36.5	-	-	-	36.9	-	-
B [kN]	35.7	65.0	27.9	20.9	34.3	94.1	49.7	9.7	37.8	50.0	20.8	37.4
BB [kN]	-	-	36.9	-	-	-	28.5	-	-	-	18.4	-
B2 [kN]	36.8	40.4	33.0	26.4	56.6	36.9	15.3	20.6	18.0	33.7	7.7	5.2
BB2 [kN]	-	-	31.9	-	-	-	35.2	-	-	-	20.4	-
C [kN]	35.6	59.2	28.5	32.5	38.2	59.8	23.1	31.5	38.4	36.9	30.7	44.5
CC [kN]	-	-	36.2	-	-	-	29.2	-	-	-	59.2	-
C2 [kN]	44.6	67.8	42.5	34.4	51.2	51.2	33.2	37.0	15.3	74.4	23.2	11.2
CC2 [kN]	-	-	37.6	-	-	-	58.3	-	-	-	24.8	-
D [kN]	45.2	58.2	34.8	38.0	32.9	48.9	31.5	43.1	21.0	77.9	33.1	32.5
D2 [kN]	41.5	52.4	34.8	31.3	59.6	68.3	47.0	27.2	28.6	49.2	43.7	29.4
E [kN]	49.1	44.2	39.5	-	58.0	47.4	39.4	58.4	26.9	62.6	37.0	39.8
E2 [kN]	50.9	-	40.1	-	62.0	-	61.1	35.7	40.9	-	51.7	23.6
F [kN]	27.8	-	-	-	40.6	-	-	48.8	34.8	-	-	33.1
F2 [kN]	35.4	-	-	-	54.4	-	-	34.1	49.3	-	-	11.2
	TB2	TB3	TB4	TB5	TB6	TB7	TB8	TB9	TB10	TB11	TB12	TB13

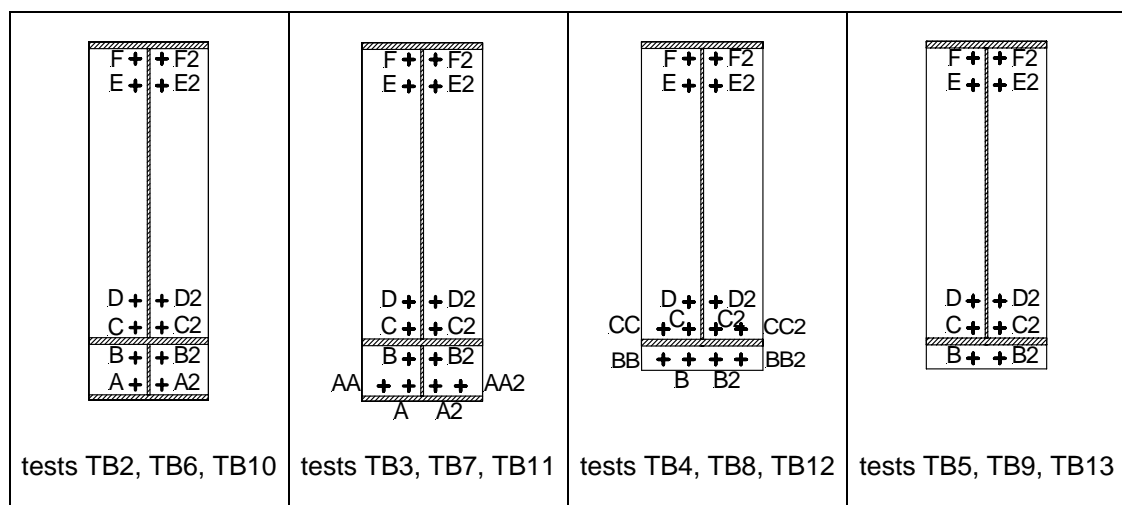


Fig C1 Positions of the load cells.

Test series II

Table C2 Measured preloads in the bolts.

bolt position	test series II name of the specimen					
	TA	TB	TC	TD	TE	TF
A [kN]	-	-	65.0	65.4	116.5	107.1
AA [kN]	-	-	-	-	114.2	106.4
A2 [kN]	-	-	76.3	77.1	90.4	87.9
AA2 [kN]	-	-	-	-	75.8	98.4
B [kN]	42.1	36.7	69.0	74.0	90.2	88.0
BB [kN]	-	-	-	-	97.7	85.6
B2 [kN]	53.7	39.8	64.5	75.2	101.1	109.3
BB2 [kN]	-	-	-	-	90.6	97.6
C [kN]	54.2	33.2	-	88.6	-	-
C2 [kN]	67.3	51.0	-	85.8	-	-
D [kN]	66.1	50.5	73.3	105.2	121.4	99.7
D2 [kN]	85.5	57.1	73.2	98.1	124.4	115.4
	TA	TB	TC	TD	TE	TF

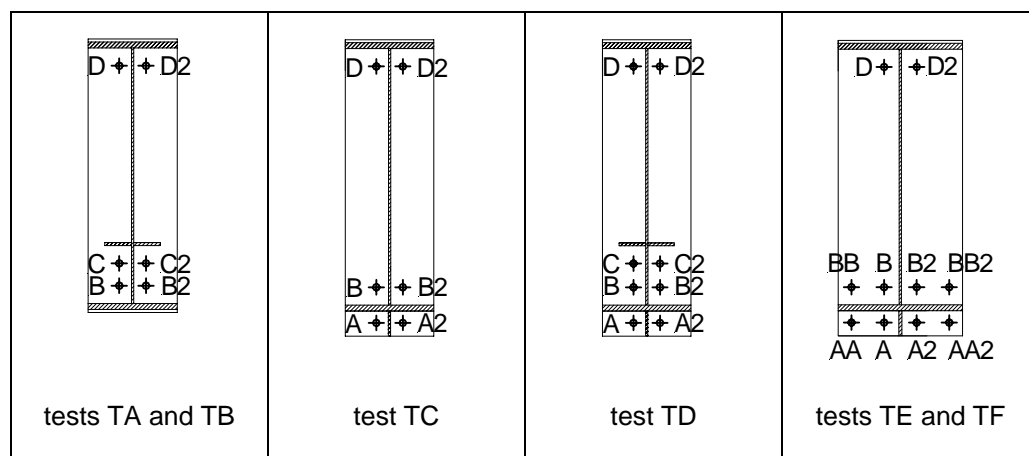


Fig C2 Positions of the load cells.

The bolts were preloaded in each test. The M20 bolts and the M24 bolts - in the fixed connection - were pre-tensioned by a maximum preload of 200 Nm and 450 Nm, respectively.

In order to get a homogeneous preload level in the bolts of the investigated connection, a three-step preload process was used. First the bolts were strained by hand, then, beginning with the bolt-row farthest from the compression flange, the bolts were preloaded by a pneumatic screwdriver, and in the third step, because of the end-plate deformations and other imperfections, the bolts were preloaded again with the pneumatic screwdriver.

Due to the following effects the achieved pre-load levels were not exactly the same:

- friction differences of the bolts (imperfect form, different coating thickness of the bolts),
- the bolt nut and/or bolt head was not exactly perpendicular to the end-plate (erection imperfection),
- the stiffness distribution in the end-plate was not homogeneous, i.e. the connected plate parts adjacent to the flange had higher stiffness than the parts near the edge.

Measuring the end-plate surface

A special equipment were developed to measure the deformation of the end-plate after the test, as shown in Figures D1, D2, D3 and D4.



Fig. D1 The testing bench.



Fig. D2 Specimens with the testing bar.



Fig. D3 Measuring wheel with inductive transducer.



Fig. D4 Magnetic scale to measure the length.

Benchmark data were collected in the web direction at each 0,25 mm, with an accuracy of 0,001 mm in terms of altitude. To measure the length a magnetic scale with an accuracy of 0,01 mm was used. The magnetic scale is shown in Figure D4.

The zero altitude level was chosen for all end-plates at the intersection of the web and the compression flange, as shown in Figure D5.

Test series I

On each end-plate eleven contour-lines in uniform distances were designated. Figure D5 shows the positions of the measured contour-lines and the identification codes.

The presented surfaces were determined by linear interpolation between the contour-lines.

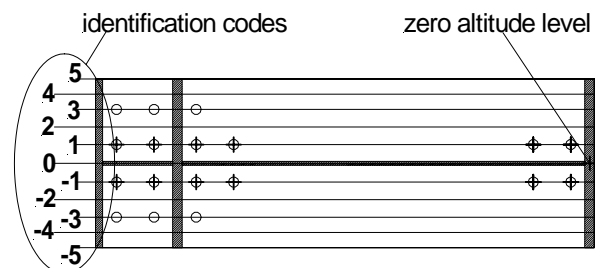


Fig. D5 Measured lines and identification codes.

1.) End-plate type I

Test specimen TB2

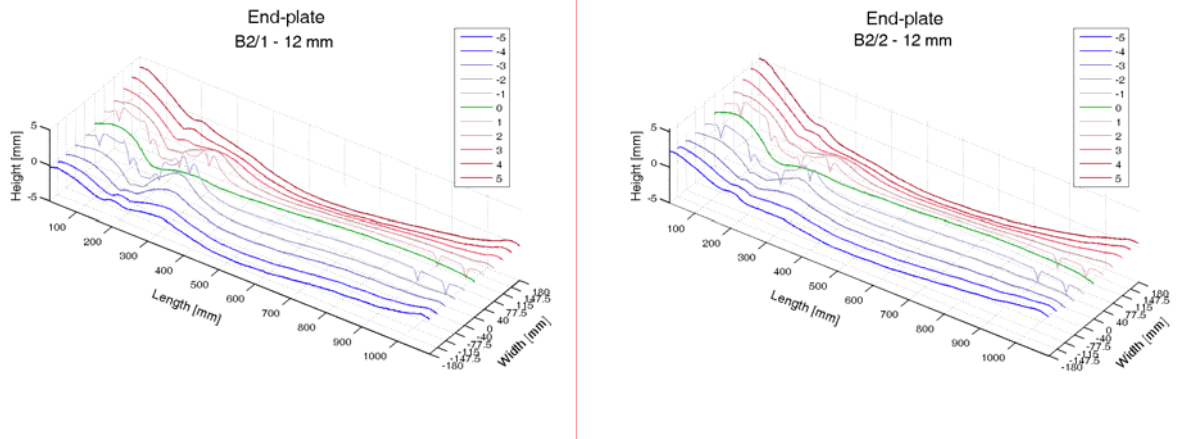


Fig. D6 Deformed end-plate contour-lines.

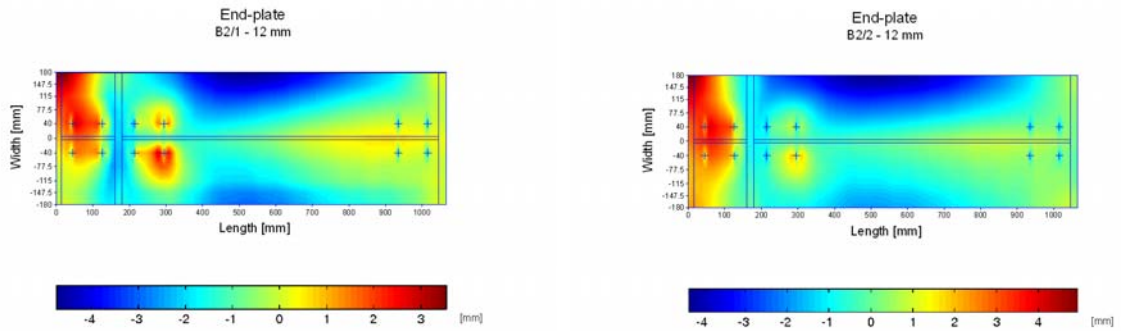


Fig. D7 The shapes of the deformed end-plates.

Test specimen TB6

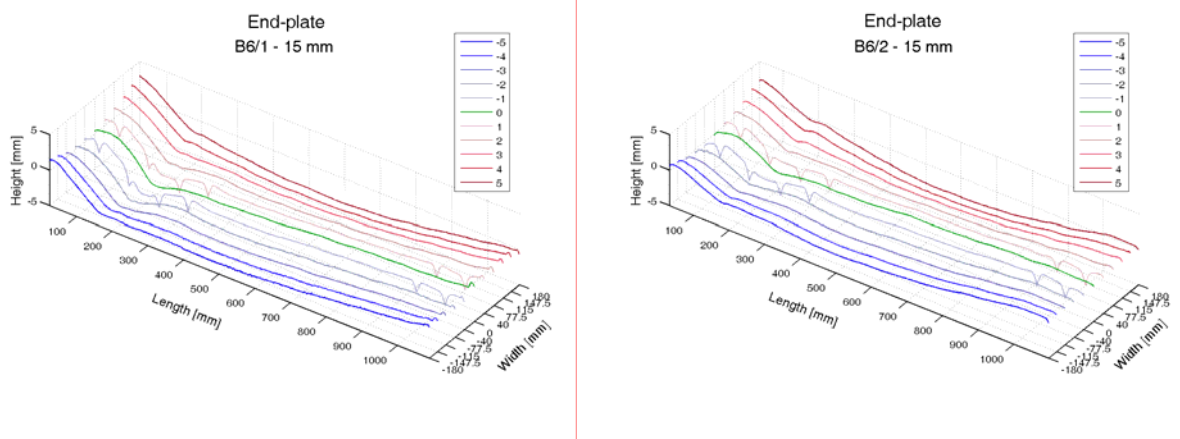


Fig. D8 Deformed end-plate contour-lines.

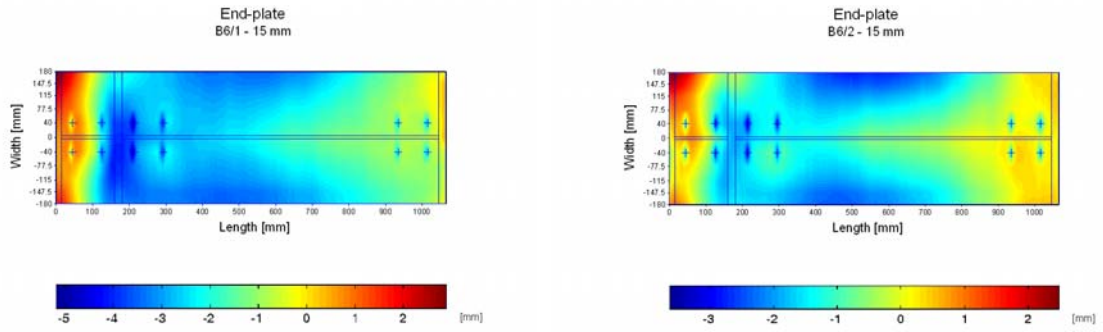


Fig. D9 The shapes of the deformed end-plates.

Test specimen TB10

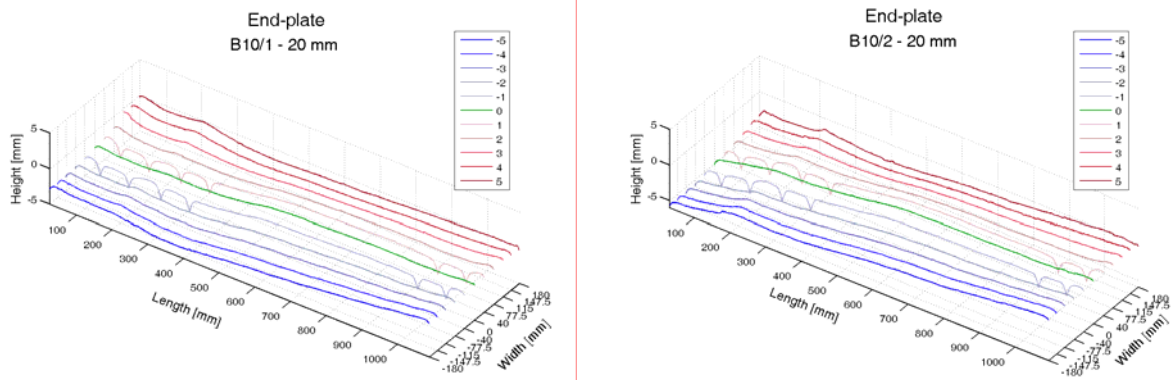


Fig. D10 Deformed end-plate contour-lines.

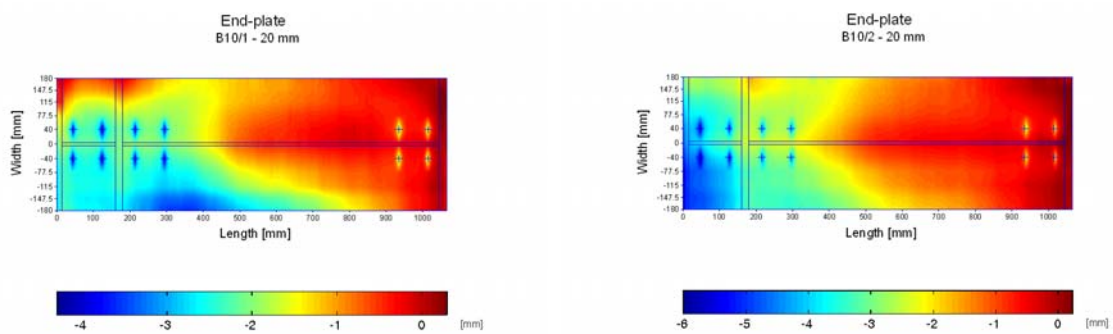


Fig. D11 The shapes of the deformed end-plates.

2.) End-plate type II

Test specimen TB3

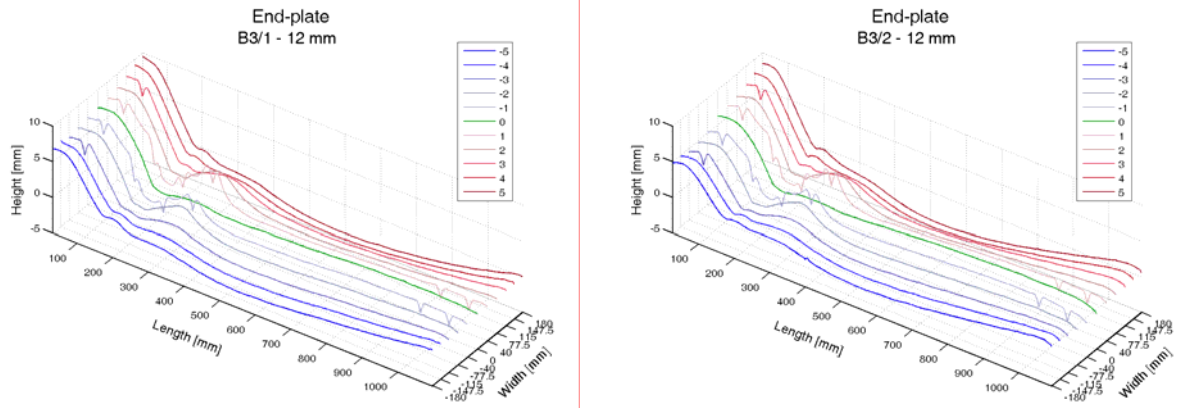


Fig. D12 Deformed end-plate contour-lines.

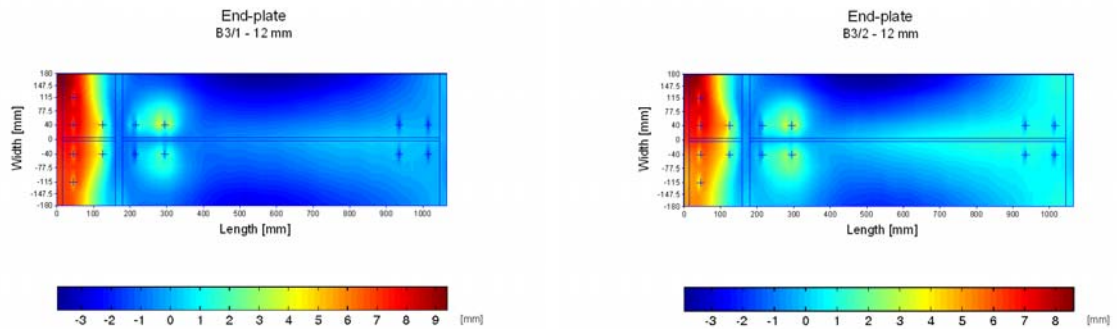


Fig. D13 The shapes of the deformed end-plates.

Test specimen TB7

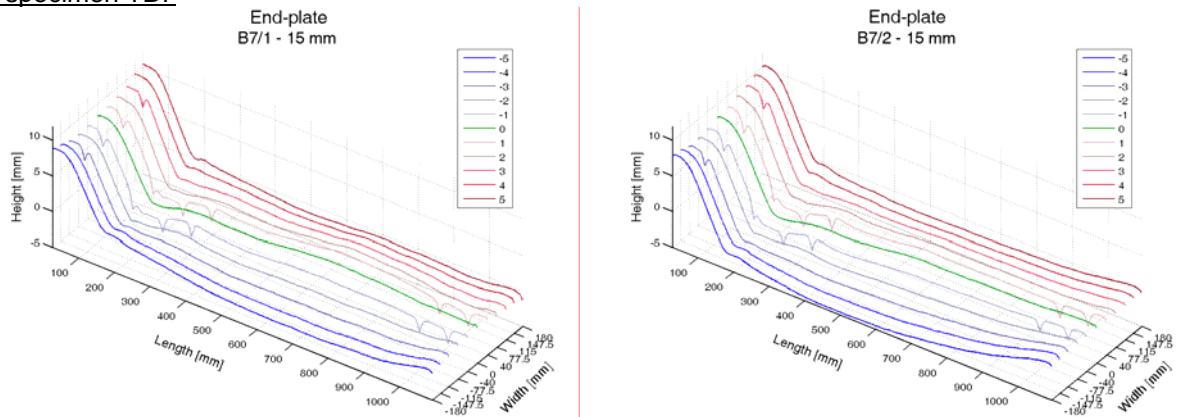


Fig. D14 Deformed end-plate contour-lines.

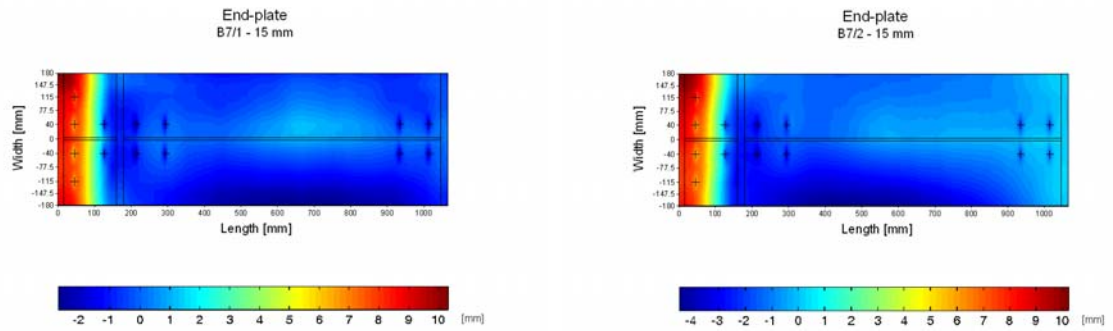


Fig. D15 The shapes of the deformed end-plates.

Test specimen TB11

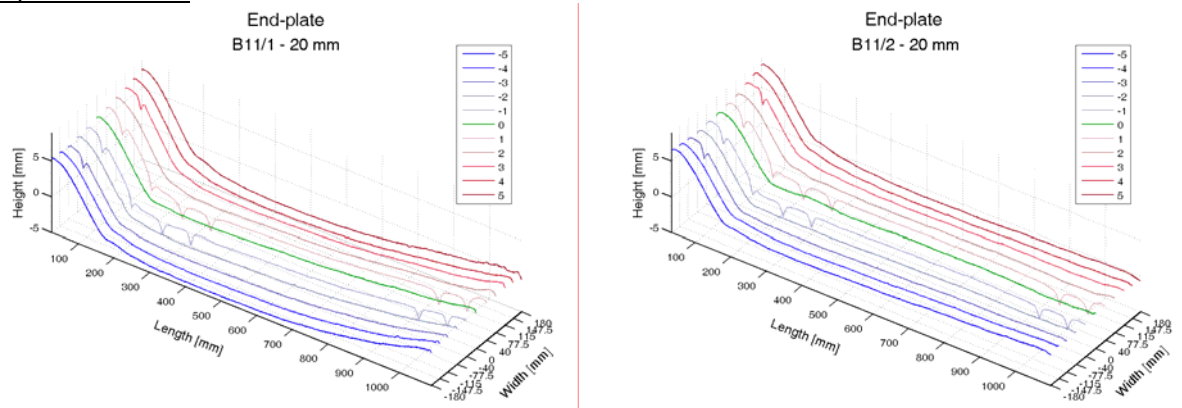


Fig. D16 Deformed end-plate contour-lines.

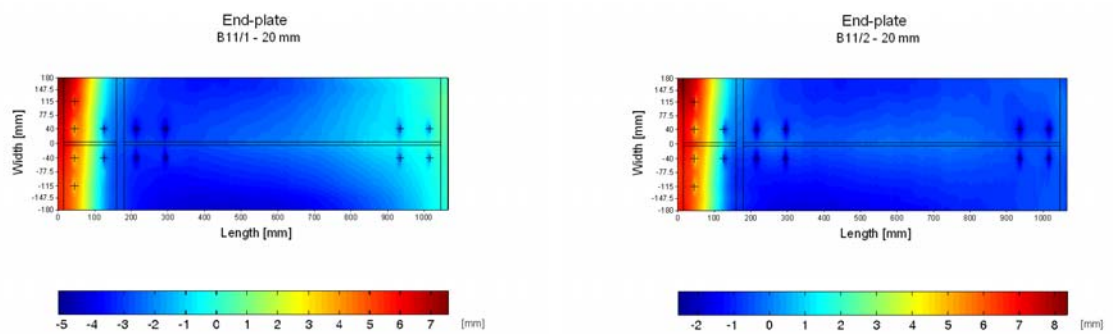


Fig. D17 The shapes of the deformed end-plates.

3.) End-plate type III

Test specimen TB4

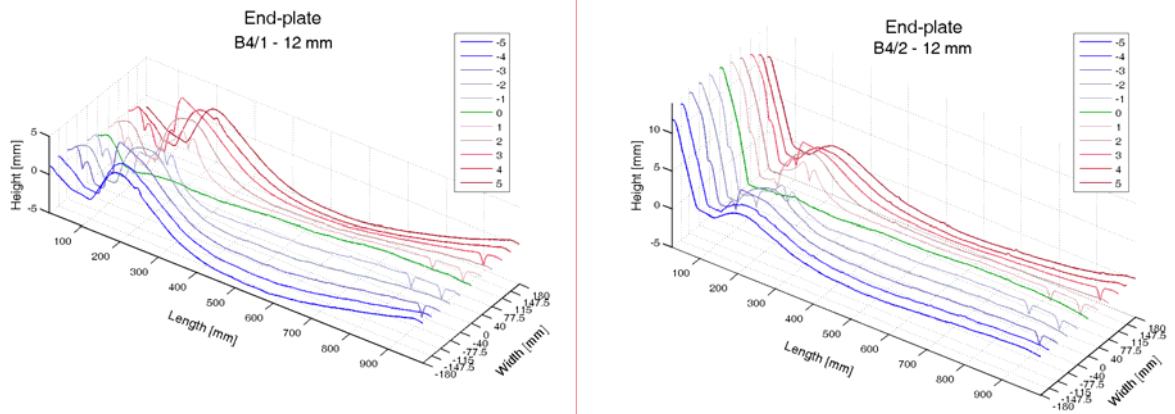


Fig. D18 Deformed end-plate contour-lines.

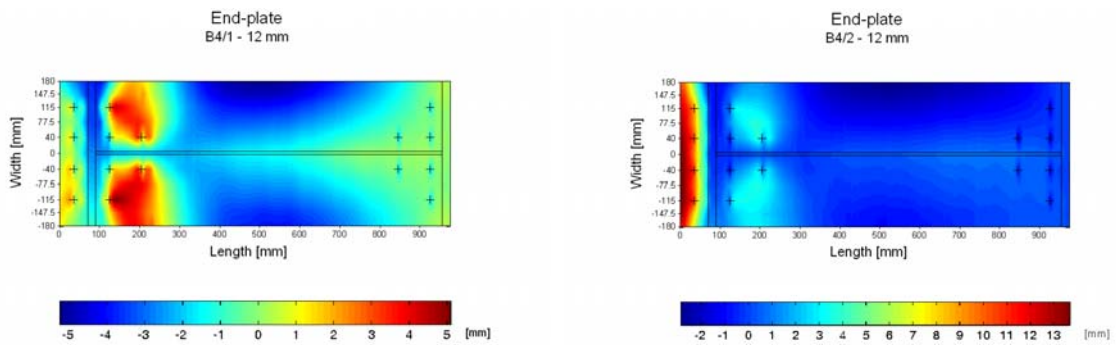


Fig. D19 The shapes of the deformed end-plates.

Test specimen TB8

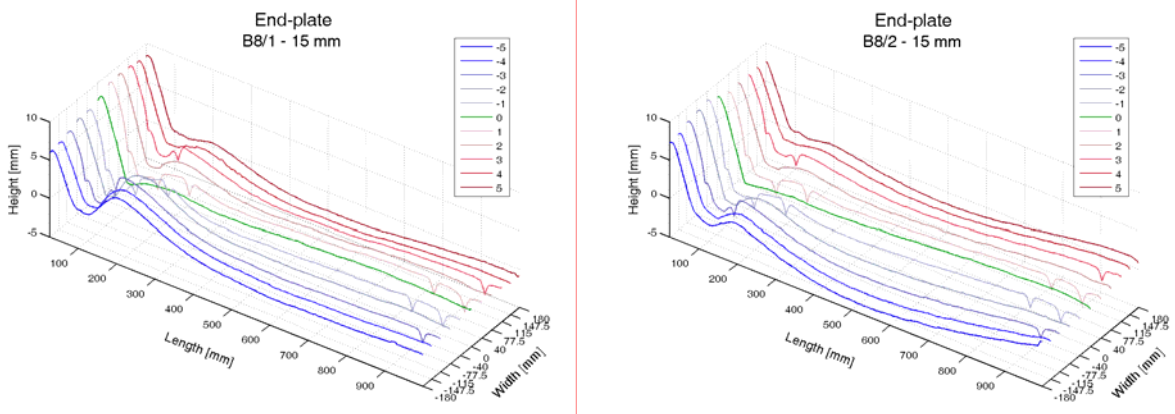


Fig. D20 Deformed end-plate contour-lines.

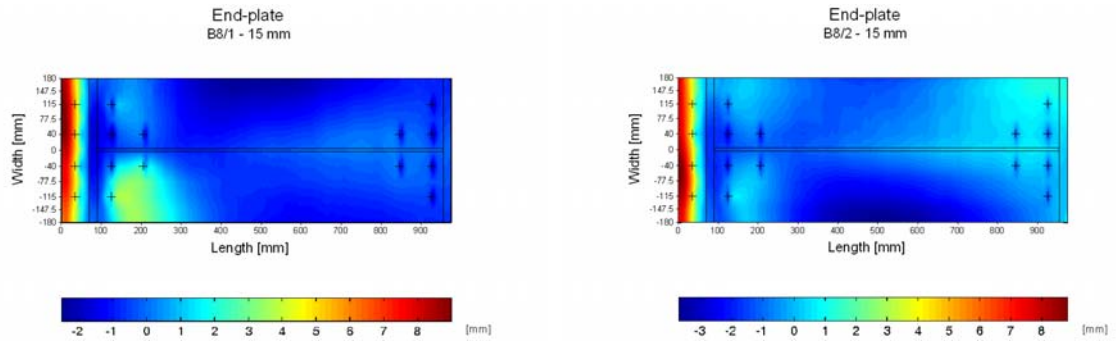


Fig. D21 The shapes of the deformed end-plates.

Test specimen TB12

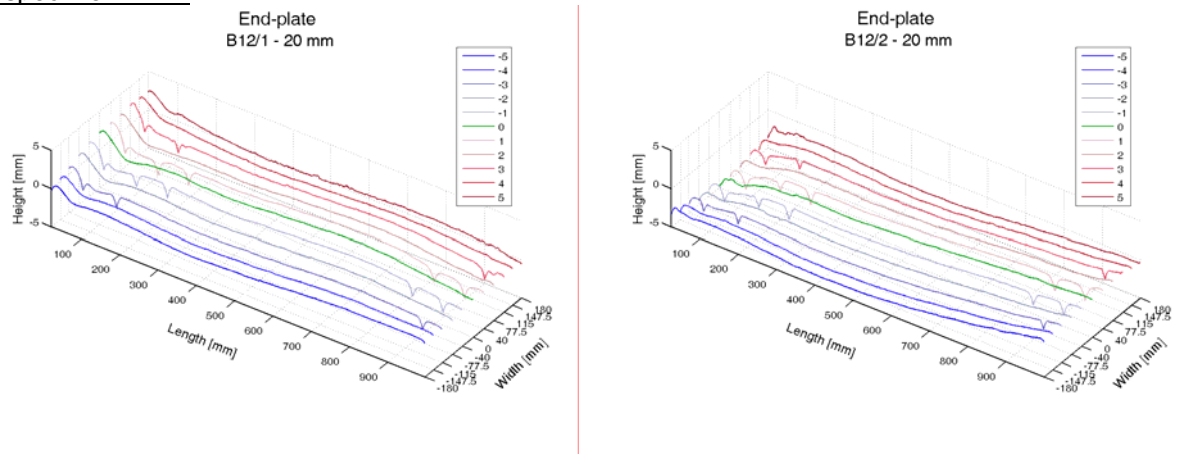


Fig. D22 Deformed end-plate contour-lines.

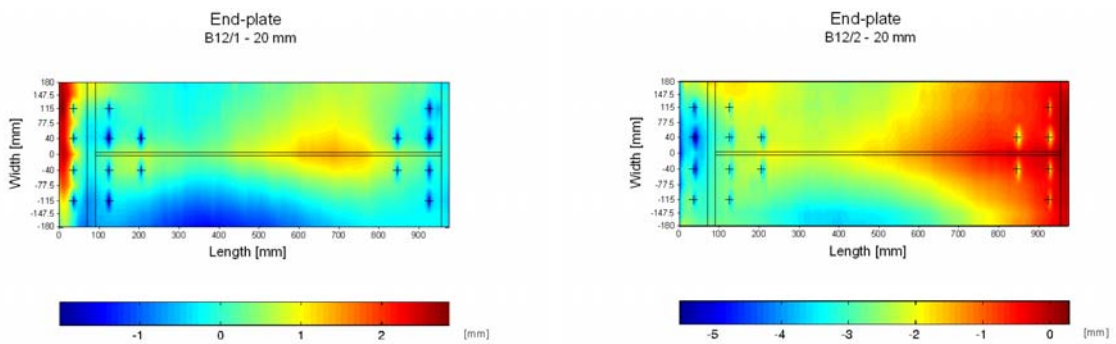


Fig. D23 The shapes of the deformed end-plates.

4.) End-plate type IV

Test specimen TB5

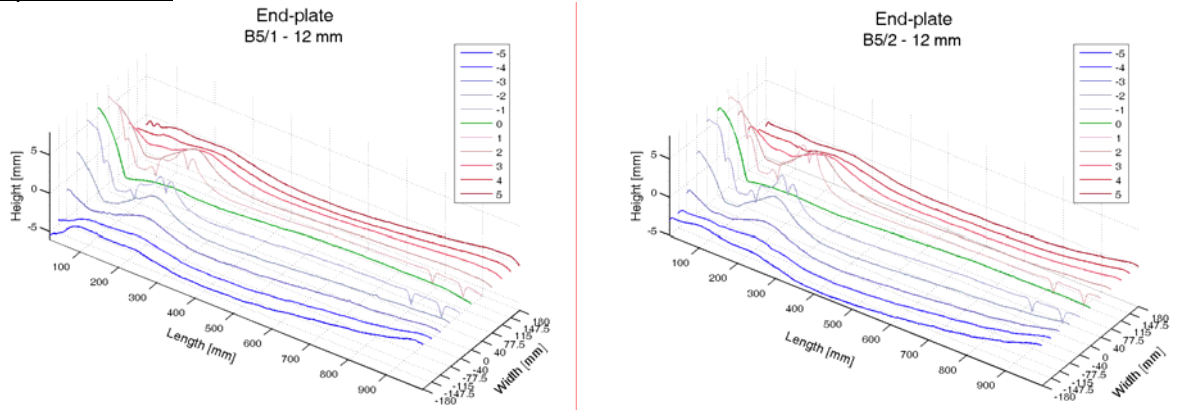


Fig. D24 Deformed end-plate contour-lines.

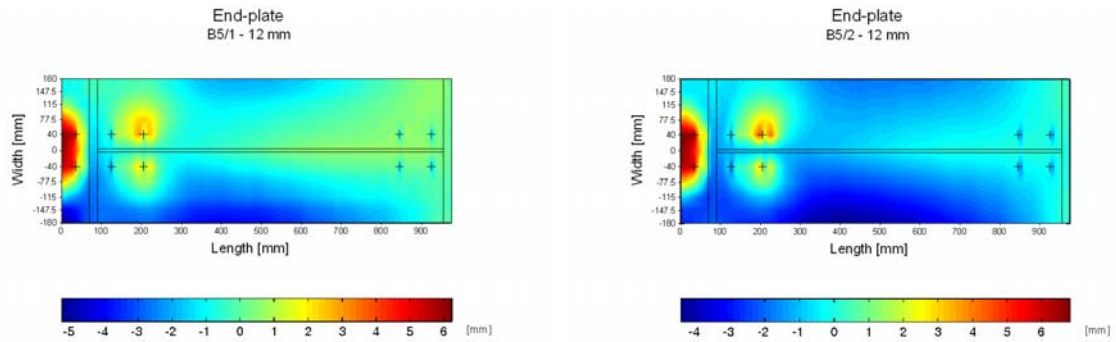


Fig. D25 The shapes of the deformed end-plates.

Test specimen TB9

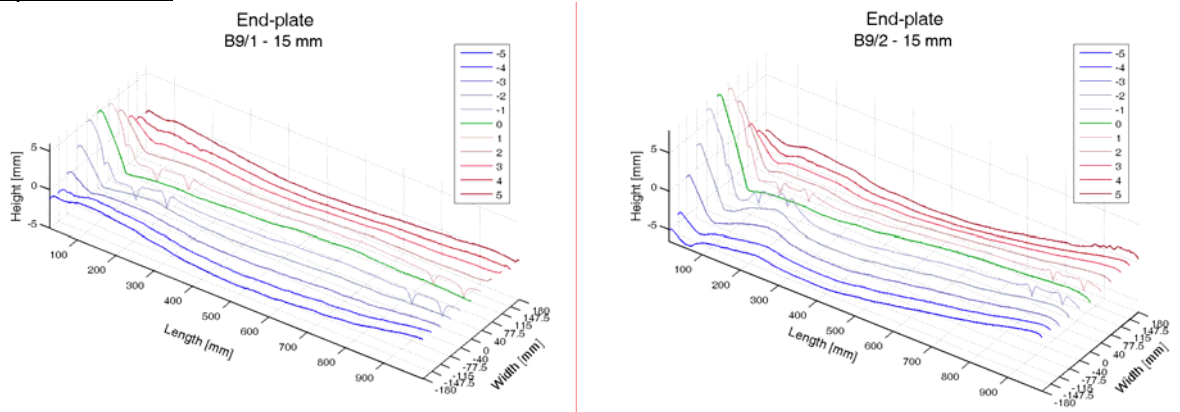


Fig. D26 Deformed end-plate contour-lines.

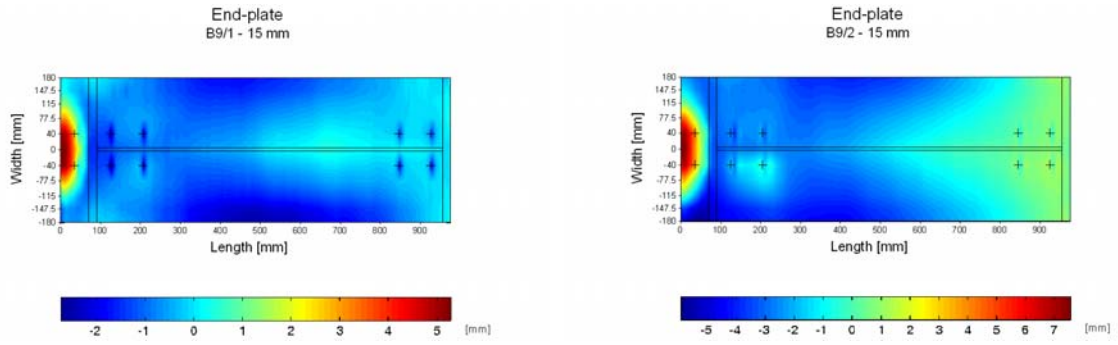


Fig. D27 D The shapes of the deformed end-plates.

Test specimen TB13

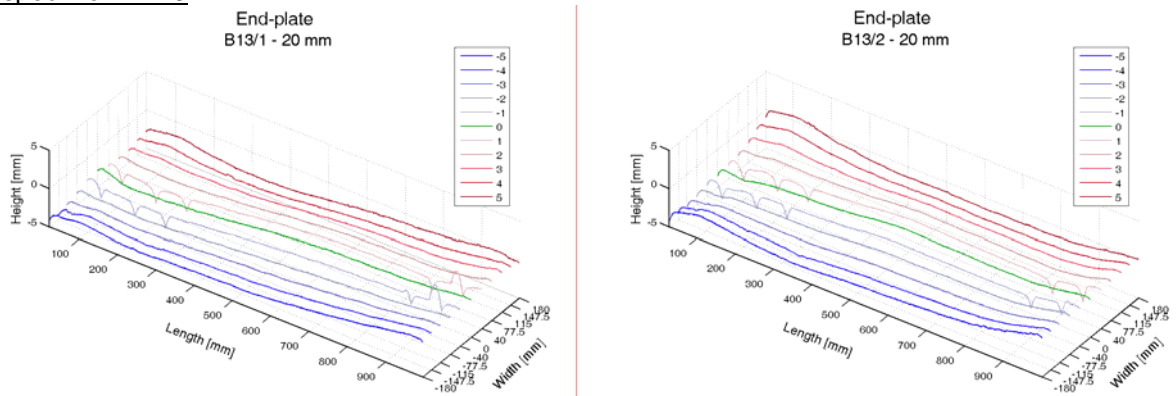


Fig. D28 Deformed end-plate contour-lines.

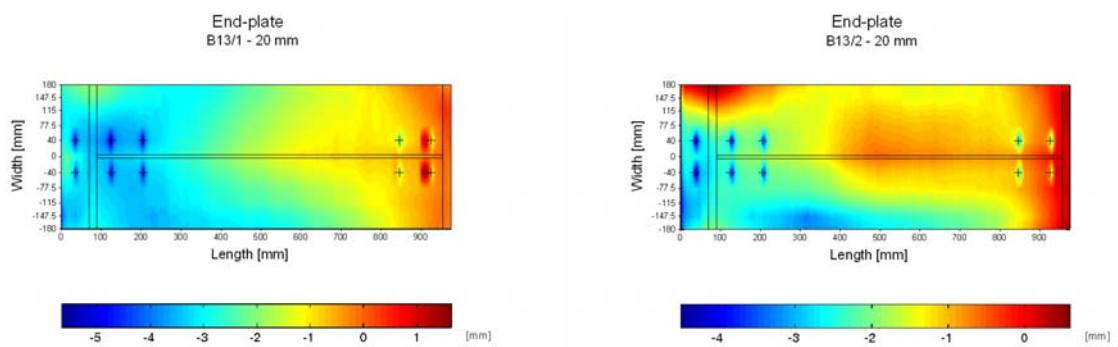


Fig. D29 The shapes of the deformed end-plates.

Test series II

The shape of the end-plates was measured before and after the tests. For all end-plates, the zero altitude level was chosen in the line of the web, on the border with the end-plate, i.e. right below the compression flange.

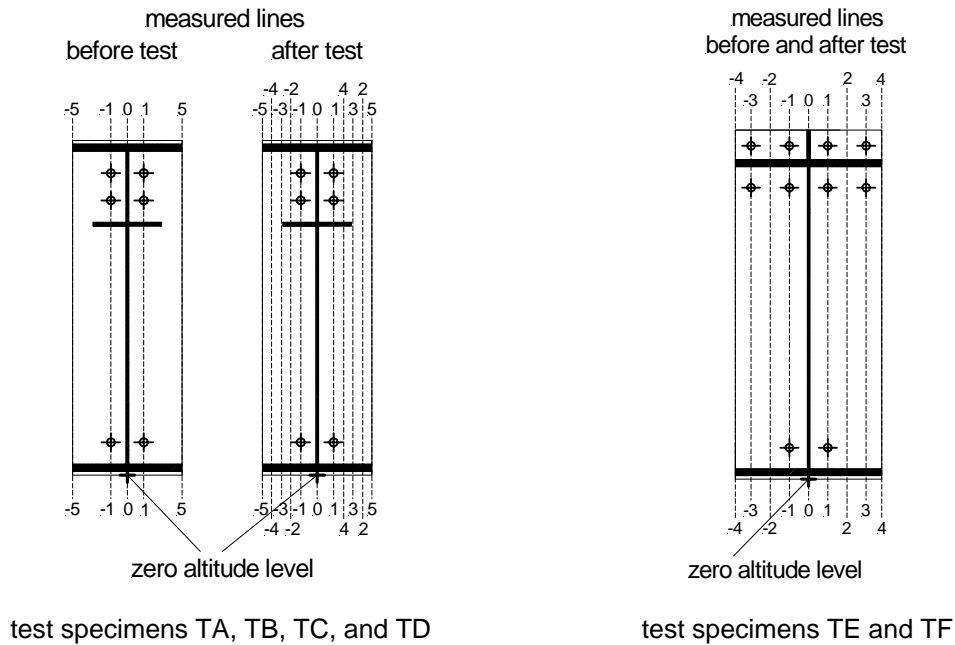


Fig. D30 Measured lines and identification on the diagrams.

Figure D30 shows the positions of the measured contour-lines and the identification for the following contour-lines diagrams. The contour-lines were measured over the web, at the end-plate border, in the axis of the bolts and at uniform distances in-between.

Test specimen TA

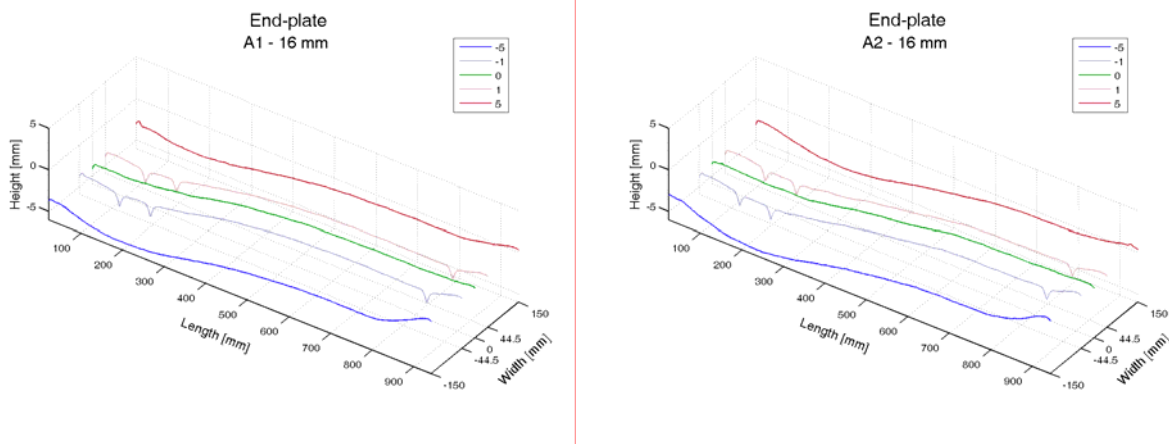


Fig. D31 Deformed end-plate contour-lines before test.

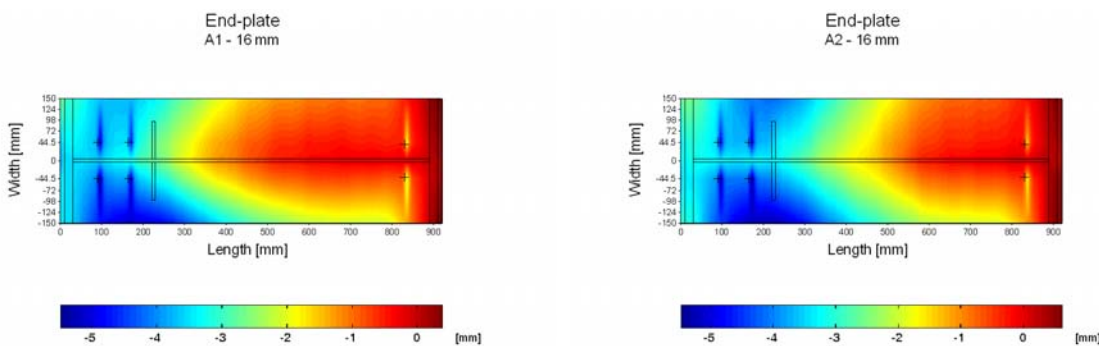


Fig. D32 The shapes of the end-plates before test.

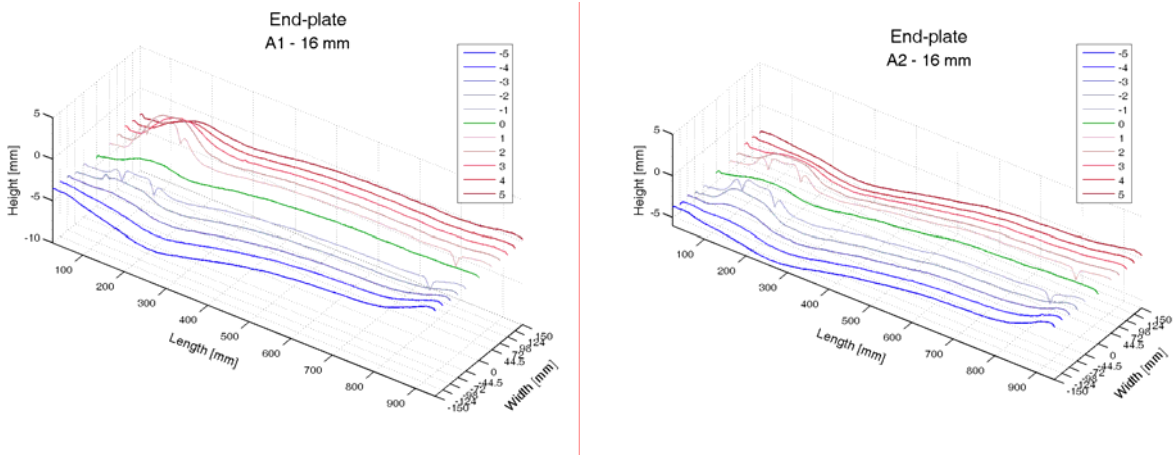


Fig. D33 Deformed end-plate contour-lines after test.

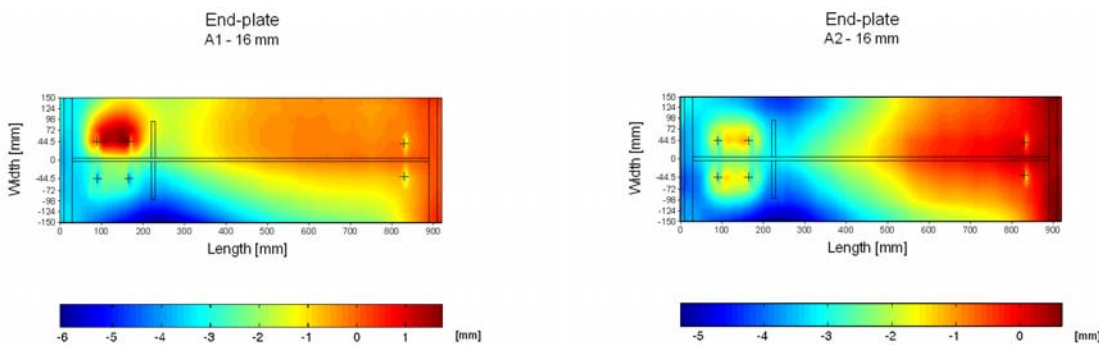
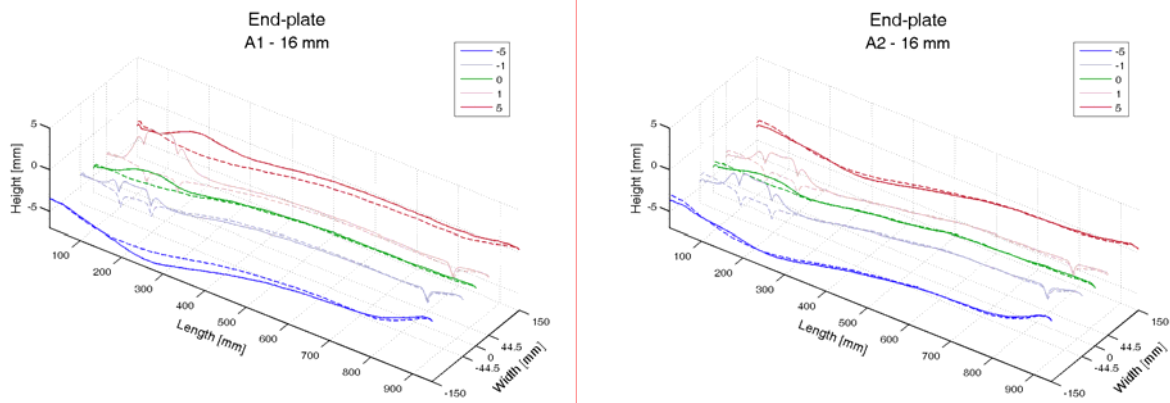


Fig. D34 The shapes of the deformed end-plates after test.



*The short dashed contour-lines were measured on the end-plate before the test, the solid lines after.

Fig. D35 Contour-lines before and after the test.

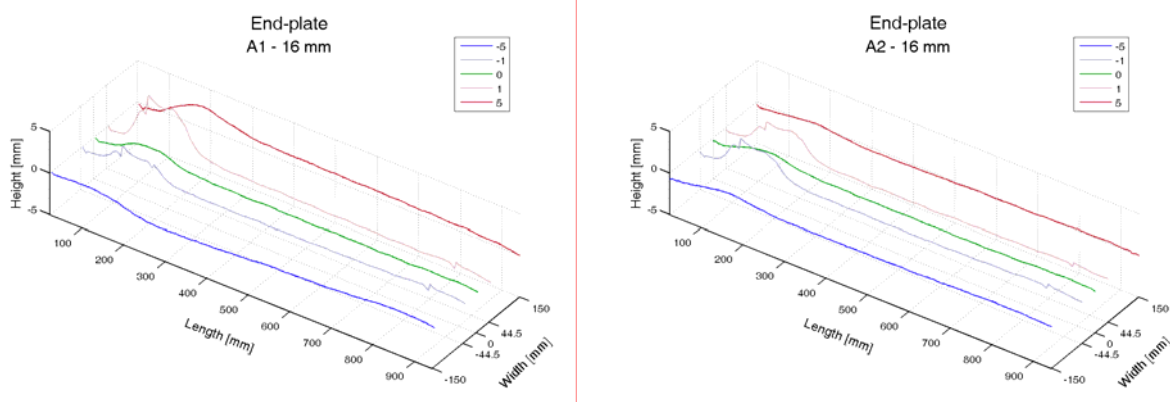


Fig. D36 Difference between the contour-lines as measured before and after test.

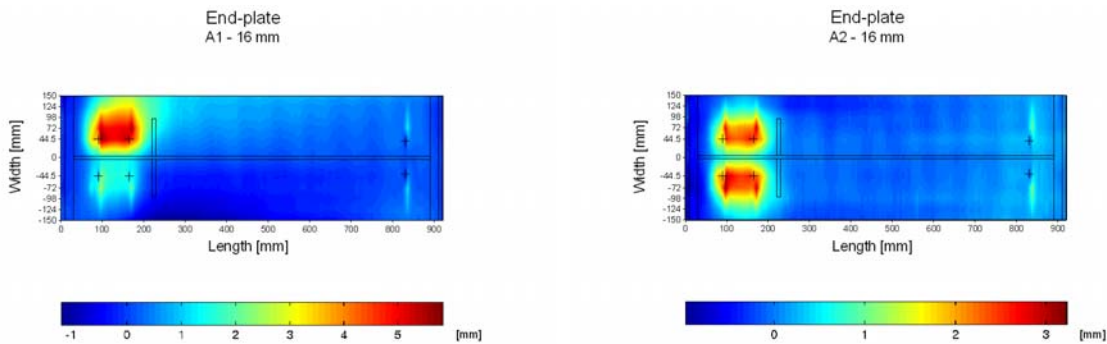


Fig. D37 Difference between the shapes as measured before and after test.

Test specimen TB

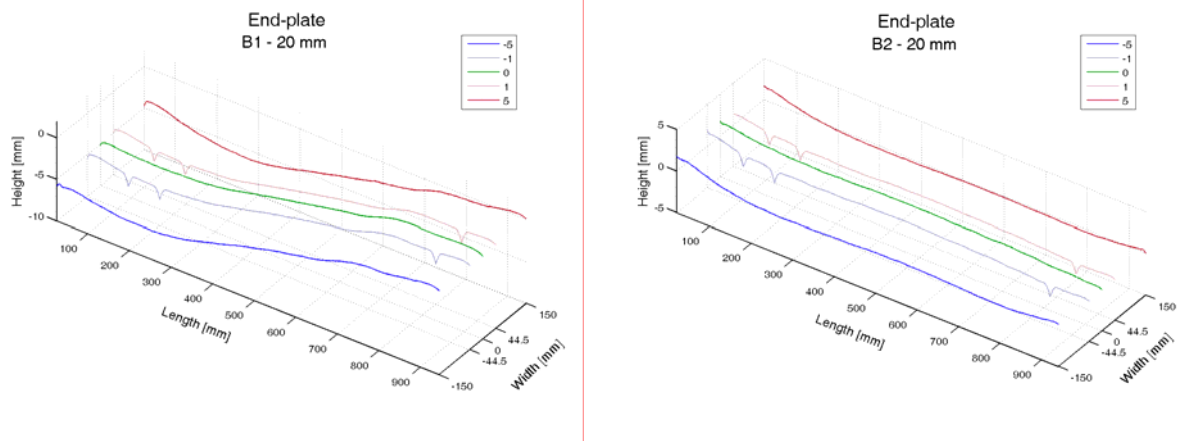


Fig. D38 Deformed end-plate contour-lines before test.

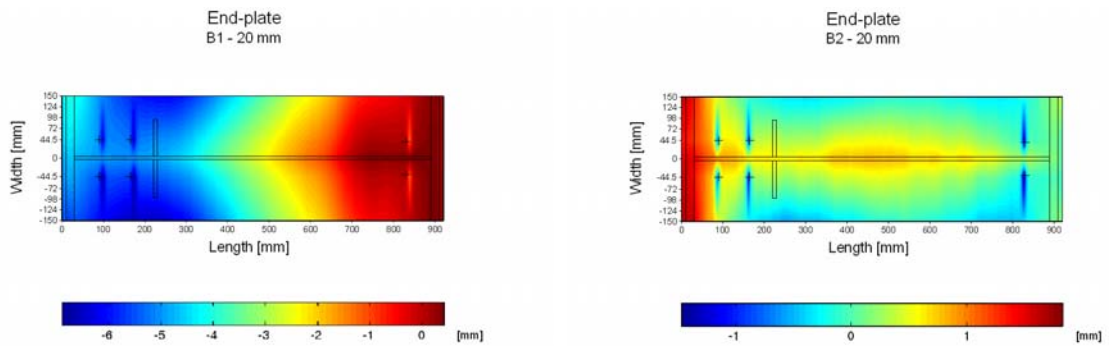


Fig. D39 The shapes of the end-plates before test.

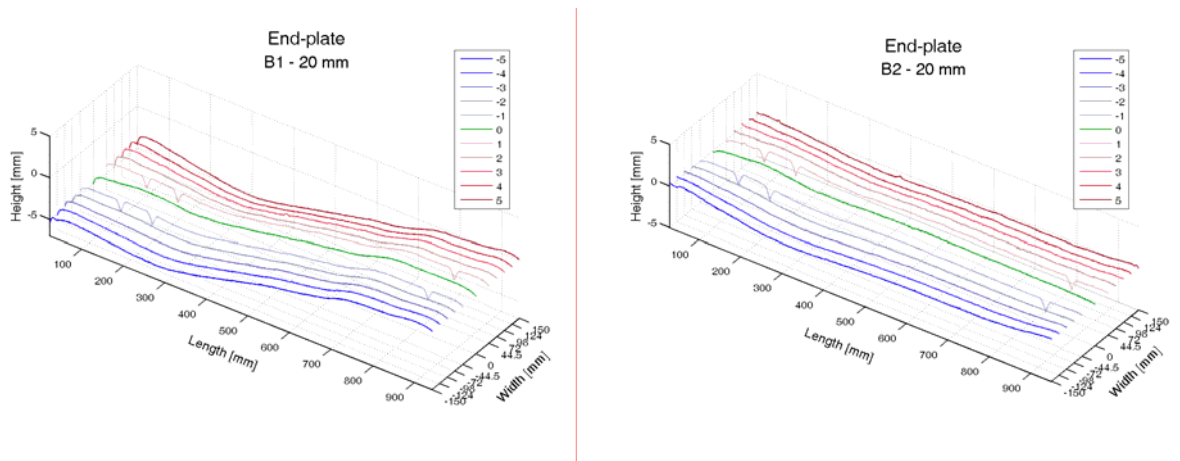


Fig. D40 Deformed end-plate contour-lines after test.

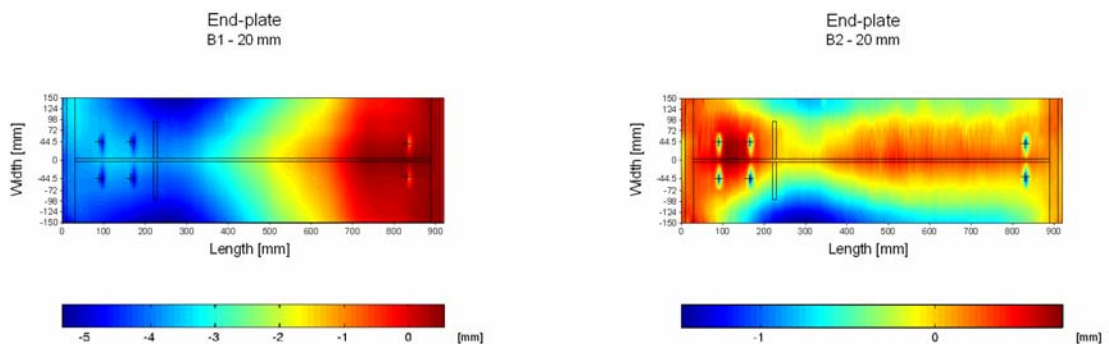


Fig. D41 The shapes of the deformed end-plates after test.

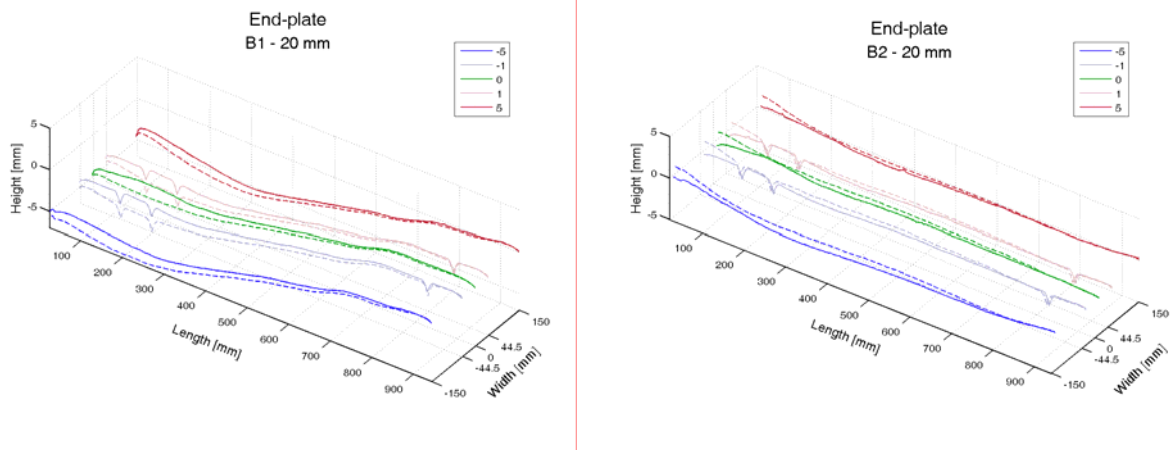


Fig. D42 Contour-lines before and after the test.

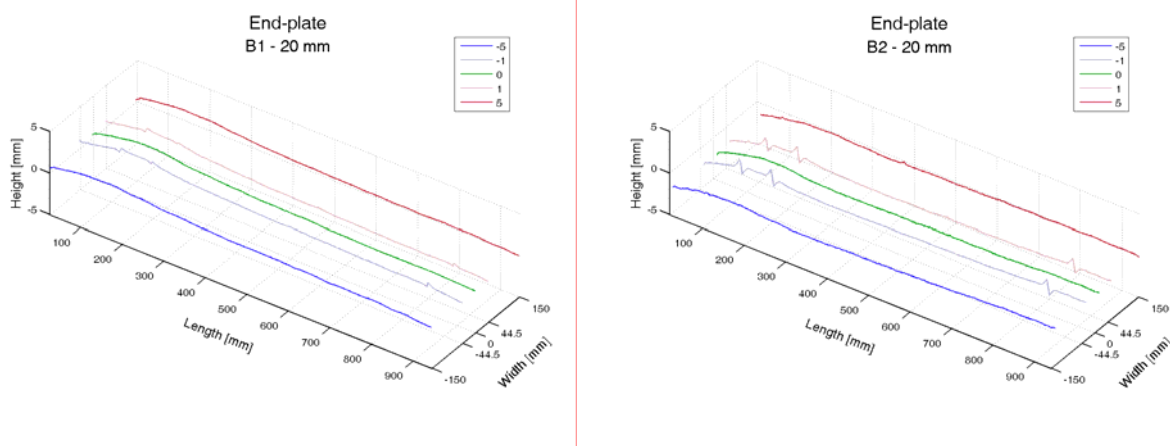


Fig. D43 Difference between the contour-lines as measured before and after test.

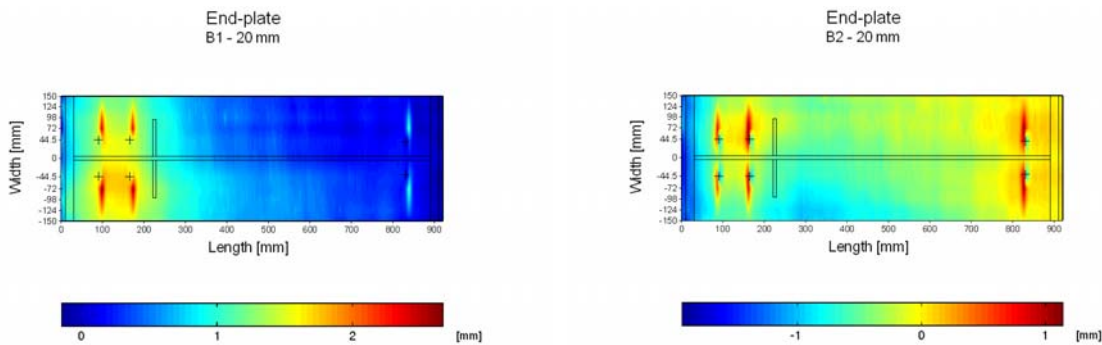


Fig. D44 Difference between the shapes as measured before and after test.

Test specimen TC

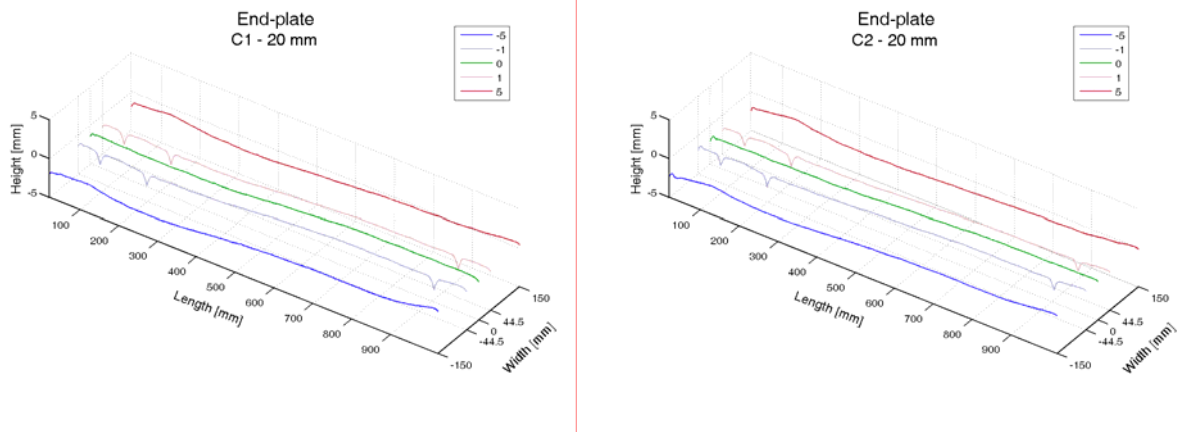


Fig. D45 Deformed end-plate contour-lines before test.

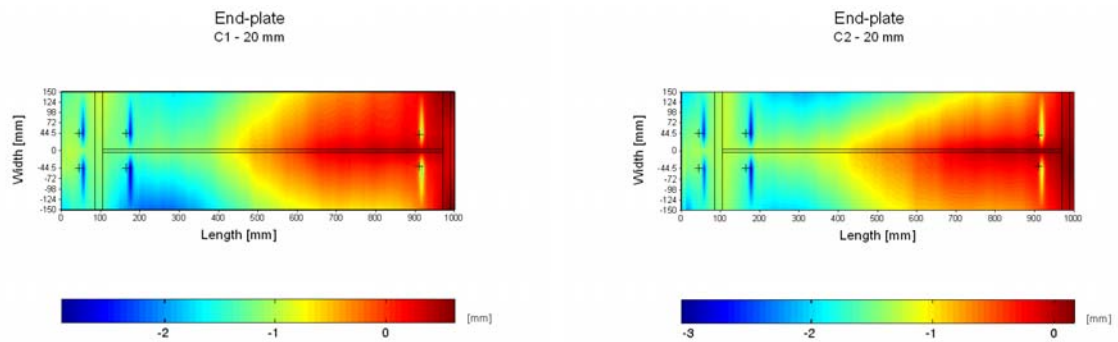


Fig. D46 The shapes of the end-plates before test.

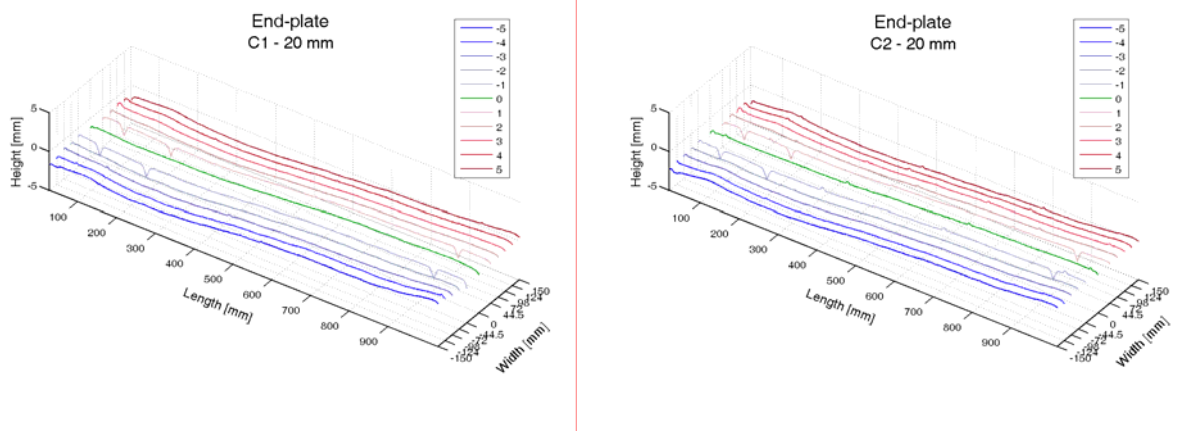


Fig. D47 Deformed end-plate contour-lines after test.

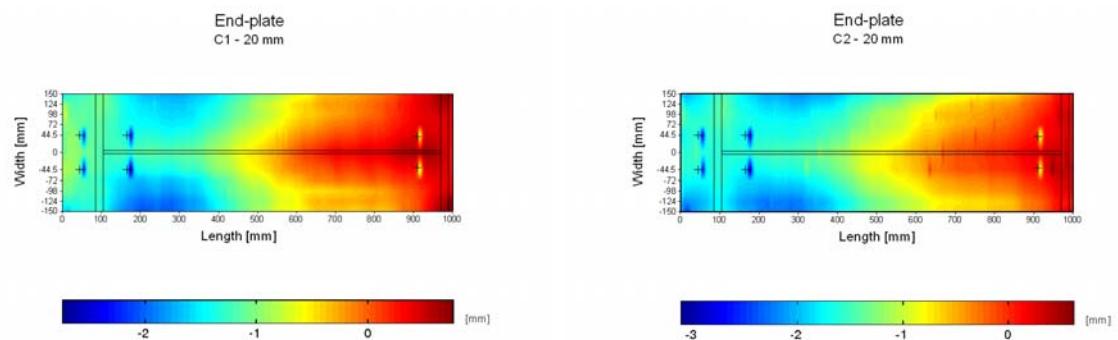


Fig. D48 The shapes of the deformed end-plates after test.

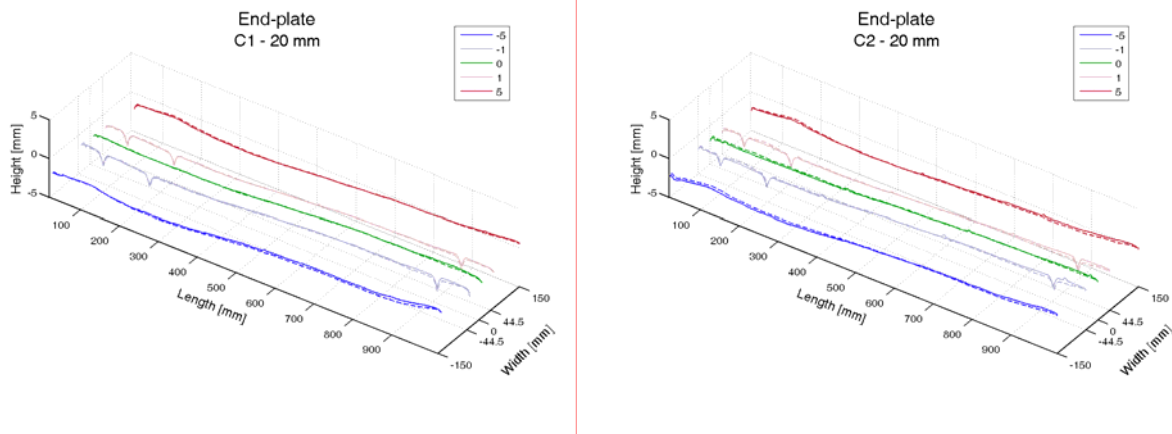


Fig. D49 Contour-lines before and after the test.

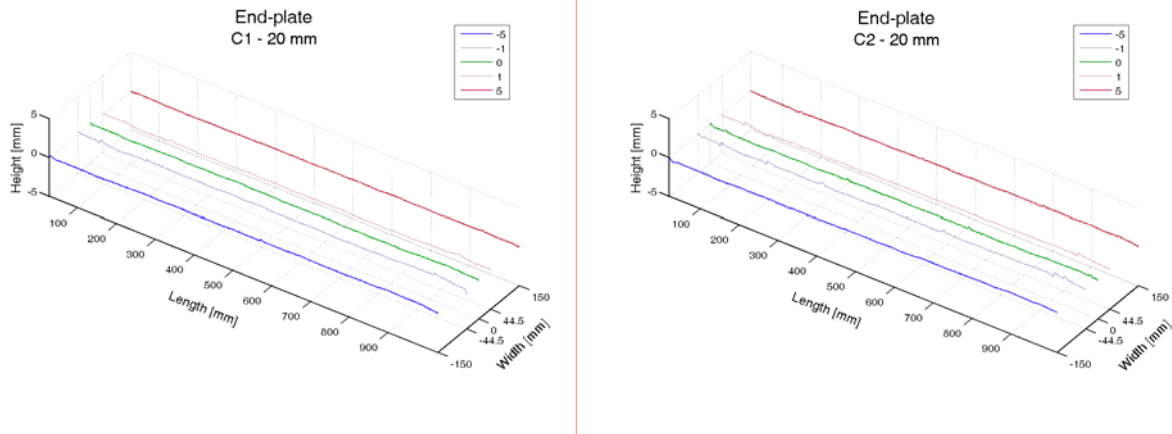


Fig. D50 Difference between the contour-lines as measured before and after test.

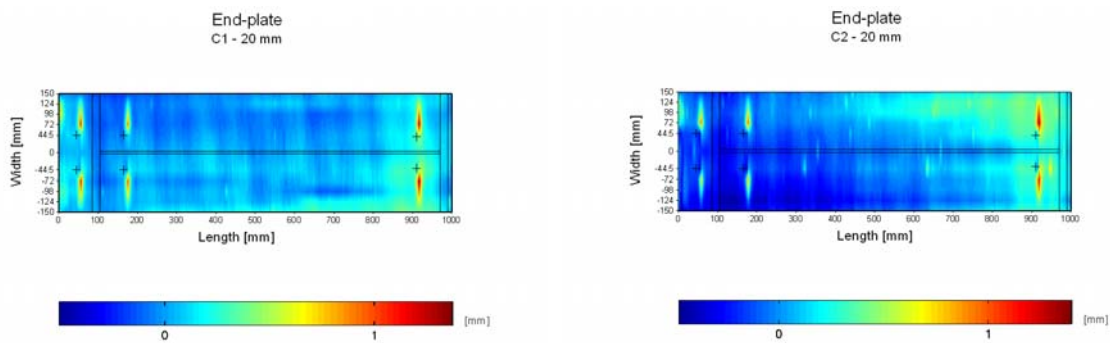


Fig. D51 Difference between the shapes as measured before and after test.

Test specimen TD

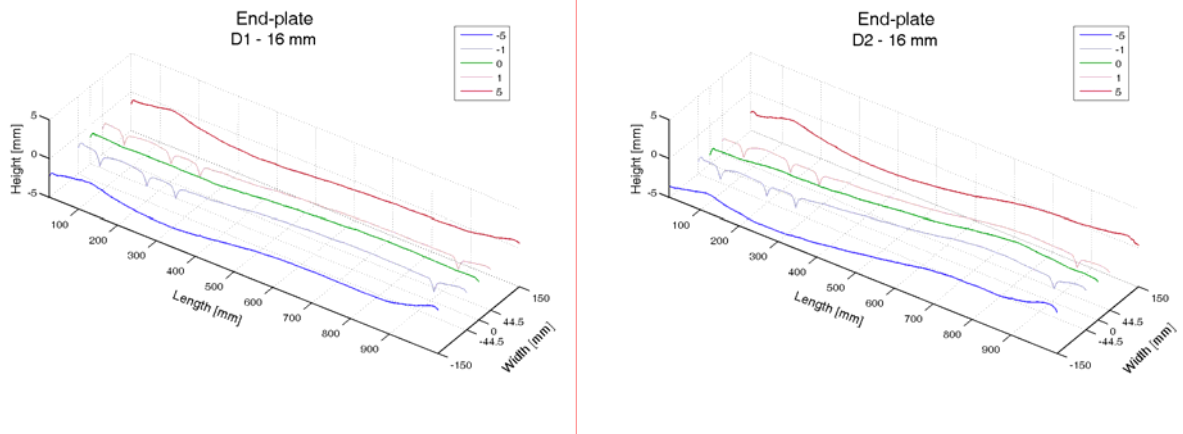


Fig. D52 Deformed end-plate contour-lines before test.

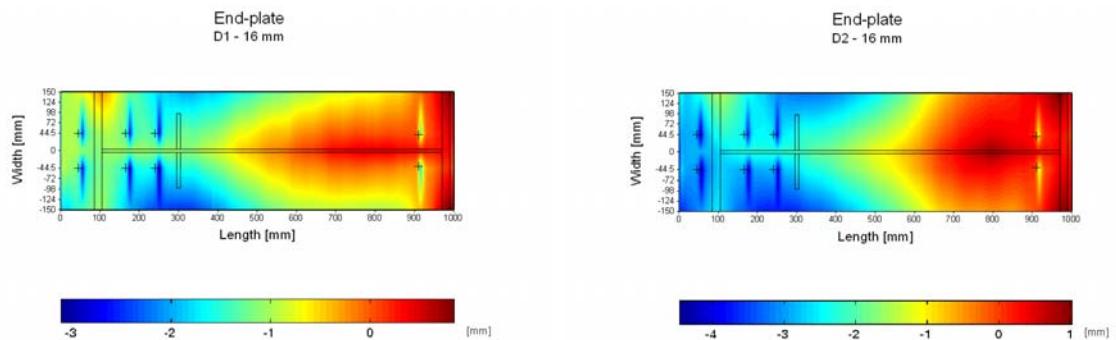


Fig. D53 The shapes of the end-plates before test.

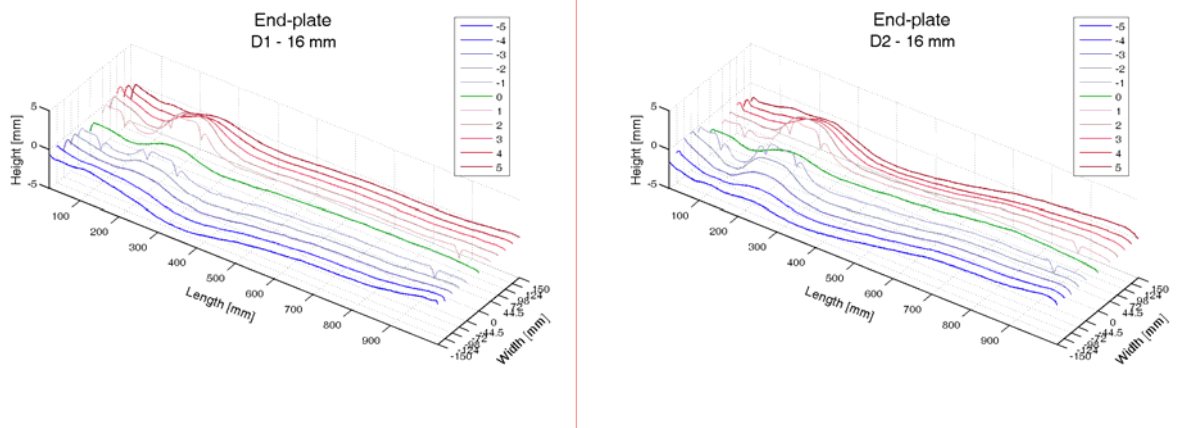


Fig. D54 Deformed end-plate contour-lines after test.

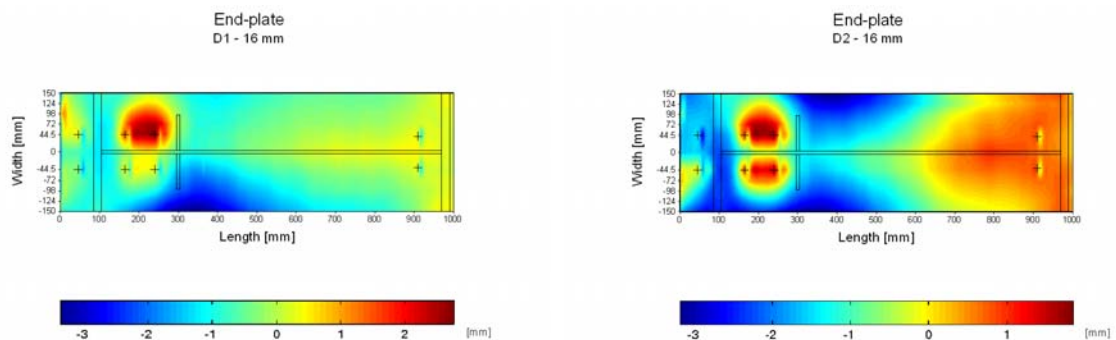


Fig. D55 The shape of the deformed end-plate after test.

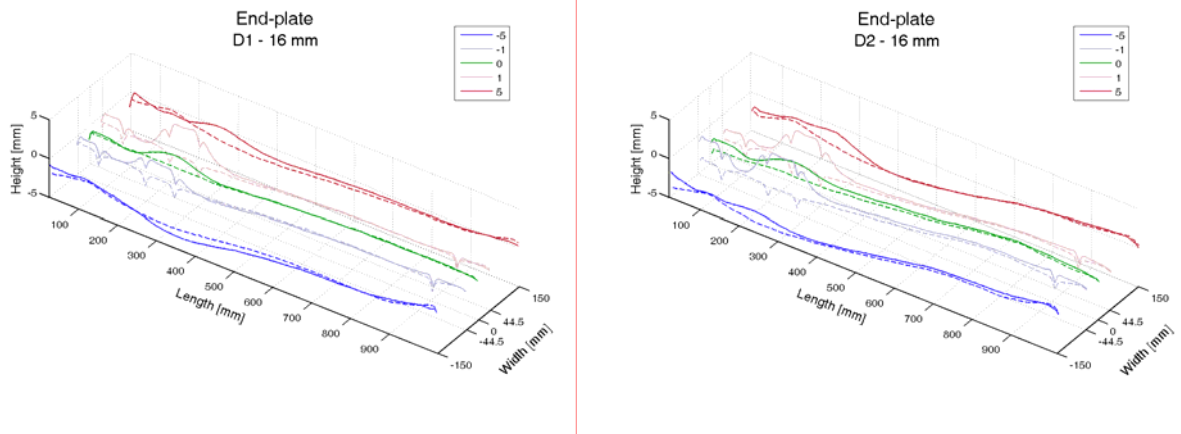


Fig. D56 Contour-lines before and after the test.

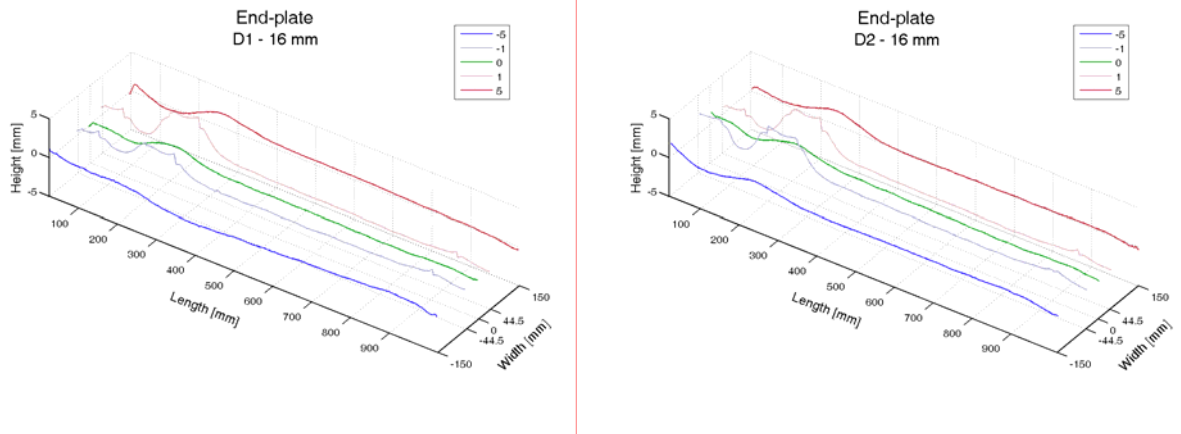


Fig. D57 Difference between the contour-lines as measured before and after test.

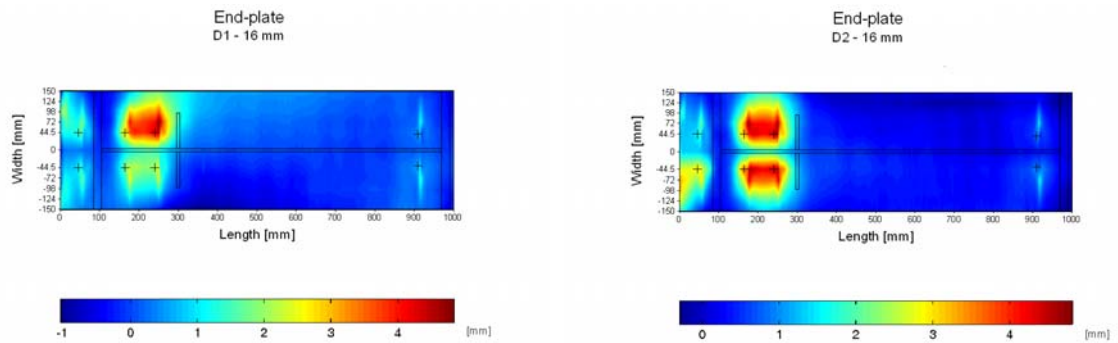


Fig. D58 Difference between the shapes as measured before and after test.

Test specimen TE

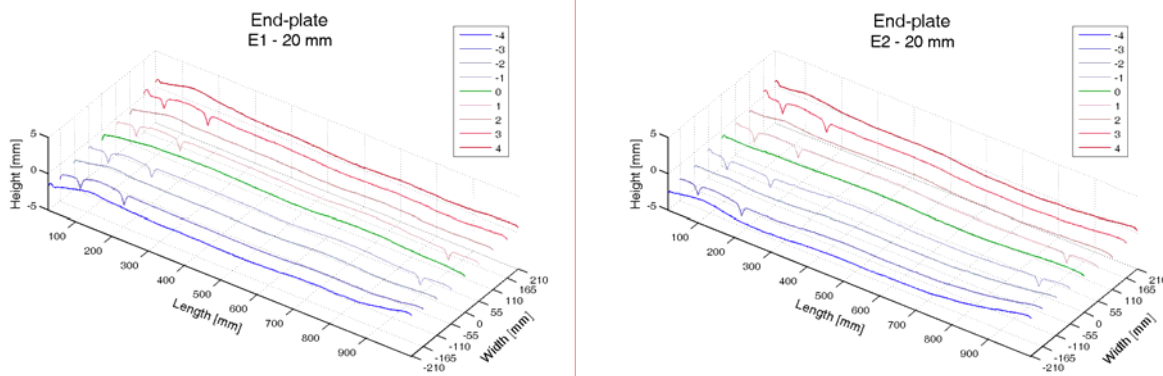


Fig. D59 Deformed end-plate contour-lines before test.

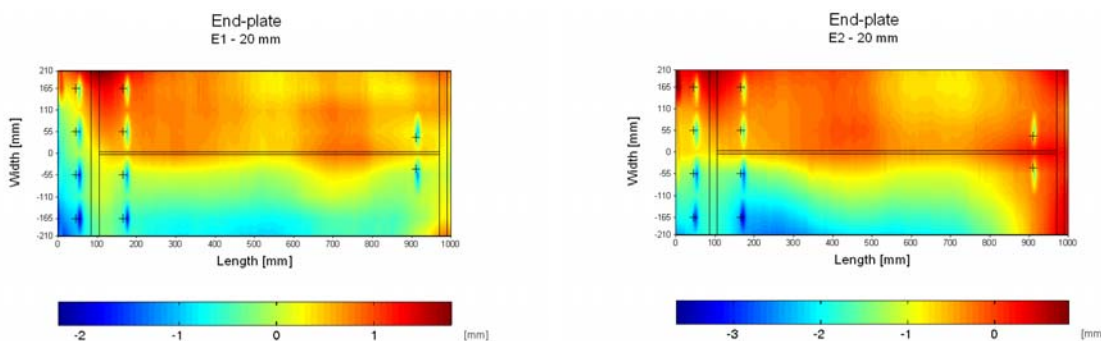


Fig. D60 The shapes of the end-plates before test.

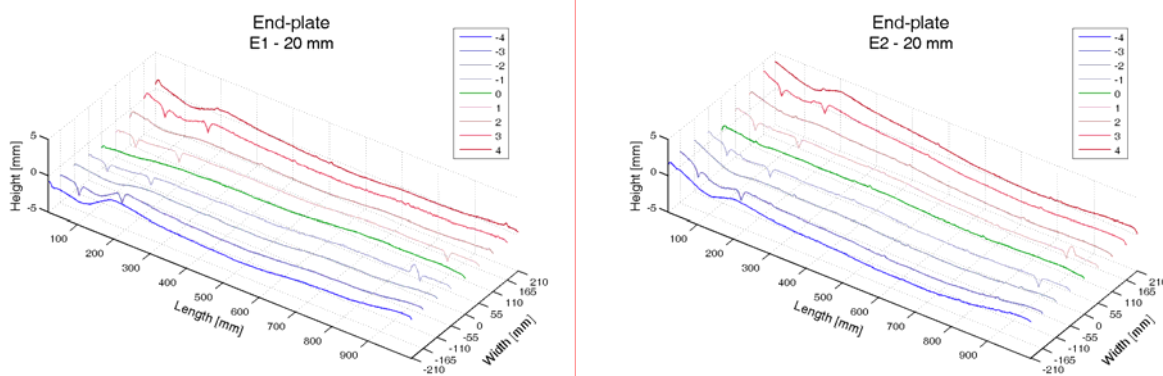


Fig. D61 Deformed end-plate contour-lines after test.

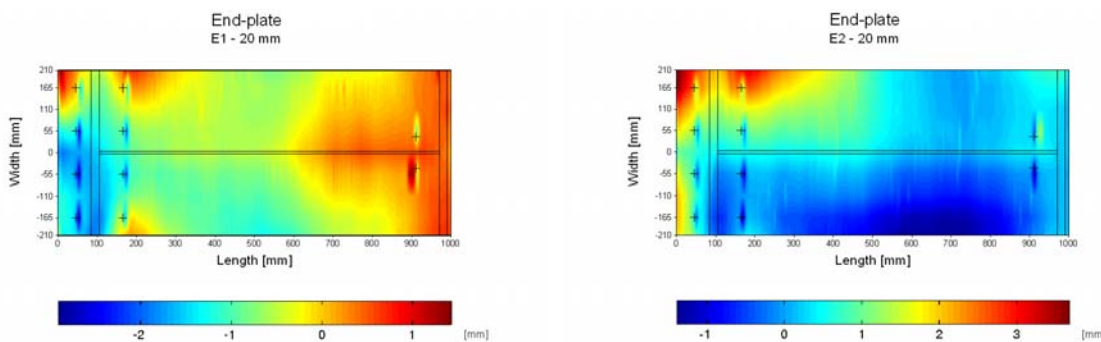


Fig. D62 The shapes of the deformed end-plates after test.

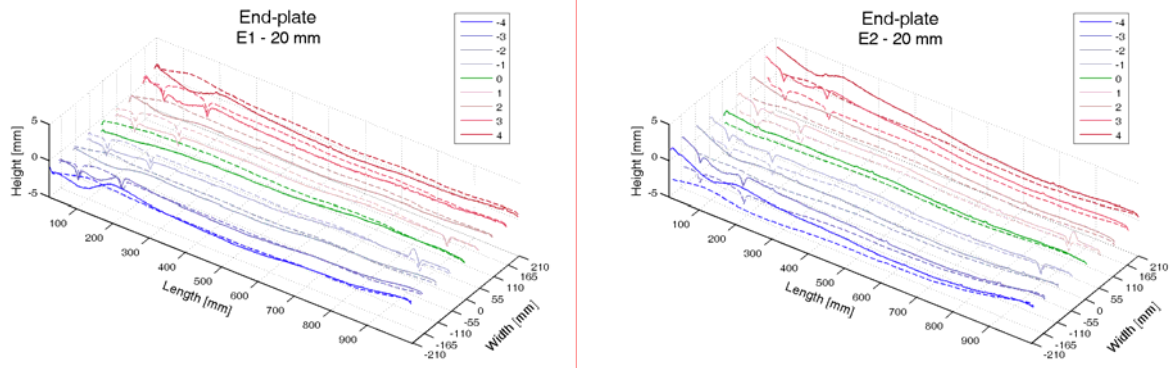


Fig. D63 Contour-lines before and after the test.

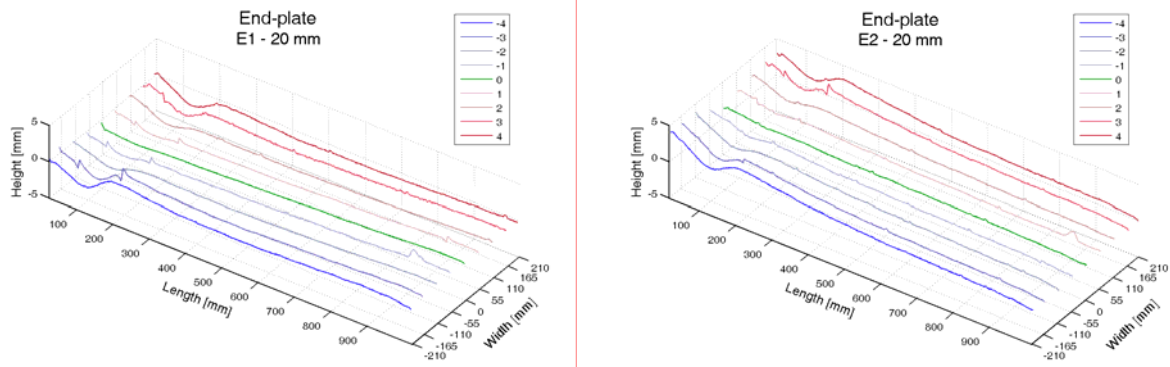


Fig. D64 Difference contour-lines between the measured lines before and after test.

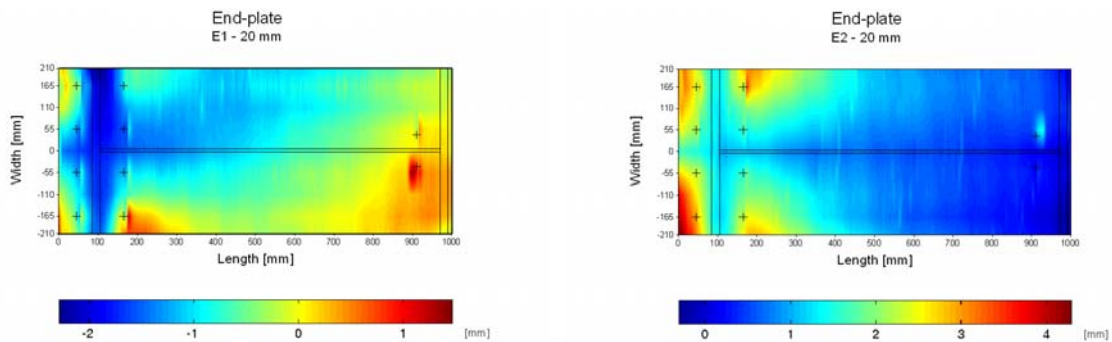


Fig. D65 Difference between the shapes as measured before and after test.

Test specimen TF

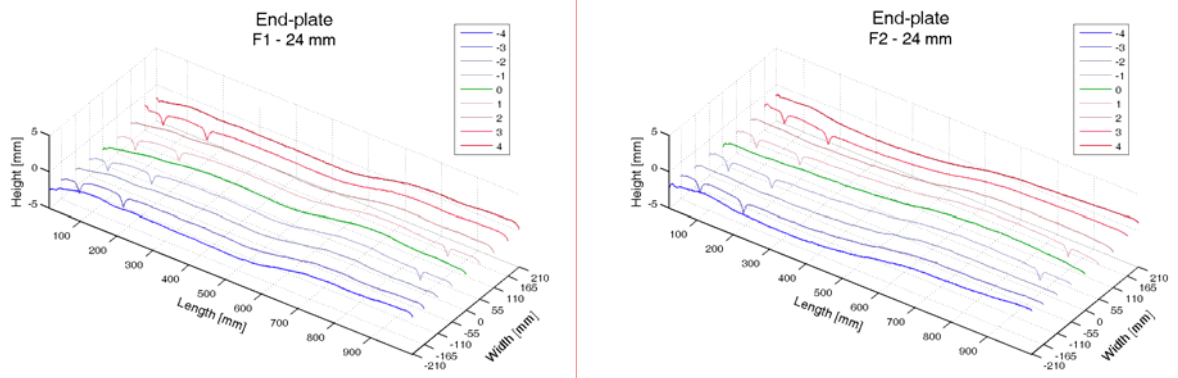


Fig. D66 Deformed end-plate contour-lines before test.

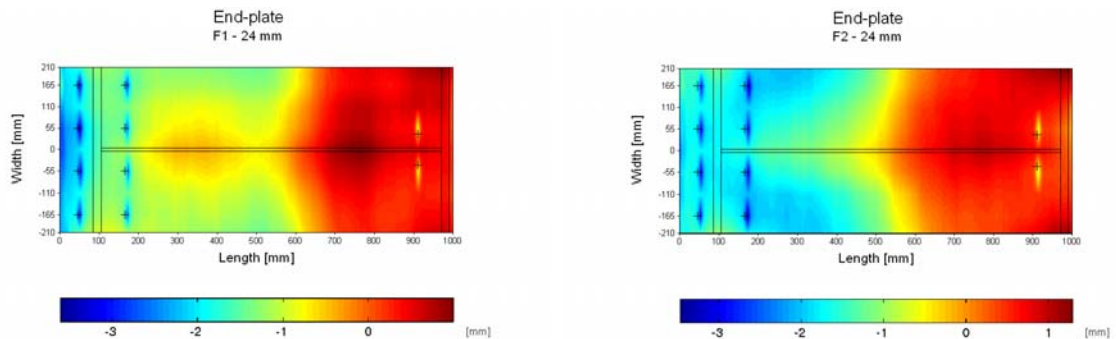


Fig. D67 The shapes of the end-plates before test.

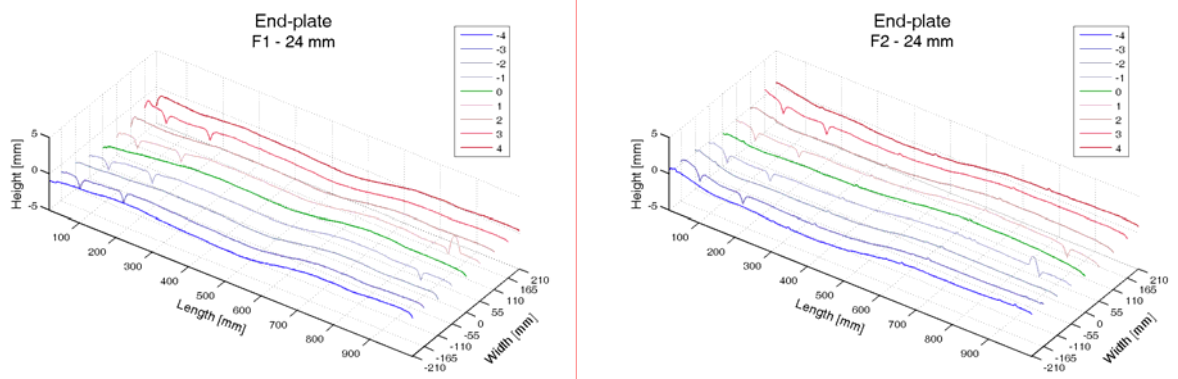


Fig. D68 Deformed end-plate contour-lines after test.

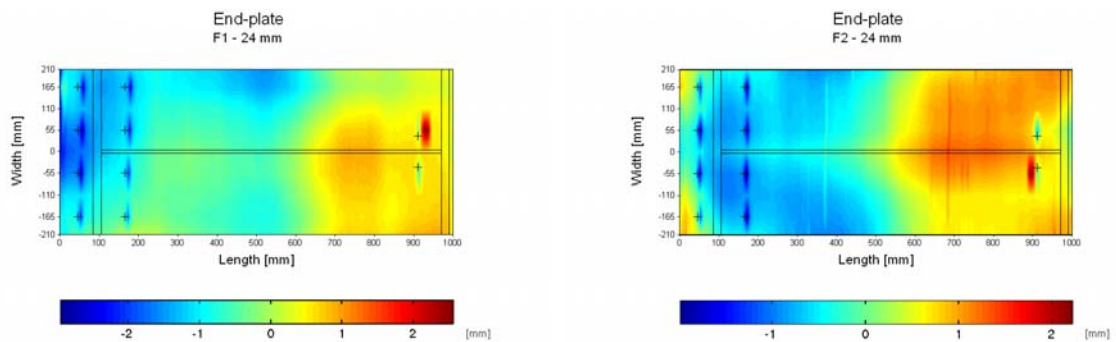


Fig. D69 The shapes of the deformed end-plates after test.

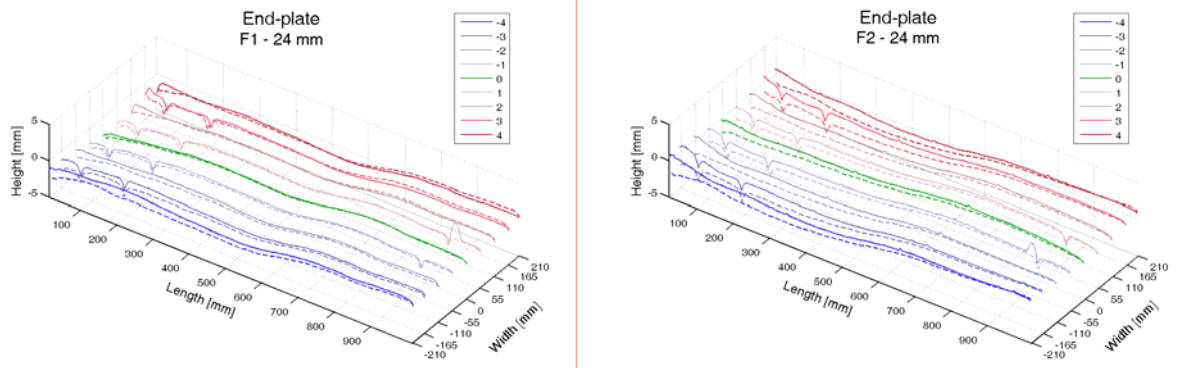


Fig. D70 Contour-lines before and after the test.

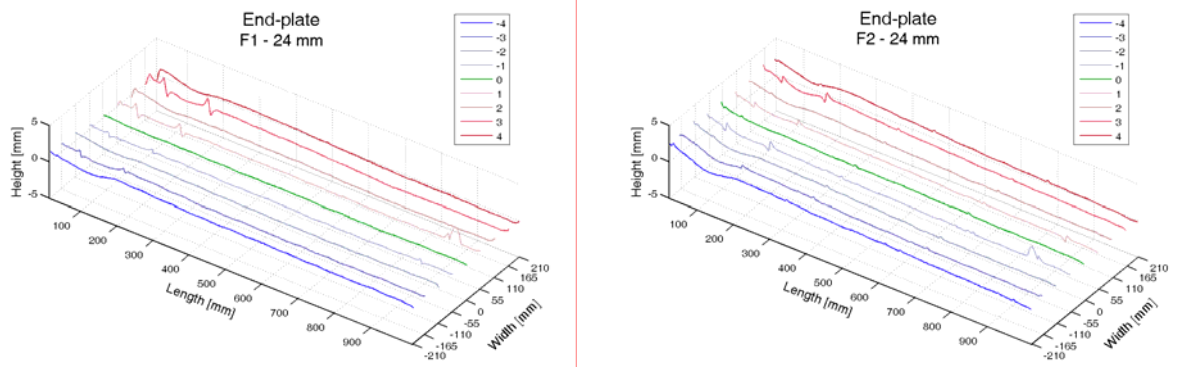


Fig. D71 Difference between the contour-lines as measured before and after test.

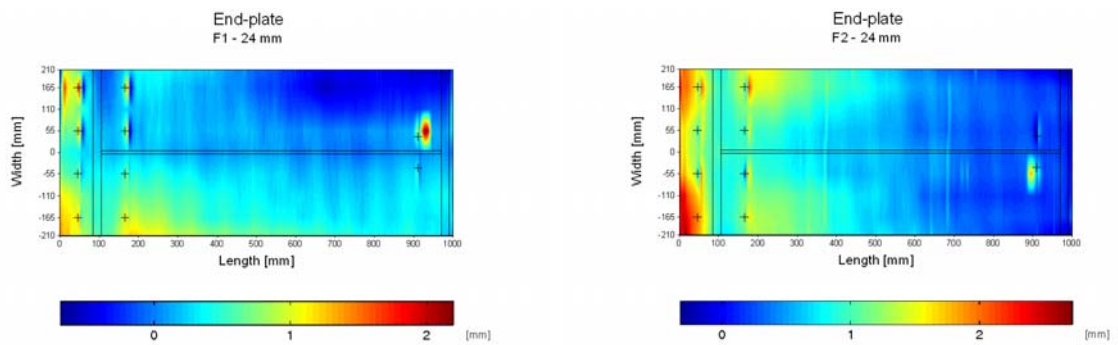


Fig. D72 Difference between the shapes as measured before and after test.

Load cell calibrations

The load cells were calibrated before test series I. The calibration load was 250 kN. The theoretical load capacity of the studied bolts (M20, 8.8) was $245 \times 800 = 196$ kN.

After test series I and before test series II the load cells were re-calibrated with a load of 300 kN. The theoretical load capacity of the studied bolts (M20, 10.9) was $245 \times 1,000 = 245$ kN.



Fig. E1 Used load cells.



Fig. E2 Load cell Nr. 14.



Fig. E3 Parts of a load cell (nut, measurement part, stovepipe).



Fig. E4 Halfbridge in the load cell.

In each load cell 4 strain gauges were arranged in the form of a halfbridge, which measures the strains. From the measured strains the stress and the load were calculated.

The following diagrams show the calibration curve of the used cells. The load and the output data from the cell were measured in mV/V. The diagrams show the measured data and the regression curve (regression line), which was used to convert the measured data to loads.

The calculated regression lines demonstrate that the used load cells have good elastic behaviour in the applied load-range.

The use of the load cells slightly modifies the bolt load distribution, because the application of the cells enlarges the elongation lengths of the bolts. This effect modifies the stiffness of the joint to a small extent and has minimal effect on the measured bolt-loads.

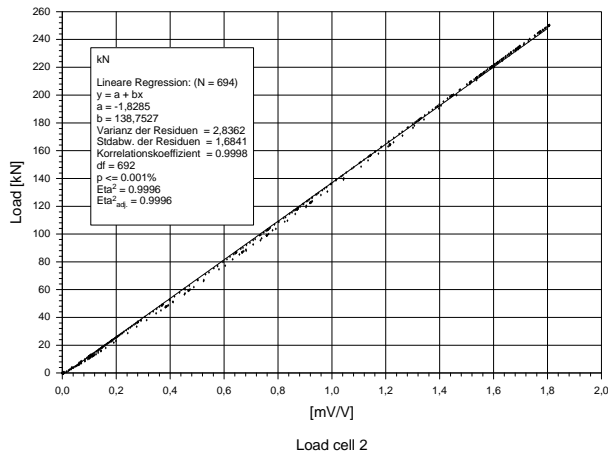


Fig. E5 Calibration curve of load cell 2.

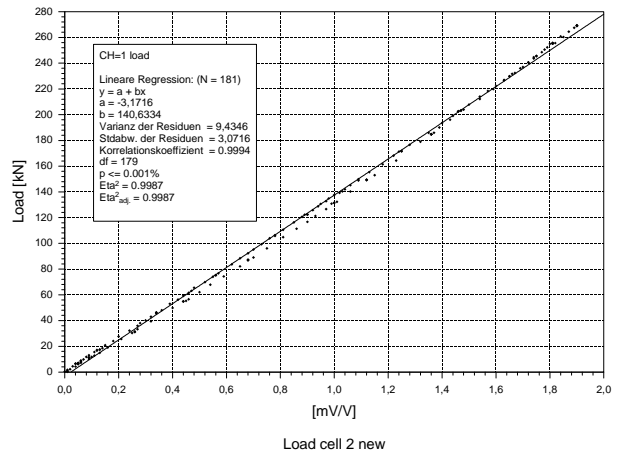


Fig. E6 Re-calibration curve of load cell 2.

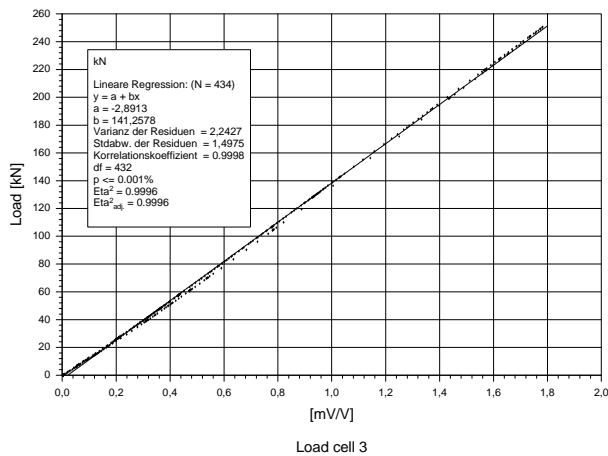


Fig. E7 Calibration curve of load cell 3.

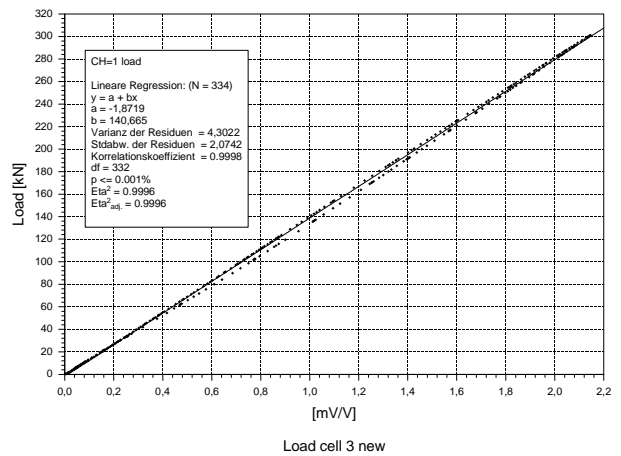


Fig. E8 Re-calibration curve of load cell 3.

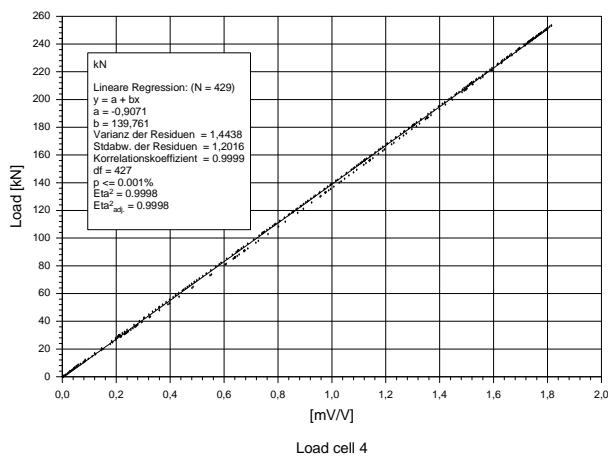


Fig. E9 Calibration curve of load cell 4.

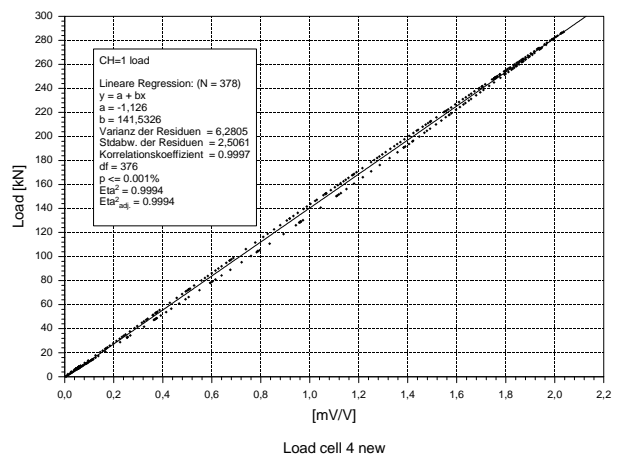


Fig. E10 Re-calibration curve of load cell 4.

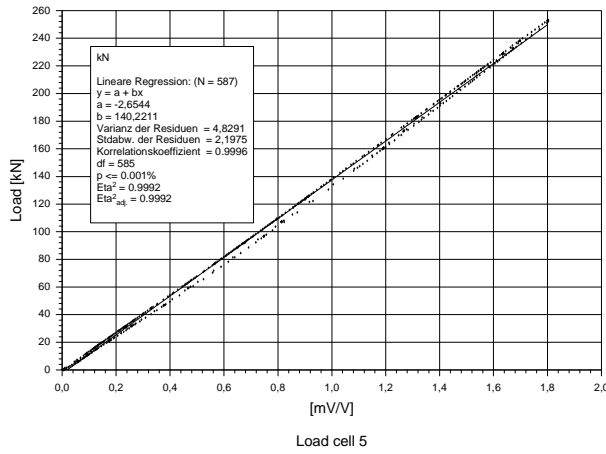


Fig. E11 Calibration curve of load cell 5.

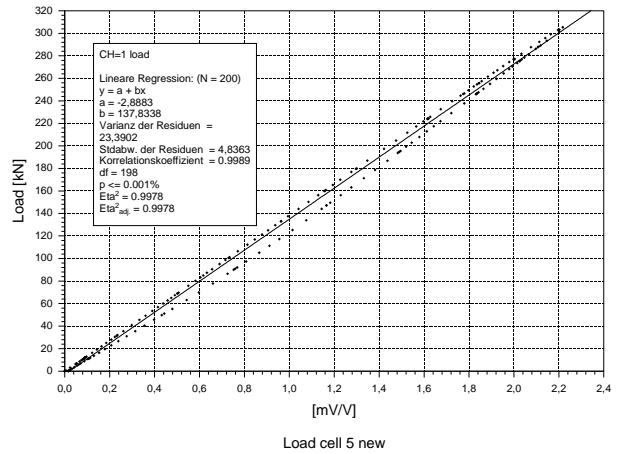


Fig. E12 Re-calibration curve of load cell 5.

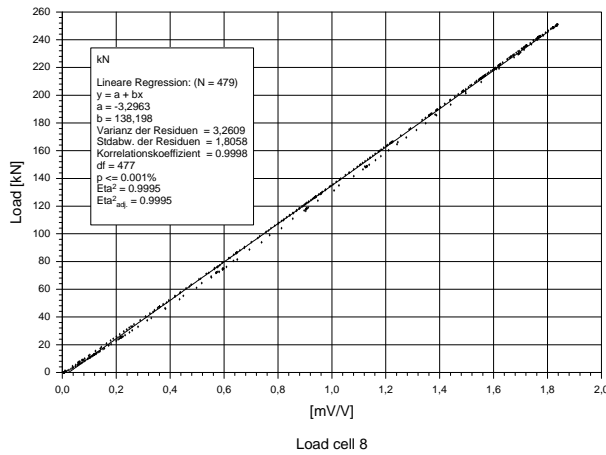


Fig. E13 Calibration curve of load cell 8.

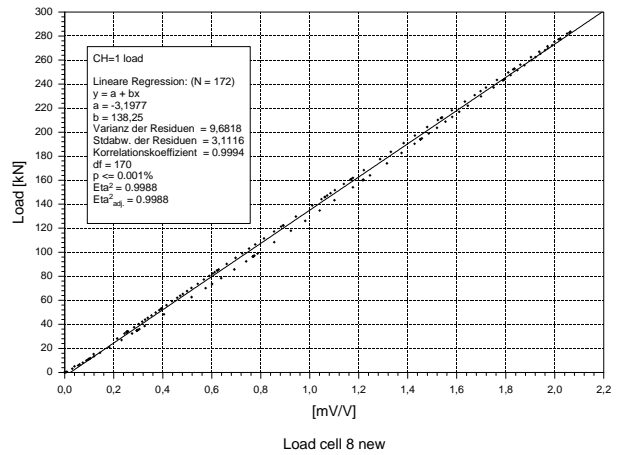


Fig. E14 Re-calibration curve of load cell 8.

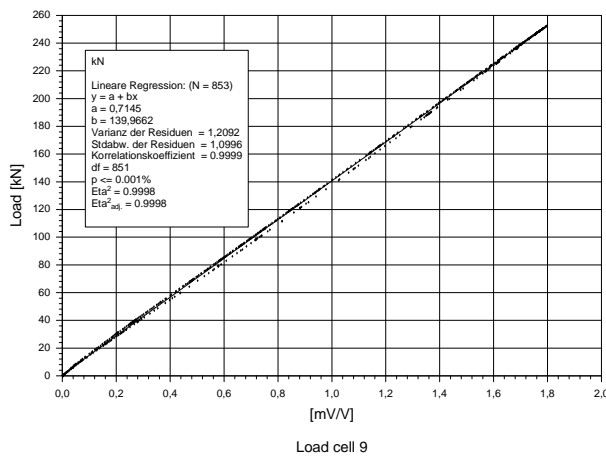


Fig. E15 Calibration curve of load cell 9.

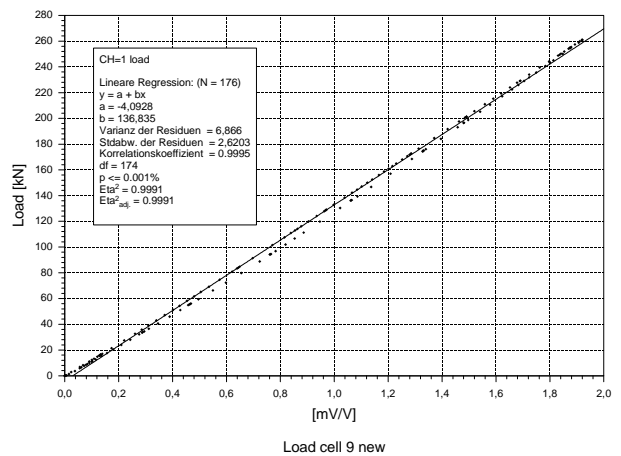


Fig. E16 Re-calibration curve of load cell 9.

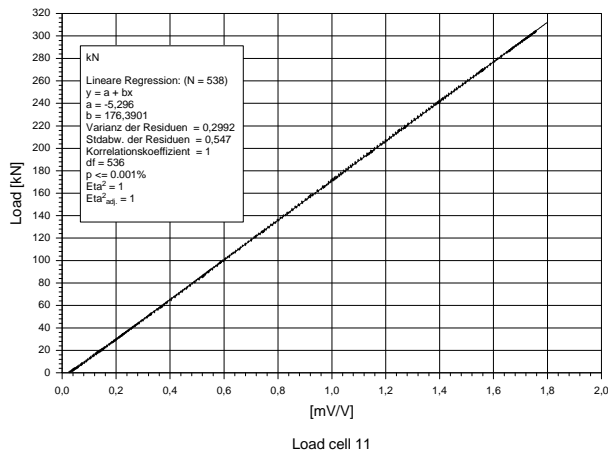


Fig. E17 Calibration curve of load cell 11.

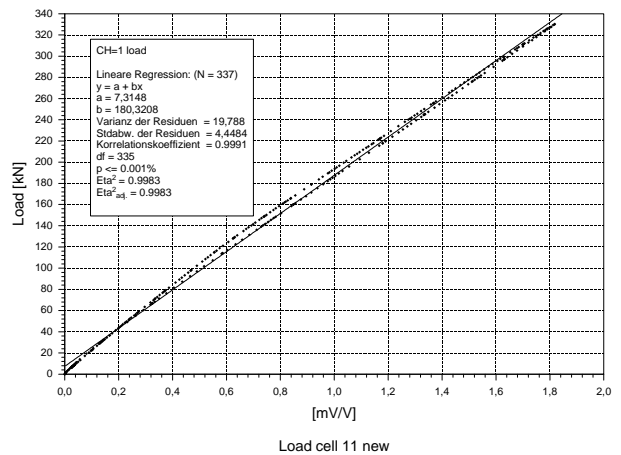


Fig. E18 Re-calibration curve of load cell 11.

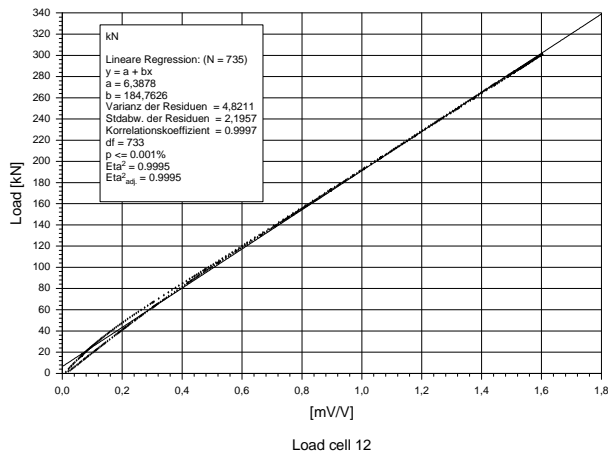


Fig. E19 Calibration curve of load cell 12.

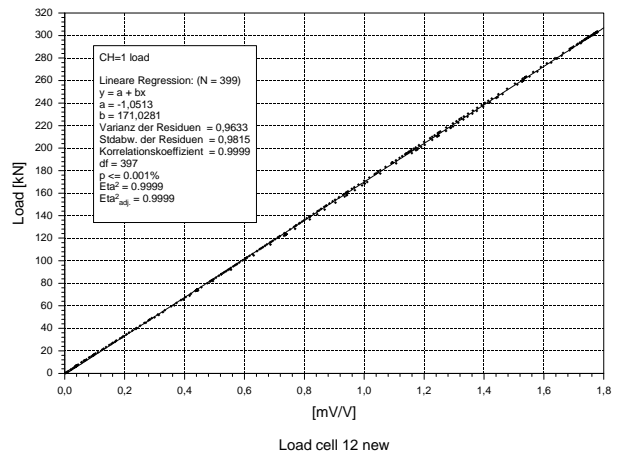


Fig. E20 Re-calibration curve of load cell 12.

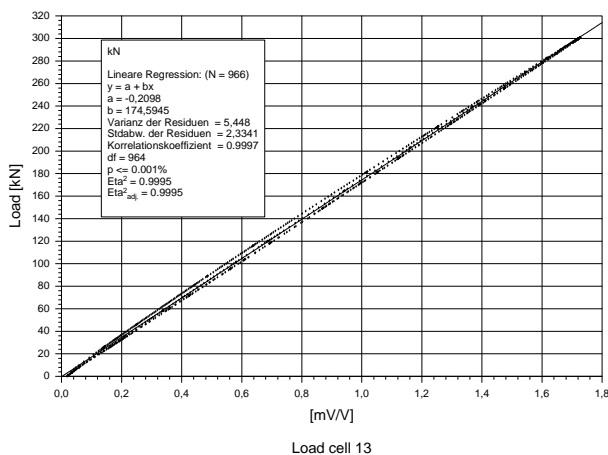


Fig. E21 Calibration curve of load cell 13.

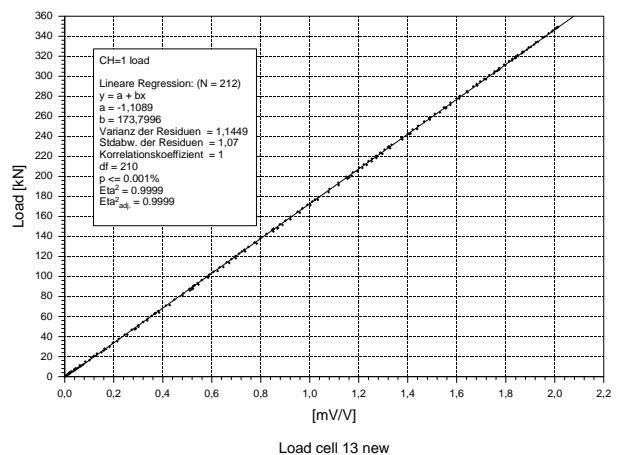


Fig. E22 Re-calibration curve of load cell 13.

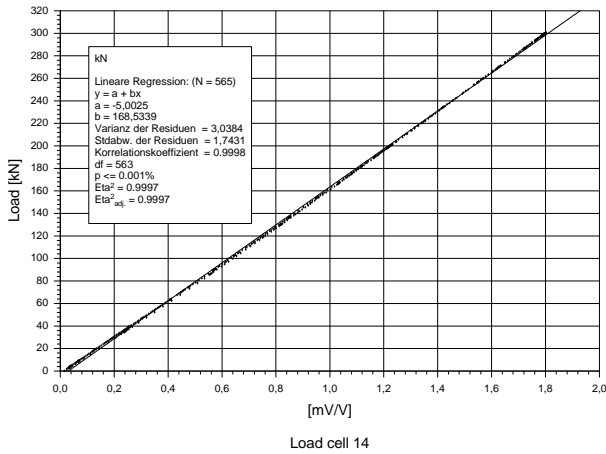


Fig. E23 Calibration curve of load cell 14.

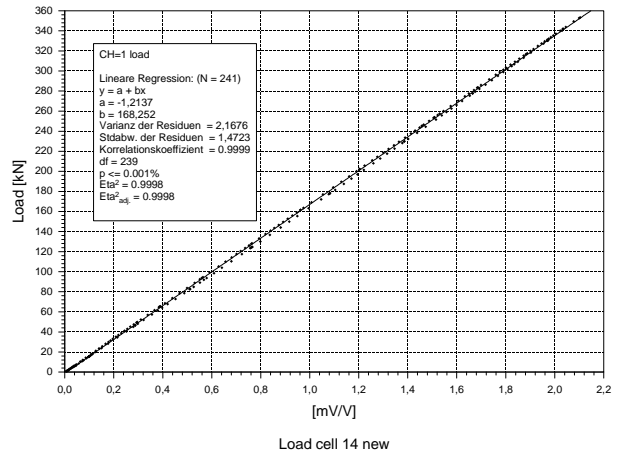


Fig. E24 Re-calibration curve of load cell 14.

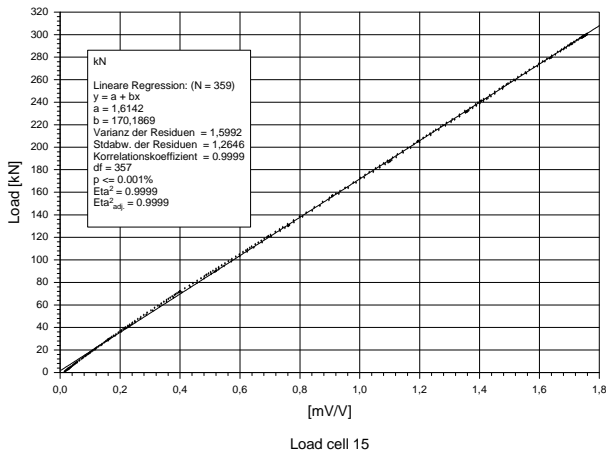


Fig. E25 Calibration curve of load cell 15.

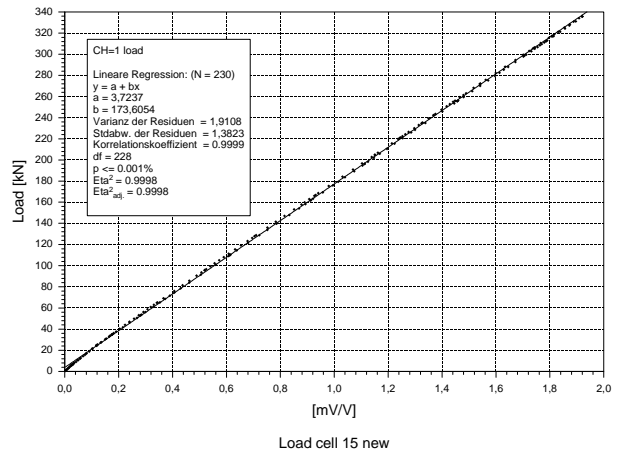


Fig. E26 Re-calibration curve of load cell 15.

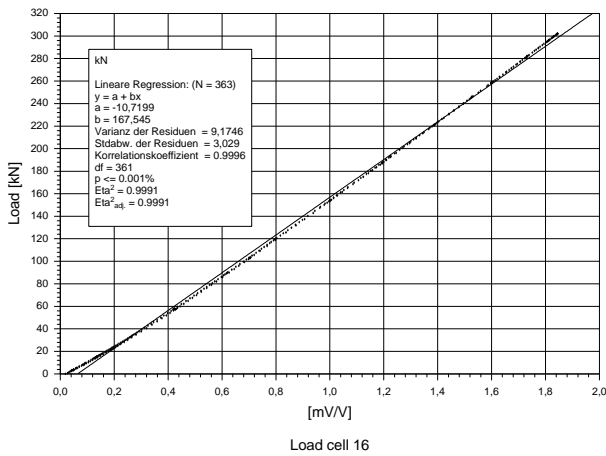


Fig. E27 Calibration curve of load cell 16.

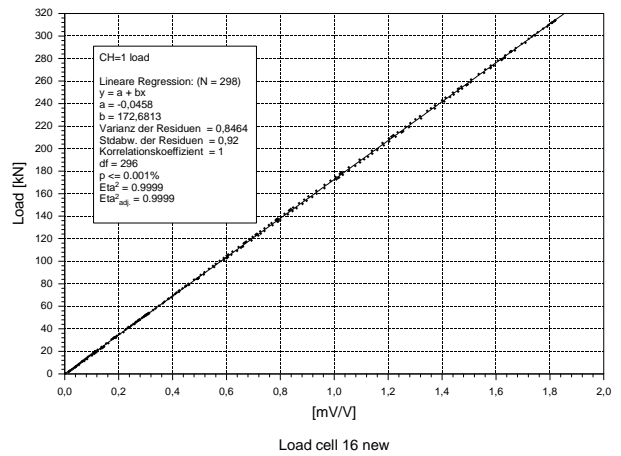


Fig. E28 Re-calibration of curve load cell 16.

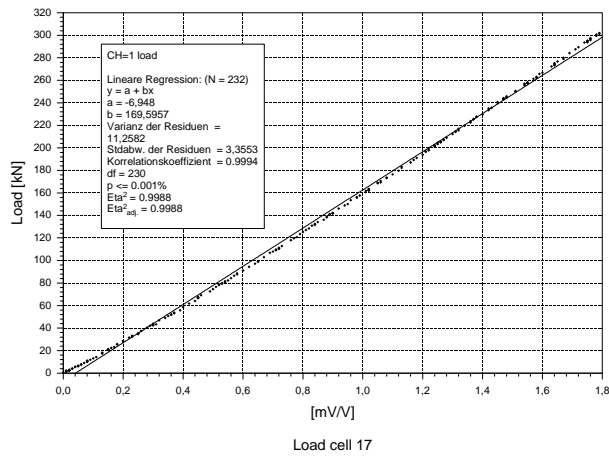


Fig. E29 Calibration curve of load cell 17.

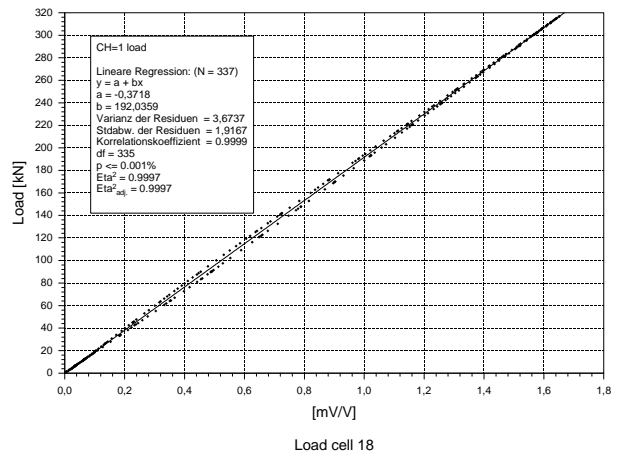


Fig. E30 Calibration curve of load cell 18.

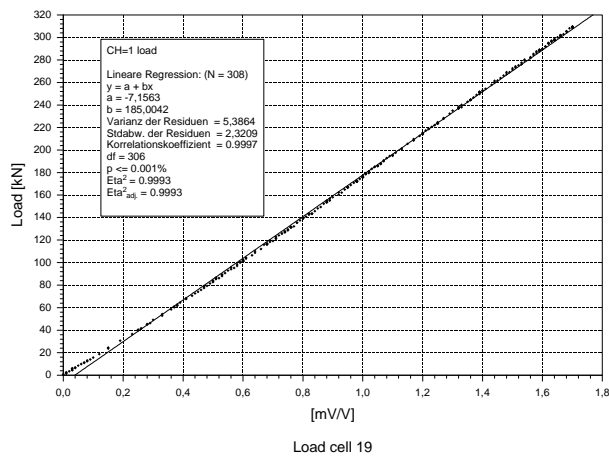


Fig. E31 Calibration curve of load cell 19.

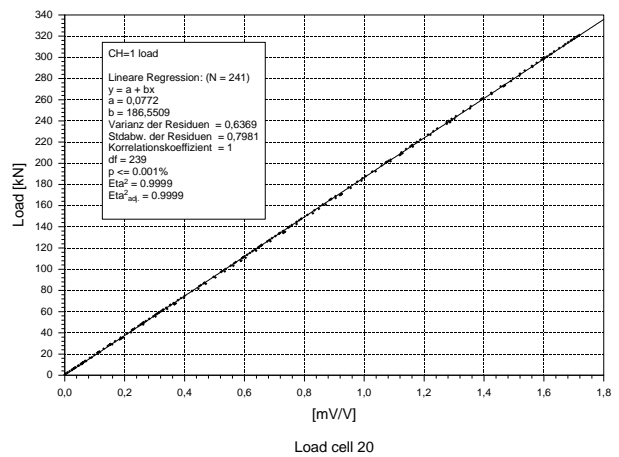


Fig. E32 Calibration curve of load cell 20.

Summary of the Eurocode 3 model

Introduction

It is well known that the rotational stiffness of the structural joints is between the two extreme cases of the rigid and the pinned behaviour.

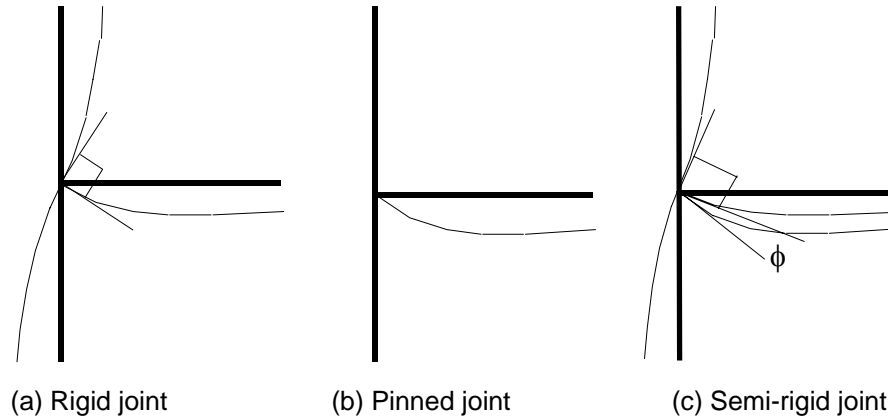


Fig. F1 Classification of joints by stiffness.

The joint is classified as rigid when all parts of the joint have sufficient rotational stiffness (i.e. their stiffness can be assumed to be infinite) and the rotations of each connected member of the joint are identical to each other, see Figure F1a. Rigid-body type rotation can be observed in the joint, called as nodal rotation in the commonly used analysis methods of frame structures.

In the case of nominally pinned joints, it is assumed that the joint has no stiffness and the beam works as a simply supported system, independently from the behaviour of any other connected member, as shown in Figure F1b.

For the intermediate case (when the stiffness is neither zero nor infinite) the joint is classified as semi-rigid, and the transferred moment is a result of the different absolute rotations of the two connected members, as shown in Figure F1c.

The simplest way to represent the rotational stiffness of the joint is a rotational (spiral) spring between the ends of the two connected members. The rotational stiffness “ S ” of this spring is the parameter which describes the relationship between the transformed moment M_j and the relative rotational difference (ϕ) between the two connected members.

When this rotational stiffness is equal to zero ($S = 0$), or when it has a relatively small value, the joint belongs to the class of nominally pinned joints. In the opposite case, when the rotational stiffness is infinite or when it is relatively large, the joint is classified as rigid.

In all the intermediate cases, the joint belongs to the semi-rigid class.

In the case of semi-rigid joints the external loads cause both a bending moment (M_j) and a relative rotational difference (ϕ) between the connected members. The moment and the relative rotation are related to each other through a constitutive law, which depends on the joint properties, as it is illustrated in Figure F2, where, for simplification, the global analysis is assumed to be performed assuming linear elastic behaviour.

The Eurocode 3 (EC3) requirements and the desire to model the behaviour of the structure in a more realistic way lead to the consideration of the semi-rigid behaviour, when it is necessary.

At the global analysis stage, if we take into consideration the semi-rigid nature of the joints - instead of the rigid or pinned joint behaviour -, it causes a modification not only of the displacements, but also of the distribution of the internal forces within the structure.

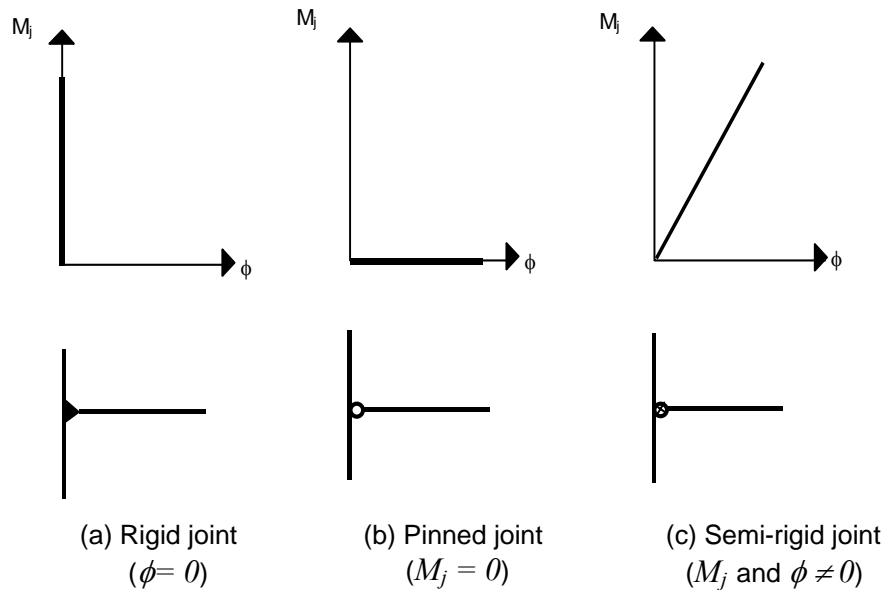


Fig. F2 Modelling of joints (elastic global analysis).

It is to be noted that the concept of rigid and pinned joints is still nevertheless included in the EC3. It is acceptable in the design process that a joint which is not fully rigid or pinned is indeed considered as fully rigid or pinned. The decision whether a joint can be considered as rigid, semi-rigid or pinned, depends on the comparison of the joint stiffness and the beam stiffness (which in turn depends on the second moment of area and the length of the beam).

Definitions of joint configuration, joint and connection

Building frames consist of beams and columns, usually made of H or I sections, which are assembled together by means of connections. These connections are between two beams, two columns, a beam and a column or a column and the foundation. The possible connection types are illustrated in Figure F3.

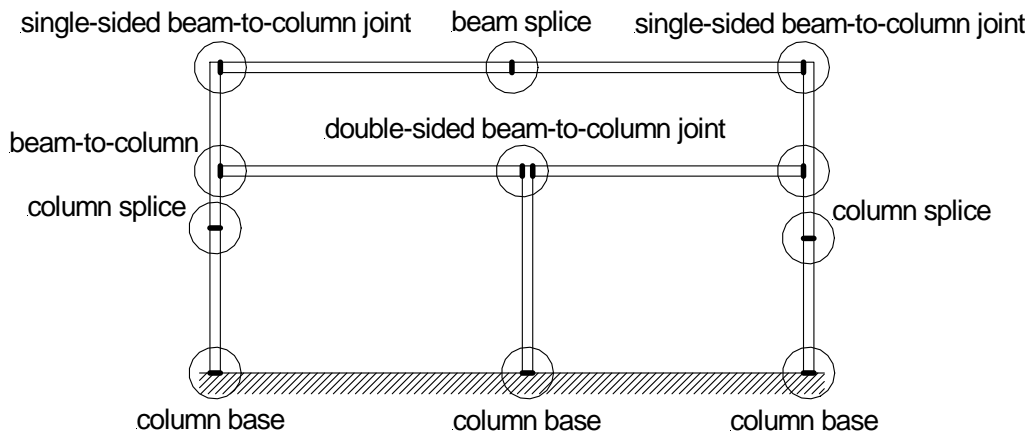


Fig. F3 Different types of connections in a building frame.

A connection is defined as the set of the physical components which mechanically fasten the connected elements.

When the connection as well as the corresponding zone of interaction between the connected members are considered together, the wording joint is used, as shown in Figure F5.

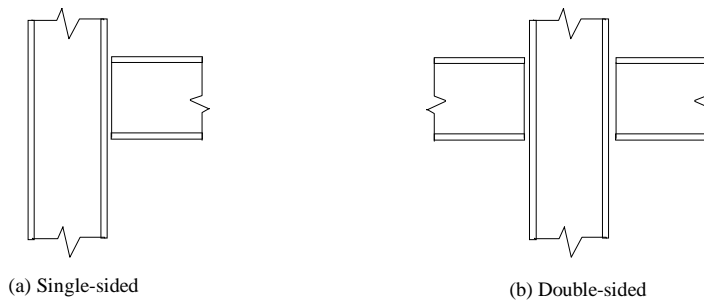


Fig. F4 In-plane joint configurations.

Depending on the number of in-plane elements connected together, single-sided and double-sided joint configurations are defined, as shown in Figure F4. In a double-sided configuration two joints, left and right, have to be considered.

The definitions illustrated in Figure F4 and F5 are also valid for other joint configurations and connection types.

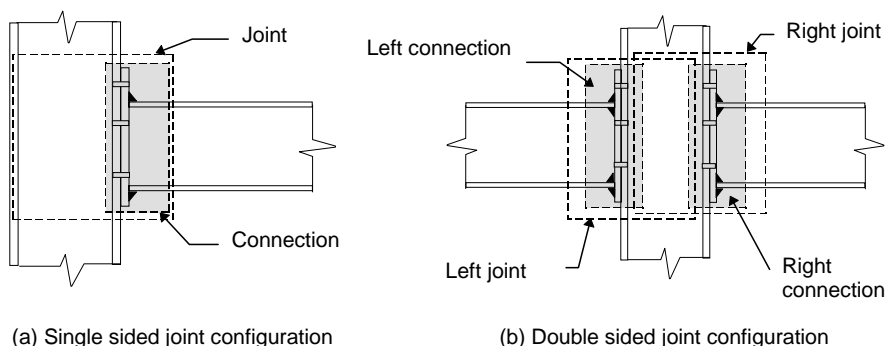


Fig. F5 Joints and connections.

As explained previously, the joints which are traditionally considered as rigid or pinned and are designed accordingly, possess, in reality, their own degree of finite flexibility or finite stiffness resulting from the deformability of all the constitutive components.

Classification of joints

Stiffness classification

The stiffness classification into rigid, semi-rigid and pinned joints is performed by comparing simply the design joint stiffness to the two stiffness boundaries (Figure F6). The stiffness boundaries have been derived so as to allow a direct comparison with the initial design joint stiffness, whatever type of joint idealization is used afterwards in the analysis.

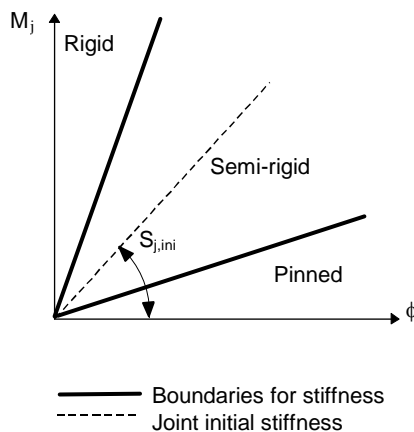


Fig. F6 Stiffness classification boundaries.

Strength classification

The strength classification simply consists of comparing the joint design moment resistance to the boundaries of the "full-strength" and "pinned" behaviour (Figure 7).

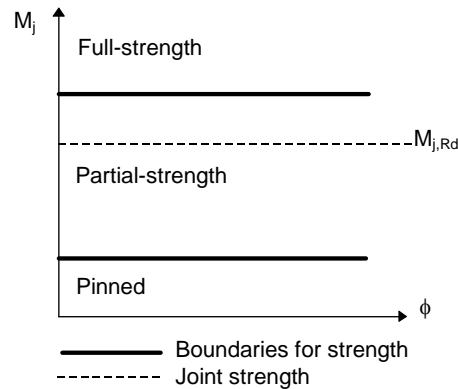


Fig. F7 Strength classification boundaries.

Boundaries for classification

It is worthwhile to stress that a classification based on the experimental $M-\phi$ characteristics of a joint is not allowed, as only design properties are of concern.

The stiffness and strength boundaries for the joint classification are given as follows:

Classification by stiffness

rigid joint $S_{j,ini} \geq 25 EI / L$ (unbraced frames)
 $S_{j,ini} \geq 8 EI / L$ (braced frames)

semi-rigid joint $0,5 EI / L < S_{j,ini} < 25 EI / L$ (unbraced frames)
 $0,5 EI / L < S_{j,ini} < 8 EI / L$ (braced frames)

pinned joint $S_{j,ini} \leq 0,5 EI / L$

Classification by strength

full-strength joint $M_{j,Rd} \geq M_{full-strength}$

partial strength joint $0,25 M_{full-strength} < M_{j,Rd} < M_{full-strength}$

pinned joint $M_{j,Rd} \leq 0,25 M_{full-strength}$

where

E = elastic modulus

I = the second moment of area of the member

L = the system length of the member

$M_{full-strength}$ = the design moment resistance of the weaker of the connected members

Joint modelling

Joint behaviour affects the structural frame response and shall therefore be modelled, just as for beams and columns, for the frame analysis and design. Traditionally, the following types of joint modelling are considered:

For rotational stiffness:

- rigid
- pinned

For resistance:

- full-strength
- partial-strength
- pinned

When the joint rotational stiffness is of concern, the wording rigid means that no relative rotation occurs between the connected members whatever is the applied moment.

The wording pinned assumes the existence of a perfect hinge between the members.

Indeed rather flexible but not fully pinned joints and rather stiff but not fully rigid joints may be considered as effectively pinned and sufficiently rigid, respectively.

For joint resistance, a full-strength joint is stronger than the weaker of the connected members, which is in contrast to a partial-strength joint. In the everyday practice, partial-strength joints are used whenever the joints are designed to transfer the internal forces but not to resist the full capacity of the connected members.

A pinned joint is considered to transfer no moment.

Consideration of rotational stiffness and joint resistance properties leads to three significant joint models:

- rigid & full-strength;
- rigid & partial-strength;
- pinned.

However, as far as the joint rotational stiffness is considered, joints designed for economy may be neither rigid nor pinned but semi-rigid. There are thus new possibilities for joint modelling:

- semi-rigid & full-strength;
- semi-rigid & partial-strength.

As a simplification we can introduce three joint models (Table F1):

Table F1 Types of joint modelling.

stiffness	resistance		
	full-strength	partial-strength	pinned
rigid	continuous	semi-continuous	-
semi-rigid	semi-continuous	semi-continuous	-
pinned	-	-	simple

continuous = covering the rigid/full-strength case only, i.e. the joint ensures a full rotational continuity between the connected members

semi-continuous = covering the rigid/partial-strength, the semi-rigid/full-strength and the semi-rigid/partial-strength cases, i.e. the joint ensures only a partial rotational continuity between the connected members

simple = covering the pinned case only, i.e. the joint prevents any rotational continuity between the connected members

The interpretation to be given to these wordings depends on the type of frame analysis to be performed. In the case of an elastic global frame analysis, only the stiffness properties of the joint are relevant for the joint modelling. In the case of a rigid-plastic analysis, the main joint feature is the resistance. In all the other cases, both the stiffness and resistance properties govern the manner in which the joints should be modelled. These possibilities are illustrated in Table F2.

Table F2 Joint modelling and frame analysis.

modelling	type of frame analyses		
	elastic analysis	rigid-plastic analysis	elastic-perfectly plastic and elastoplastic analysis
continuous	rigid	full-strength	rigid/full-strength
semi-continuous	semi-rigid	partial-strength	rigid/partial-strength semi-rigid/full-strength semi-rigid/partial-strength
simple	pinned	pinned	pinned

Joint characterization

An important step when designing a frame consists of the characterization of the rotational response of the joints, i.e. the evaluation of the mechanical properties in terms of stiffness, strength and ductility.

Three main approaches may be followed:

- experimental,
- numerical,
- analytical.

The only practical option for the designer is the analytical approach. Analytical procedures have been developed which enable a prediction of the joint response based on the knowledge of the mechanical and geometrical properties of the joint components, termed component method. It applies to any type of steel or composite joints, whatever is the geometrical configuration, the type of loading (axial force and/or bending moment, ...) and the type of member sections.

Introduction to the component method

The component method considers any joint as a set of individual basic components. The components are the following:

Compression zone:

- column web in compression;
- beam flange and web in compression;

Tension zone:

- column web in tension;
- column flange in bending;
- bolts in tension;
- end-plate in bending;
- beam web in tension;

Shear zone:

- column web panel in shear.

Each of these basic components possesses its own strength and stiffness either in tension or in compression or in shear. The column web is subject to coincident compression, tension and shear. This co-existence of several components within the same joint element can obviously lead to stress interactions that are likely to decrease the resistance of the individual basic components. To derive the mechanical properties of the whole joint from those of all the individual constituent components requires a preliminary distribution of the forces acting on the joint into internal forces acting on the components in a way that satisfies equilibrium.

The application of the component method requires the following steps:

- identification of the active components in the joint being considered;
- evaluation of the stiffness and/or resistance characteristics for each individual basic component;
- assembly of all the constituent components and evaluation of the stiffness and/or resistance characteristics of the whole joint.

The application of the component method requires a sufficient knowledge of the behaviour of the basic components. Those covered by EC3 are listed in Table F3.

The combination of these components allows one to cover a wide range of joint configurations, which should be sufficient to satisfy the needs of practitioners as far as beam-to-column joints and beam splices in bending are concerned.

Table F3/a List of components covered by Eurocode 3 (EC3 EN 1993-1-8: 2005).

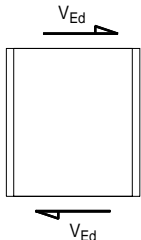
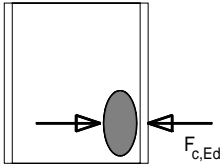
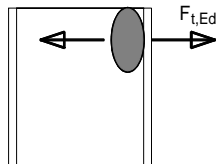
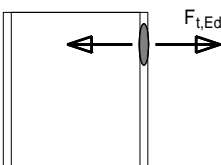
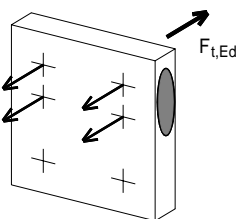
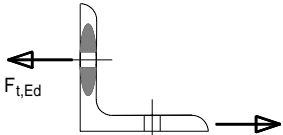
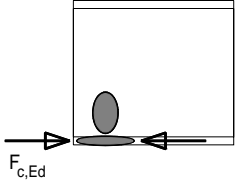
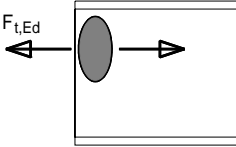
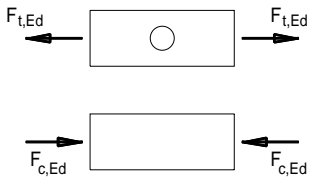
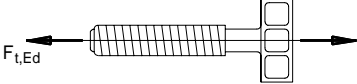
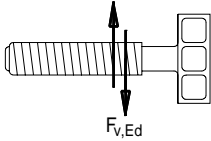
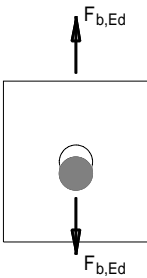
Component		Design resistance	Stiffness coefficient	
1.	Column web pane in shear		6.2.6.1	6.3.2
2.	Column web in transverse compression		6.2.6.2	6.3.2
3.	Column web in transverse tension		6.2.6.3	6.3.2
4.	Column flange in bending		6.2.6.4	6.3.2
5.	End-plate in bending		6.2.6.5	6.3.2
6.	Flange cleat in bending		6.2.6.6	6.3.2

Table 3/b List of components covered by Eurocode 3 (EC3 EN 1993-1-8: 2005).

Component		Design resistance	Stiffness coefficient	
7.	Beam or column flange and web in compression		6.2.6.7	6.3.2
8.	Beam web in tension		6.2.6.8	6.3.2
9.	Plate in tension or compression		In tension: EN 1993-1-1 In compr.: EN 1993-1-1	6.3.2
10.	Bolts in tension		With column flange: 6.2.6.4 with end-plate 6.2.6.5 with flange cleat: 6.2.6.6	6.3.2
11.	Bolts in shear		3.6	6.3.2
12.	Bolts in bearing (on beam flange, column flange, end-plate or cleat)		3.6	6.3.2

Joint idealization

The non-linear behaviour of the isolated flexural spring which characterizes the actual joint response does not lend itself towards everyday design practice. However the moment-rotation characteristic curve may be idealized without significant loss of accuracy. One of the most simple idealizations possible is the elastic-perfectly plastic relationship. This modelling has the advantage of being quite similar to that used traditionally for the modelling of member cross-sections subject to bending.

The initial stiffness $S_{j,ini}$ is derived from the elastic stiffness of the components. The elastic behaviour of each component is represented by an extensional spring. The force-deformation relationship of this spring is given by:

$$F_i = k_i \cdot E \cdot \Delta_i$$

where: F_i is the force in the spring i;
 k_i is the stiffness coefficient of the component i;
 E is the Young modulus;
 Δ_i is the deformation of the spring i.

The spring components in a joint are combined into a spring model. As an example the spring model for an unstiffened welded beam-to-column joint is shown in Figure F8.

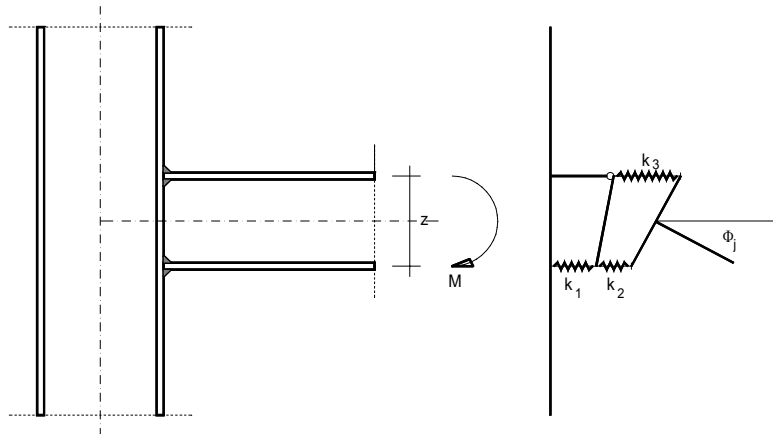


Fig. F8 Spring model for an unstiffened welded joint.

The force in each spring is equal to F . The moment M acting on the spring model is equal to $F \cdot z$, where z is the distance between the centre of tension (for welded joints, located in the centre of the upper beam flange) and the centre of compression (for welded joints, located in the centre of the lower beam flange). The rotation ϕ in the joint is equal to $(\Delta_1 + \Delta_2 + \Delta_4) / z$. In other words:

$$S_{j,ini} = \frac{M}{\phi} = \frac{Fz}{\frac{\Sigma \Delta_i}{z}} = \frac{Fz^2}{\frac{F}{E} \Sigma \frac{1}{k_i}} = \frac{Ez^2}{\Sigma \frac{1}{k_i}}$$

The spring model adopted for end-plate joints with two or more bolt-rows in tension is shown in Figure F9. It is assumed that the bolt-row deformations for all rows are proportional to the distance to the point of compression, but that the elastic forces in each row are dependent on the stiffness of the components.

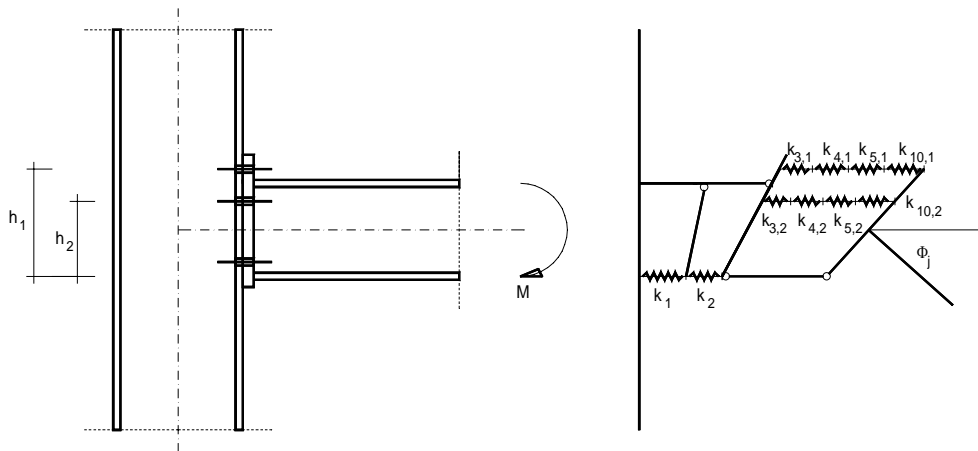


Fig. F9 Spring model for a beam-to-column end-plate joint with more than one bolt-row in tension.

Strength assembly

For the connection represented in Figure F10 the distribution of internal forces is quite easy to obtain: the compressive force is transferred at the centroid of the beam flange, while the tension force is at the level of the upper bolt-row. The resistance possibly associated with the lower bolt-row is usually neglected as it contributes in a very modest way to the transfer of bending moment in the joint (small level arm).

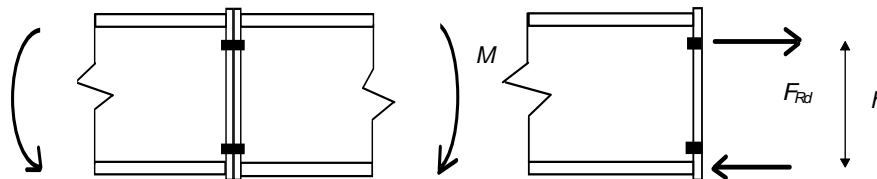


Fig. F10 Joint with one bolt-row in tension.

The design resistance of the joint $M_{j,Rd}$ is associated with the design resistance F_{Rd} of the weakest joint component which can be one of the following:

- the beam and web in compression,
- the beam web in tension,
- the plate in bending or
- the bolts in tension.

For the two last components (plate and bolts), reference is made to the concept of "idealized T-stub" introduced in EC3. The bending resistance becomes:

$$M_{j,Rd} = F_{Rd} \cdot z$$

where $z = h$ = the lever arm.

When more than one bolt-row has to be considered in the tension zone (Figure F11), the distribution of internal forces is more complex.

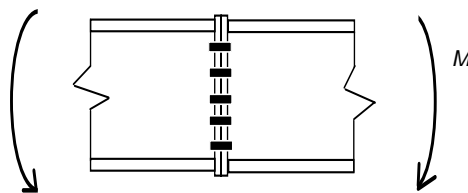


Fig. F11 Joint with more than one bolt-row in tension.

Assume, initially, that the design of the joint leads to the adoption of a particularly thick end-plate in comparison to the bolt diameter – see Figure F12. In this case, the distribution of internal forces between the different bolt-rows is linear according to the distance from the centre of compression. The compression force F_c which equilibrates the tension forces acts at the level of the centroid of the lower beam flange.

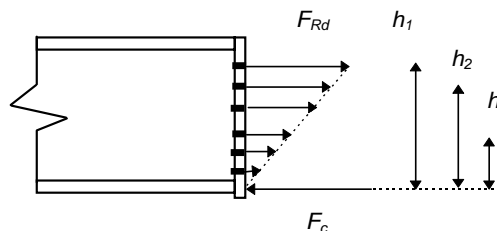


Fig. F12 Internal force distribution in a joint with a thick end-plate.

The design resistance $M_{j,Rd}$ of the joint is reached as soon as the bolt-row subjected to the highest stresses - in reality that which is located the farthest from the centre of compression - reaches its design resistance in tension $2B_{t,Rd}$.

Because of a limited deformation capacity of the bolts in tension no redistribution of forces is allowed to take place between bolt-rows.

It is assumed here that the design resistance of the beam flange and web in compression is sufficient to transfer the compression force F_c . The tensile resistance of the beam web is also assumed not to limit the design resistance of the joint. $M_{j,Rd}$ is so expressed as:

$$M_{j,Rd} = \frac{F_{Rd}}{h_1} \sum h_i^2$$

For thinner end-plates, the distribution of internal forces requires much more attention. When an initial moment is applied to the joint, the forces distribute between the bolt-rows according to the relative stiffnesses of the T-stubs. This stiffness is namely associated to that of the part of the end-plate adjacent to the considered bolt-row. In the particular case of Figure F13, the upper bolt-row is characterized by a higher stiffness because of the presence of the beam flange and the web welded to the end-plate.

Because of the higher stiffness, the upper bolt-row is capable of transferring a higher load than the lower bolt-rows – illustrated in Figure F13/b.

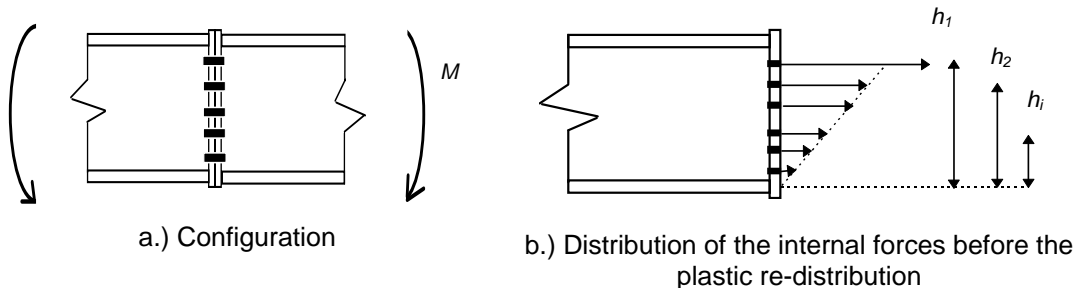


Fig. F13 Joint with a thin end-plate.

The design resistance of the upper bolt-row may be associated with one of the following components:

- the end-plate only (Mode 1),
- the bolts-plate assembly (Mode 2) or
- the bolts only (Mode 3),
- the beam web in tension.

If its failure mode is ductile, a redistribution of forces between the bolt-rows can take place: as soon as the upper bolt-row reaches its design resistance, any additional bending moment applied to the joint will be carried by the lower bolt-rows, each of which in their turn may reach its own design resistance.

The failure of a T-stub may occur in three different ways as shown Table F4.

Table 4 Failure modes of a T-stub.

	<p>mode 1 Complete yielding of the flange</p>
	<p>mode 2 Bolt failure with yielding of the flange</p>
	<p>mode 3 Bolt failure</p>

The plastic redistribution of the internal forces extends to all bolt-rows when they have sufficient deformation capacity.

The design moment resistance $M_{j,Rd}$ is expressed as - see Figure F14:

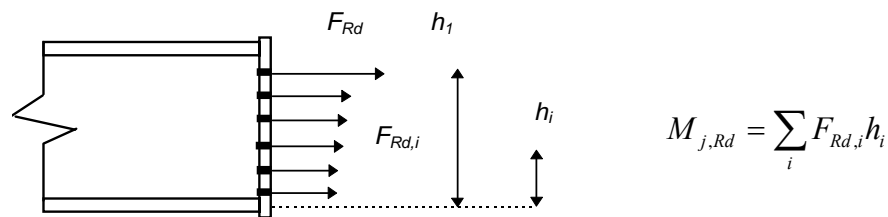


Fig. F14 Plastic distribution of internal forces.

The plastic forces $F_{Rd,i}$ vary from one bolt-row to another according to the failure modes.

EC3 considers that a bolt-row possesses a sufficient deformation capacity to allow a plastic redistribution of internal force to take place when:

$F_{Rd,i}$ is associated to the failure of the beam web in tension; or

$F_{Rd,i}$ is associated to the failure of the T-sub and:

$$F_{Rd,i} \leq 1.9 B_{t,Rd}$$

The plastic redistribution of forces is interrupted because of the lack of deformation capacity in the last bolt-row (k) which has reached its design resistance.

In the bolt-rows located lower than bolt-row k, the forces are then linearly distributed according to their distance to the point of compression (Figure F15).

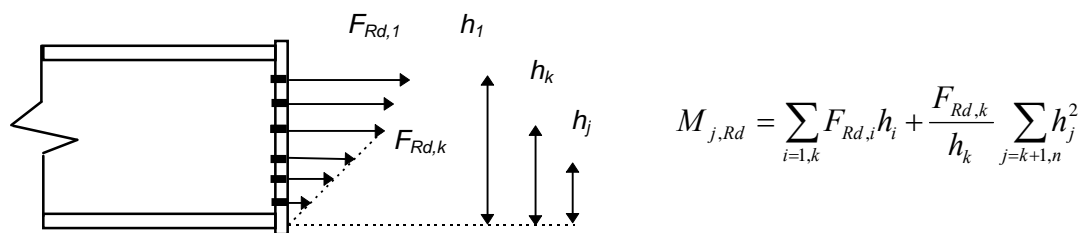


Fig. F15 Elasto-plastic distribution of internal forces.

where: n is the total number of bolt-rows;

k is the number of the bolt-row, the deformation capacity of which is not sufficient.

In this case, the distribution is "elasto-plastic".

The plastic or elasto-plastic distribution of internal forces is interrupted because the compression force F_c attains the design resistance of the beam flange and web in compression. The moment resistance $M_{j,Rd}$ is evaluated with the formula

$$M_{j,Rd} = \sum_{i=1,k} F_{Rd,i} h_i + \frac{F_{Rd,k}}{h_k} \sum_{j=k+1,n} h_j^2$$

In which, obviously, only a limited number of bolt-rows are taken into consideration. These bolt rows are such that:

$$\sum_{\ell=1,m} F_{\ell} = F_{c,Rd}$$

- where: m is the number of the last bolt-row transferring a tensile force;
 F_ℓ is the tensile force in bolt-row number ℓ ;
 $F_{c,Rd}$ is the design resistance of the beam flange and web in compression.

The application of the above-described principles to beam-to-column joints is quite similar. The design moment resistance M_{Rd} is, as for the beam splices, likely to be limited by the resistance of:

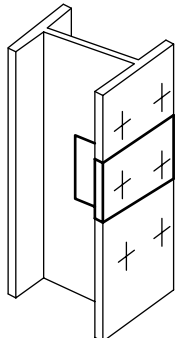
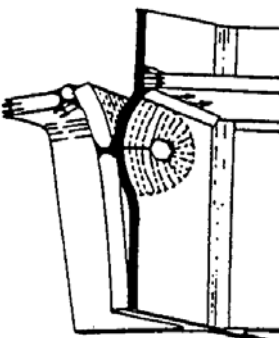
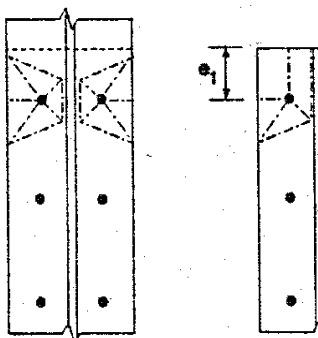
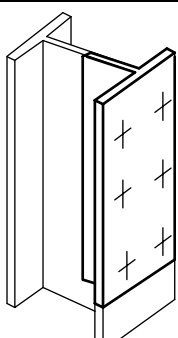
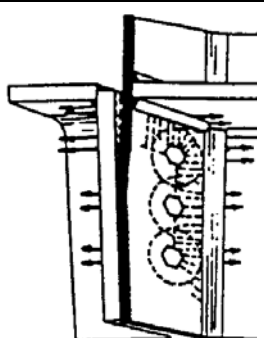
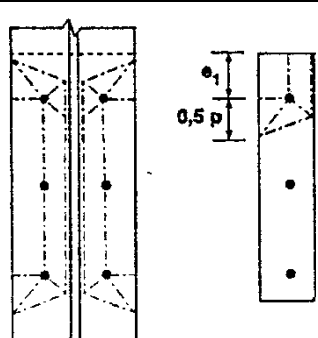
- the end-plate in bending,
 - the bolts in tension,
 - the beam web in tension,
 - the beam flange and web in compression,
- but also by that of:
- the column web in tension,
 - the column flange in bending,
 - the column web in compression,
 - the column web panel in shear.

To each of these mechanisms are associated specific design resistances.

The resistance, which can be evaluated for a certain bolt row assuming the failure of the group of fasteners, is always smaller than the resistance of that certain bolt row in single failure mode.

Table F5 shows examples of yield line patterns for individual bolt-row failure and for the failure of groups of bolt-rows.

Table F5 Example of plastic mechanisms.

a) Individual:		$l_{eff,1} = 4m + 1,25e$
		
b) Group mechanism:		$l_{eff,g} = 4m + 1,25e + 2p$
		

Classification of cross-section according to EN 1993-1-1

Input data:

material properties: S 355 $f_y := 355 \frac{\text{N}}{\text{mm}^2}$ $E := 210000 \frac{\text{N}}{\text{mm}^2}$ $\nu := 0.3$ $G := \frac{E}{2 \cdot (1 + \nu)}$

partial factor: $\gamma_{M,0} := 1.0$

loads: $M_{Ed} := 100 \text{ kN} \cdot \text{m}$ $N_{Ed} := 0 \text{ kN}$ $V_{Ed} := 0 \text{ kN}$

The dimensions of the welds are in this calculation neglected!

Dimensions:

$a := 360 \text{ mm}$ $e := 360 \text{ mm}$ $x := 0 \text{ mm}$

$b := 20 \text{ mm}$ $f := 20 \text{ mm}$

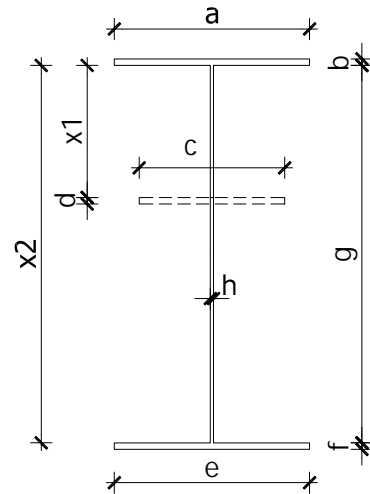
$c := 0 \text{ mm}$ $g := 860 \text{ mm}$

$d := 0 \text{ mm}$ $h := 8 \text{ mm}$

$g1 := x - \frac{d}{2}$ $g1 = 0 \text{ mm}$

$g2 := g - x - \frac{d}{2}$ $g2 = 860 \text{ mm}$

$h_b := b + g + f$ $h_b = 900 \text{ mm}$



$$A_n := a \cdot b + (c - h) \cdot d + e \cdot f + g \cdot h \quad \sqrt{A_n = 212.8 \text{ cm}^2}$$

$$S_{y_n} := (a \cdot b) \cdot \frac{-b}{2} + (c - h) \cdot d \cdot x + e \cdot f \cdot \left(g + \frac{f}{2} \right) + g1 \cdot h \cdot \frac{g1}{2} + g2 \cdot h \cdot \left(x + \frac{d}{2} + \frac{g2}{2} \right)$$

$$\overline{S_{y_n}} := (a \cdot b) \cdot \frac{-b}{2} + (c - h) \cdot d \cdot x + e \cdot f \cdot \left(g + \frac{f}{2} \right) + g \cdot h \cdot \left(x + \frac{d}{2} + \frac{g}{2} \right) \quad S_{y_n} = 9150.4 \text{ cm}^3$$

$$s_{y_n} := \frac{S_{y_n}}{A_n} \quad \sqrt{s_{y_n} = 430 \text{ mm}}$$

$$y2_n := g + f - s_{y_n} \quad y2_n = 450 \text{ mm} \quad y1_n := g + 2 \cdot f - y2_n \quad y1_n = 450 \text{ mm}$$

$$y_{\max, n} := \max(s_{y_n}, y2_n) \quad y_{\max, n} = 450 \text{ mm}$$

$$S_{y, n, \text{half}} := a \cdot b \cdot \left(y1_n - \frac{b}{2} \right) + h \cdot s_{y_n} \cdot \frac{s_{y_n}}{2} \quad S_{y, n, \text{half}} = 3907.6 \text{ cm}^3$$

$$I_{y, n} := a \cdot \frac{b^3}{12} + a \cdot b \cdot \left(\frac{b}{2} \right)^2 + c \cdot \frac{d^3}{12} + c \cdot d \cdot x^2 + e \cdot \frac{f^3}{12} + e \cdot f \cdot \left(g + \frac{f}{2} \right)^2 + h \cdot \frac{g1^3}{12} + g1 \cdot h \cdot \left(\frac{g1}{2} \right)^2 + h \cdot \frac{g2^3}{12} \dots$$

$$+ g2 \cdot h \cdot \left(x + \frac{d}{2} + \frac{g2}{2} \right)^2 - A_n \cdot s_{y_n}^2 \quad \sqrt{I_{y, n} = 321235.733 \text{ cm}^4}$$

$$W_{y, n} := \frac{I_{y, n}}{y_{\max, n}} \quad \sqrt{W_{y, n} = 7138.572 \text{ cm}^3} \quad W_{y, \text{pl}, n} := 2 \cdot S_{y, n, \text{half}} \quad \sqrt{W_{y, \text{pl}, n} = 7815.2 \text{ cm}^3}$$

$$A_v := g \cdot h \quad A_v = 68.8 \text{ cm}^2$$

Cross-section uner compression (N)

classification

upper flange:

$$\varepsilon_{\text{w}} := \sqrt{\frac{235 \frac{\text{N}}{\text{mm}^2}}{f_y}} \quad \varepsilon = 0.814 \quad C_{\text{w}} := \frac{a}{2} \quad C = 18 \text{ cm} \quad \frac{C}{b} = 9$$

$$\text{upper_flange_N} := \begin{cases} 1 & \text{if } \frac{C}{b} \leq 9 \cdot \varepsilon \\ 2 & \text{if } 9 \cdot \varepsilon < \frac{C}{b} \leq 10 \cdot \varepsilon \\ 3 & \text{if } 10 \cdot \varepsilon < \frac{C}{b} \leq 14 \cdot \varepsilon \\ 4 & \text{otherwise} \end{cases} \quad \text{upper_flange_N} = 3 \quad \text{class 3}$$

web plate:

$$\frac{g}{h} = 107.5$$

$$\text{web_plate_N} := \begin{cases} 1 & \text{if } \frac{g}{h} \leq 33 \cdot \varepsilon \\ 2 & \text{if } 33 \cdot \varepsilon < \frac{g}{h} \leq 38 \cdot \varepsilon \\ 3 & \text{if } 38 \cdot \varepsilon < \frac{g}{h} \leq 42 \cdot \varepsilon \\ 4 & \text{otherwise} \end{cases} \quad \text{web_plate_N} = 4 \quad \text{class 4}$$

lower flange:

$$\varepsilon_{\text{w}} := \sqrt{\frac{235 \frac{\text{N}}{\text{mm}^2}}{f_y}} \quad \varepsilon = 0.814 \quad C_{\text{w}} := \frac{e}{2} \quad C = 18 \text{ cm} \quad \frac{C}{f} = 9$$

$$\text{lower_flange_N} := \begin{cases} 1 & \text{if } \frac{C}{f} \leq 9 \cdot \varepsilon \\ 2 & \text{if } 9 \cdot \varepsilon < \frac{C}{f} \leq 10 \cdot \varepsilon \\ 3 & \text{if } 10 \cdot \varepsilon < \frac{C}{f} \leq 14 \cdot \varepsilon \\ 4 & \text{otherwise} \end{cases} \quad \text{lower_flange_N} = 3 \quad \text{class 3}$$

$$\text{cross_section_compression} := \max(\text{upper_flange_N}, \text{web_plate_N}, \text{lower_flange_N})$$

$$\boxed{\text{cross_section_compression}} = 4 \quad \text{class 4}$$

Cross-section uner bending (M)

classification

upper flange is under tension \rightarrow

upper_flange_M := 1

class 1

web plate:

$$\frac{g}{h} = 107.5$$

$$\text{web_plate_M} := \begin{cases} 1 & \text{if } \frac{g}{h} \leq 72 \cdot \varepsilon \\ 2 & \text{if } 72 \cdot \varepsilon < \frac{g}{h} \leq 83 \cdot \varepsilon \\ 3 & \text{if } 83 \cdot \varepsilon < \frac{g}{h} \leq 124 \cdot \varepsilon \\ 4 & \text{otherwise} \end{cases}$$

web_plate_M = 4

class 4

lower flange is under compression. \rightarrow

lower_flange_M := 3

class 3

cross_section_bending := max(upper_flange_M, web_plate_M, lower_flange_M)

$$\overline{\text{cross_section_bending}} = 4$$

class 4

Resistances for class 1 and 2 cross-sectionsshear:

$$\eta := 1.2$$

$$A_w := \eta \cdot g \cdot h$$

$$V_{pl.Rd.I} := \frac{A_w \cdot f_y}{2 \cdot \sqrt{3} \cdot \gamma_{M.0}}$$

$$\overline{V_{pl.Rd.I}} = 846.072 \text{ kN}$$

bending:

$$M_{c.Rd.I} := \frac{W_{y.pl.n} \cdot f_y}{\gamma_{M.0}}$$

$$\overline{M_{c.Rd.I}} = 2774.396 \text{ kN}\cdot\text{m}$$

compression / tension:

$$N_{c.Rd.I} := \frac{A_n \cdot f_y}{\gamma_{M.0}}$$

$$\overline{N_{c.Rd.I}} = 7554.4 \text{ kN}$$

Resistances for class 3 cross-sectionsbending:

$$M_{c.Rd.III} := \frac{W_{y.n} \cdot f_y}{\gamma_{M.0}}$$

$$\overline{M_{c.Rd.III}} = 2534.193 \text{ kN}\cdot\text{m}$$

compression:

$$N_{c.Rd.III} := \frac{A_n \cdot f_y}{\gamma_{M.0}}$$

$$\overline{N_{c.Rd.III}} = 7554.4 \text{ kN}$$

Effective cross-section under compression (N)

upper flange:

$$B := \frac{a}{2} - \frac{h}{2} \quad t := b \quad B = 176 \text{ mm} \quad \psi := 1 \quad k_{\sigma} := 0.43$$

$$\lambda_p := \frac{\frac{B}{t}}{28.4 \cdot \varepsilon \cdot \sqrt{k_{\sigma}}} \quad \lambda_p = 0.581$$

$$\rho := \text{if} \left(\frac{\lambda_p - 0.188}{\lambda_p^2} > 1, 1, \frac{\lambda_p - 0.188}{\lambda_p^2} \right) \quad \rho = 1$$

$$b_{\text{eff}} := \rho \cdot B \quad b_{\text{eff}} = 176 \text{ mm} \quad a_{\text{eff}} := 2 \cdot b_{\text{eff}} + h$$

$$a_{\text{eff}} := \text{if}(\text{upper_flange_N} < 4, a_n, a) \quad a = 360 \text{ mm}$$

web plate:

$$B_{\text{eff}} := g \quad t_{\text{eff}} := h \quad \psi_{\text{eff}} := 1 \quad k_{\sigma_{\text{eff}}} := 4.0$$

$$\lambda_{p_{\text{eff}}} := \frac{\frac{B_{\text{eff}}}{t_{\text{eff}}}}{28.4 \cdot \varepsilon \cdot \sqrt{k_{\sigma_{\text{eff}}}}} \quad \lambda_{p_{\text{eff}}} = 2.326$$

$$\rho_{\text{eff}} := \text{if} \left[\frac{\lambda_{p_{\text{eff}}} - 0.055 \cdot (3 + \psi)}{\lambda_{p_{\text{eff}}}^2} > 1, 1, \frac{\lambda_{p_{\text{eff}}} - 0.055 \cdot (3 + \psi)}{\lambda_{p_{\text{eff}}}^2} \right] \quad \rho_{\text{eff}} = 0.389$$

$$b_{\text{eff}_{\text{eff}}} := \rho_{\text{eff}} \cdot B_{\text{eff}} \quad b_{\text{eff}_{\text{eff}}} = 334.742 \text{ mm}$$

$$g_{\text{eff}} := \frac{b_{\text{eff}_{\text{eff}}}}{2} \quad g_{\text{eff}} = 167.371 \text{ mm}$$

$$g_{\text{eff}} := \text{if}(\text{web_plate_N} < 4, g_n, g_{\text{eff}}) \quad g_{\text{eff}} = 167.371 \text{ mm}$$

$$k_{\text{eff}} := \frac{b_{\text{eff}_{\text{eff}}}}{2} \quad k_{\text{eff}} = 167.371 \text{ mm}$$

$$k_{\text{eff}} := \text{if}(\text{web_plate_N} < 4, 0, k_{\text{eff}}) \quad k_{\text{eff}} = 167.371 \text{ mm}$$

lower flange:

$$B_{\text{eff}} := \frac{e}{2} - \frac{h}{2} \quad t_{\text{eff}} := 1 \quad \psi_{\text{eff}} := 1 \quad k_{\sigma_{\text{eff}}} := 0.43$$

$$\lambda_{p_{\text{eff}}} := \frac{\frac{B_{\text{eff}}}{t_{\text{eff}}}}{28.4 \cdot \varepsilon \cdot \sqrt{k_{\sigma_{\text{eff}}}}} \quad \lambda_{p_{\text{eff}}} = 0.581$$

$$\rho := \text{if} \left(\frac{\lambda_p - 0.188}{\lambda_p^2} > 1, 1, \frac{\lambda_p - 0.188}{\lambda_p^2} \right) \quad \rho = 1$$

$$b_{\text{eff}} := \rho \cdot B \quad b_{\text{eff}} = 176 \text{ mm}$$

$$e := 2 \cdot b_{\text{eff}} + h \quad e = 360 \text{ mm}$$

$$e := \text{if}(\text{lower_flange_N} < 4, e_n, e) \quad e = 360 \text{ mm}$$

The dimensions of the effective cross-section

$$a = 360 \text{ mm} \quad b = 20 \text{ mm} \quad x1 := 0 \text{ mm} \quad x2 := g_n$$

$$e = 360 \text{ mm} \quad f = 20 \text{ mm}$$

$$g = 167.371 \text{ mm} \quad h = 8 \text{ mm} \quad k = 167.371 \text{ mm}$$

$$i := 0 \text{ mm} \quad j := 0 \text{ mm}$$

$$A_{\text{eff.N}} := a \cdot b + c \cdot d + e \cdot f + (g + i + j + k) \cdot h \quad A_{\text{eff.N}} = 170.779 \text{ cm}^2$$

$$S_{y,\text{eff.N}} := (a \cdot b) \cdot \frac{-b}{2} + c \cdot d \cdot x1 + e \cdot f \cdot \left(x2 + \frac{f}{2} \right) + g \cdot h \cdot \frac{g}{2} + i \cdot h \cdot \left(x1 - \frac{d}{2} - \frac{i}{2} \right) + j \cdot h \cdot \left(x1 + \frac{d}{2} + \frac{j}{2} \right) + k \cdot h \cdot \left(x2 - \frac{k}{2} \right) \dots$$

$$s_{y,\text{N}} := \frac{S_{y,\text{eff.N}}}{A_{\text{eff.N}}} \quad s_{y,\text{N}} = 430 \text{ mm} \quad S_{y,\text{eff.N}} = 7343.512 \text{ cm}^3$$

$$I_{y,\text{N.IV}} := a \cdot \frac{b^3}{12} + a \cdot b \cdot \left(\frac{b}{2} \right)^2 + c \cdot \frac{d^3}{12} + c \cdot d \cdot x1^2 + e \cdot \frac{f^3}{12} + e \cdot f \cdot \left(x2 + \frac{f}{2} \right)^2 + h \cdot \frac{g^3}{12} + h \cdot g \cdot \left(\frac{g}{2} \right)^2 + \left(h \cdot \frac{i^3}{12} \right) + h \cdot i \cdot \left(x1 - \frac{d}{2} - \frac{i}{2} \right)^2 + \left(h \cdot \frac{j^3}{12} \right) + j \cdot h \cdot \left(x1 + \frac{d}{2} + \frac{j}{2} \right)^2 + h \cdot \frac{k^3}{12} + k \cdot h \cdot \left(x2 - \frac{k}{2} \right)^2 - A_{\text{eff.N}} \cdot s_{y,\text{N}}^2$$

$$I_{y,\text{N.IV}} = 311574.618 \text{ cm}^4$$

$$y2 := x2 + f - s_{y,\text{N}} \quad y2 = 450 \text{ mm}$$

$$y_{\text{max,eff.N}} := \max(s_{y,\text{N}}, y2) \quad y_{\text{max,eff.N}} = 450 \text{ mm}$$

$$W_{y,\text{eff.N}} := \frac{I_{y,\text{N.IV}}}{y_{\text{max,eff.N}}} \quad W_{y,\text{eff.N}} = 6923.88 \text{ cm}^3$$

Resistance of the effective cross-section under compression

$$N_{\text{C.Rd.IV}} := \frac{A_{\text{eff.N}} \cdot f_y}{\gamma_{\text{M.0}}} \quad N_{\text{C.Rd.IV}} = 6062.667 \text{ kN}$$

Effective cross-section under bending (M)

$$\underline{a} := a_n \quad b = 20 \text{ mm}$$

$$\underline{e} := e_n \quad f = 20 \text{ mm}$$

$$\underline{g} := g_n \quad h = 8 \text{ mm} \quad g_1 := y_{2n} - b \quad g_2 := y_{1n} - f$$

stresses:

from bending (M_{Ed})

$$\sigma_{Mf.f} := \frac{-M_{Ed}}{I_{y.n}} \cdot (g_1 + b) \quad \sigma_{Mf.f} = -1.401 \frac{\text{kN}}{\text{cm}^2} \quad (\text{stress in upper flange})$$

$$\sigma_{Mf.a} := \frac{M_{Ed}}{I_{y.n}} \cdot (g_2 + f) \quad \sigma_{Mf.a} = 1.401 \frac{\text{kN}}{\text{cm}^2} \quad (\text{stress in lower flange})$$

$$\sigma_{Mw1} := \frac{-M_{Ed}}{I_{y.n}} \cdot (g_1) \quad \sigma_{Mw1} = -1.339 \frac{\text{kN}}{\text{cm}^2} \quad (\text{max. compr. stress in web plate})$$

$$\sigma_{Mw2} := \frac{M_{Ed}}{I_{y.n}} \cdot (g_2) \quad \sigma_{Mw2} = 1.339 \frac{\text{kN}}{\text{cm}^2} \quad (\text{max. tension stress in web plate})$$

upper flange:

$$\underline{B} := \frac{a}{2} - \frac{h}{2} \quad \underline{t} := b \quad \underline{\psi} := 1 \quad \underline{k_{\sigma}} := 0.43$$

$$\lambda_{p,\sigma} := \frac{\frac{B}{t}}{28.4 \cdot \varepsilon \cdot \sqrt{k_{\sigma}}} \quad \lambda_p = 0.581$$

$$\underline{\rho} := \frac{\lambda_p - 0.188}{\lambda_p^2} \quad \rho = 1.164$$

$$\underline{\rho}_{\sigma} := \text{if}(\rho < 1, \rho, 1)$$

$$\underline{b_{eff}} := \begin{cases} B & \text{if } \sigma_{Mf.f} \leq 0 \\ \rho \cdot B & \text{otherwise} \end{cases} \quad b_{eff} = 176 \text{ mm}$$

$$\underline{a} := 2 \cdot b_{eff} + h \quad a = 360 \text{ mm}$$

$$\underline{a} := \text{if}(\text{upper_flange_M} < 4, a_n, 2 \cdot b_{eff} + h) \quad a = 360 \text{ mm}$$

web plate:

$$\underline{B} := g \quad \underline{t} := h \quad \sigma_{Mw2} = 1.339 \frac{\text{kN}}{\text{cm}^2} \quad \sigma_{Mw1} = -1.339 \frac{\text{kN}}{\text{cm}^2}$$

$$\underline{\psi} := \frac{\sigma_{Mw1}}{\sigma_{Mw2}} \quad \psi = -1$$

$$k_{\text{Mw}} := \begin{cases} 4.0 & \text{if } \psi = 1 \\ \frac{8.2}{1.05 + \psi} & \text{if } 1 > \psi > 0 \\ 7.81 & \text{if } \psi = 0 \\ 7.81 - 6.29 \cdot \psi + 9.78 \cdot \psi^2 & \text{if } 0 > \psi > -1 \\ 23.9 & \text{if } \psi = -1 \\ 5.89 \cdot (1 - \psi)^2 & \text{if } -1 > \psi > -2 \end{cases} \quad k_{\sigma} = 23.9$$

$$\lambda_{\text{Mp}} := \frac{\frac{B}{t}}{28.4 \cdot \varepsilon \cdot \sqrt{k_{\sigma}}} \quad \lambda_p = 0.952$$

$$\rho_{\text{w}} := \frac{\lambda_p - 0.055 \cdot (3 + \psi)}{\lambda_p^2} \quad \rho = 0.929$$

$$\rho_{\text{w}} := \text{if}(\rho < 1, \rho, 1)$$

$$b_c := \frac{B}{1 - \psi} \quad b_c = 430 \text{ mm}$$

$$b_t := B - b_c \quad b_t = 430 \text{ mm}$$

$$b_{\text{eff}} := \rho \cdot b_c \quad b_{\text{eff}} = 399.623 \text{ mm}$$

$$b_{e,1} := 0.4 \cdot b_{\text{eff}} \quad b_{e,1} = 159.849 \text{ mm}$$

$$b_{e,2} := 0.6 \cdot b_{\text{eff}} \quad b_{e,2} = 239.774 \text{ mm}$$

$$g_{\text{M}} := \begin{cases} b_{e,1} & \text{if } \sigma_{\text{Mw}1} > 0 \\ b_t + b_{e,2} & \text{otherwise} \end{cases} \quad g = 669.774 \text{ mm}$$

$$g_{\text{M}} := \text{if}(\text{web_plate_M} < 4, g_n, g) \quad g = 669.774 \text{ mm}$$

$$k_{\text{M}} := \begin{cases} b_{e,1} & \text{if } \sigma_{\text{Mw}2} > 0 \\ b_t + b_{e,2} & \text{otherwise} \end{cases} \quad k = 159.849 \text{ mm}$$

$$k_{\text{M}} := \text{if}(\text{web_plate_M} < 4, 0 \text{ mm}, k) \quad k = 159.849 \text{ mm}$$

lower flange:

$$B_{\text{w}} := \frac{e}{2} - \frac{h}{2} \quad t_{\text{M}} := t \quad \sigma_2 := 1 \quad \sigma_1 := 1 \quad \psi_{\text{M}} := 1$$

$$\lambda_{\text{Mp}} := \frac{\frac{B}{t}}{28.4 \cdot \varepsilon \cdot \sqrt{k_{\sigma}}} \quad \lambda_p = 0.078 \quad k_{\text{Mw}} := 0.43$$

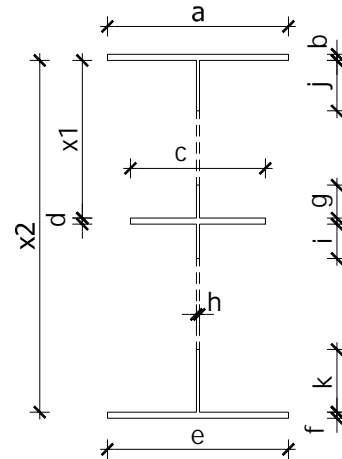
$$\rho_{\omega} := \frac{\lambda_p - 0.188}{\lambda_p^2} \quad \rho = -18.142$$

$$\rho_{\omega} := \text{if}(\rho < 1, \rho, 1)$$

$$b_{\text{eff}} := \begin{cases} B & \text{if } \sigma_{Mf.a} \leq 0 \\ \rho \cdot B & \text{otherwise} \end{cases} \quad b_{\text{eff}} = -3193.03 \text{ mm}$$

$$e := 2 \cdot b_{\text{eff}} + h \quad e = -6378.059 \text{ mm}$$

$$e := \text{if}(\text{lower_flange_M} < 4, e_n, e) \quad e = 360 \text{ mm}$$



The dimensions of the effective cross-section

$$a = 360 \text{ mm} \quad b = 20 \text{ mm} \quad x1 := 0 \text{ mm} \quad x2 := g_n$$

$$e = 360 \text{ mm} \quad f = 20 \text{ mm}$$

$$g = 669.774 \text{ mm} \quad h = 8 \text{ mm}$$

$$i := 0 \text{ mm} \quad j := 0 \text{ mm} \quad k = 159.849 \text{ mm}$$

$$A_{\text{eff.M}} := a \cdot b + c \cdot d + e \cdot f + (g + i + j + k) \cdot h \quad A_{\text{eff.M}} = 210.37 \text{ cm}^2$$

$$S_{y,\text{eff.M}} := (a \cdot b) \cdot \frac{-b}{2} + c \cdot d \cdot x1 + e \cdot f \cdot \left(x2 + \frac{f}{2}\right) + g \cdot h \cdot \frac{g}{2} + i \cdot h \cdot \left(x1 - \frac{d}{2} - \frac{i}{2}\right) \dots$$

$$+ j \cdot h \cdot \left(x1 + \frac{d}{2} + \frac{j}{2}\right) + k \cdot h \cdot \left(x2 - \frac{k}{2}\right) \quad S_{y,\text{eff.M}} = 8983.944 \text{ cm}^3$$

$$s_{y.M} := \frac{S_{y,\text{eff.M}}}{A_{\text{eff.M}}} \quad s_{y.M} = 427.055 \text{ mm}$$

$$I_{y.M.IV} := a \cdot \frac{b^3}{12} + a \cdot b \cdot \left(\frac{b}{2}\right)^2 + c \cdot \frac{d^3}{12} + c \cdot d \cdot x1^2 + e \cdot \frac{f^3}{12} + e \cdot f \cdot \left(x2 + \frac{f}{2}\right)^2 + h \cdot \frac{g^3}{12} + h \cdot g \cdot \left(\frac{g}{2}\right)^2 + \left(h \cdot \frac{i^3}{12}\right) \dots$$

$$+ h \cdot i \cdot \left(x1 - \frac{d}{2} - \frac{i}{2}\right)^2 + \left(h \cdot \frac{j^3}{12}\right) + j \cdot h \cdot \left(x1 + \frac{d}{2} + \frac{j}{2}\right)^2 + h \cdot \frac{k^3}{12} + k \cdot h \cdot \left(x2 - \frac{k}{2}\right)^2 - A_{\text{eff.M}} \cdot s_{y.M}^2$$

$$I_{y.M.IV} = 319635.875 \text{ cm}^4$$

$$y2 := x2 + f - s_{y.M} \quad y2 = 452.945 \text{ mm}$$

$$y1 := s_{y.M} + b \quad y1 = 447.055 \text{ mm}$$

$$y1 + y2 = 900 \text{ mm}$$

$$y_{\text{max.M}} := \max(y1, y2) \quad y_{\text{max.M}} = 452.945 \text{ mm}$$

$$W_{y,\text{eff.M}} := \frac{I_{y.M.IV}}{y_{\text{max.M}}} \quad W_{y,\text{eff.M}} = 7056.832 \text{ cm}^3$$

$$M_{c,\text{Rd.IV}} := \frac{W_{y,\text{eff.M}} \cdot f_y}{\gamma_{M.0}} \quad M_{c,\text{Rd.IV}} = 2505.175 \text{ kN}\cdot\text{m}$$

Resistance of the effective cross-section under bending (M)

$$M_{c,Rd} := \begin{cases} M_{c,Rd.I} & \text{if } \text{cross_section_bending} = 1 \\ M_{c,Rd.I} & \text{if } \text{cross_section_bending} = 2 \\ M_{c,Rd.III} & \text{if } \text{cross_section_bending} = 3 \\ M_{c,Rd.IV} & \text{if } \text{cross_section_bending} = 4 \end{cases} \quad \overline{M_{c,Rd}} = 2505.175 \text{ kN}\cdot\text{m}$$

$$N_{c,Rd} := \begin{cases} N_{c,Rd.I} & \text{if } \text{cross_section_bending} < 4 \\ N_{c,Rd.IV} & \text{if } \text{cross_section_bending} = 4 \end{cases} \quad \overline{N_{c,Rd}} = 6062.667 \text{ kN}$$

Calculation of the effective lengths**bolt-row B:**

$$l_{\text{eff.B.ind.1.1}} := 2 \cdot \Pi \cdot m_B$$

$$l_{\text{eff.B.ind.1.1}} = 219.3389 \text{ mm}$$

$$l_{\text{eff.B.ind.1.2}} := \Pi \cdot m_B + 2 \cdot 140 \cdot \text{mm}$$

$$l_{\text{eff.B.ind.1.2}} = 389.6694 \text{ mm}$$

$$l_{\text{eff.B.ind.2.1}} := 4 \cdot m_B + 1.25 \cdot e_B$$

$$l_{\text{eff.B.ind.2.1}} = 183.3853 \text{ mm}$$

$$l_{\text{eff.B.gr.1.1}} := \Pi \cdot m_B + w$$

$$l_{\text{eff.B.gr.1.1}} = 189.6694 \text{ mm}$$

$$l_{\text{eff.B.gr.1.2}} := \Pi \cdot \frac{m_B}{2} + \frac{w}{2} + e_B$$

$$l_{\text{eff.B.gr.1.2}} = 129.8347 \text{ mm}$$

$$l_{\text{eff.B.gr.2.1}} := 2 \cdot m_B + 0.625 \cdot e_B + \frac{w}{2}$$

$$l_{\text{eff.B.gr.2.1}} = 131.6927 \text{ mm}$$

$$l_{\text{eff.B.gr.2.2}} := w + 2 \cdot 140 \cdot \text{mm}$$

$$l_{\text{eff.B.gr.2.2}} = 360 \text{ mm}$$

$$l_{\text{eff.B.ind.2}} := l_{\text{eff.B.ind.2.1}}$$

$$l_{\text{eff.B.ind.2}} = 183.3853 \text{ mm}$$

$$l_{\text{eff.B.ind.1}} := \min(l_{\text{eff.B.ind.1.1}}, l_{\text{eff.B.ind.1.2}}, l_{\text{eff.B.ind.2}})$$

$$l_{\text{eff.B.ind.1}} = 183.3853 \text{ mm}$$

$$l_{\text{eff.B.gr.2}} := \min(l_{\text{eff.B.gr.2.1}}, l_{\text{eff.B.gr.2.2}})$$

$$l_{\text{eff.B.gr.2}} = 131.6927 \text{ mm}$$

$$l_{\text{eff.B.gr.1}} := \min(l_{\text{eff.B.gr.1.1}}, l_{\text{eff.B.gr.1.2}}, l_{\text{eff.B.gr.2}})$$

$$l_{\text{eff.B.gr.1}} = 129.8347 \text{ mm}$$

$$M_{B,\text{pl.ind.1.Rd}} := \frac{1}{4} \cdot l_{\text{eff.B.ind.1}} \cdot t_{\text{ep}}^2 \cdot \frac{f_y}{\gamma_{M,0}}$$

$$M_{B,\text{pl.ind.1.Rd}} = 2.5945 \text{ kN} \cdot \text{m}$$

$$M_{B,\text{pl.ind.2.Rd}} := \frac{1}{4} \cdot l_{\text{eff.B.ind.2}} \cdot t_{\text{ep}}^2 \cdot \frac{f_y}{\gamma_{M,0}}$$

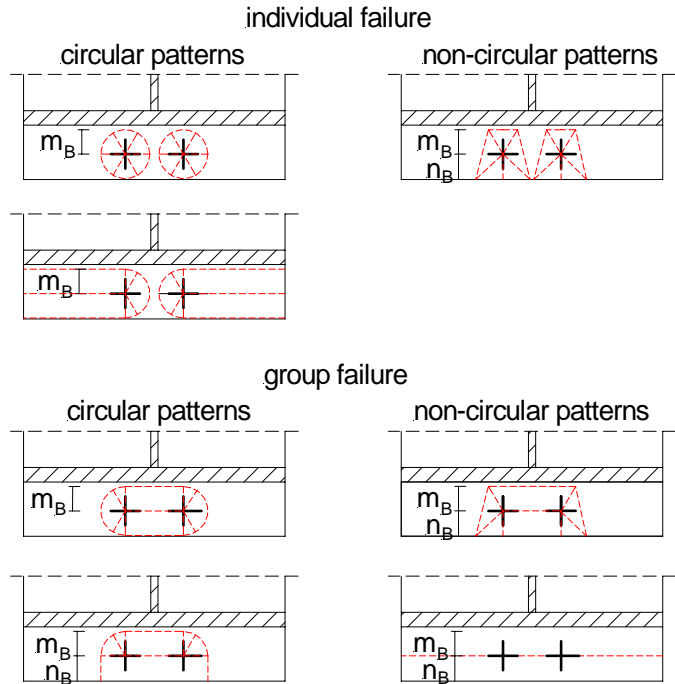
$$M_{B,\text{pl.ind.2.Rd}} = 2.5945 \text{ kN} \cdot \text{m}$$

$$M_{B,\text{pl.gr.1.Rd}} := \frac{1}{4} \cdot l_{\text{eff.B.gr.1}} \cdot t_{\text{ep}}^2 \cdot \frac{f_y}{\gamma_{M,0}}$$

$$M_{B,\text{pl.gr.1.Rd}} = 1.8369 \text{ kN} \cdot \text{m}$$

$$M_{B,\text{pl.gr.2.Rd}} := \frac{1}{4} \cdot l_{\text{eff.B.gr.2}} \cdot t_{\text{ep}}^2 \cdot \frac{f_y}{\gamma_{M,0}}$$

$$M_{B,\text{pl.gr.2.Rd}} = 1.8632 \text{ kN} \cdot \text{m}$$



Design resistance of the T-stub

Bolt in tension:
$$F_{T.Rd} := \frac{k_2 \cdot f_{u.b} \cdot A_s}{\gamma_{M.2}}$$

Bolt-row considered individually:

Mode 1:
$$F_{T.Rd.1.B.ind} := \frac{4 \cdot M_{B.pl.ind.1.Rd}}{m_B} \quad F_{T.Rd.1.B.ind} = 297.2927 \text{ kN}$$

Mode 2:
$$F_{T.Rd.2.B.ind} := \frac{2 \cdot M_{B.pl.ind.2.Rd} + n_B \cdot 2 \cdot F_{T.Rd}}{m_B + n_B} \quad F_{T.Rd.2.B.ind} = 298.988 \text{ kN}$$

Mode 3:
$$F_{T.Rd.3} := 2 \cdot F_{T.Rc} \quad F_{T.Rd.3} = 448.938 \text{ kN}$$

$$F_{T.Rd.B.ind} := \min(F_{T.Rd.1.B.ind} \quad F_{T.Rd.2.B.ind} \quad F_{T.Rd.3}) \quad F_{T.Rd.B.ind} = 297.2927 \text{ kN}$$

Bolt-row considered as "horizontal" group:

Mode 1:
$$F_{T.Rd.1.B.gr} := \frac{4 \cdot M_{B.pl.gr.1.Rd}}{m_B} \quad F_{T.Rd.1.B.gr} = 210.4799 \text{ kN}$$

Mode 2:
$$F_{T.Rd.2.B.gr} := \frac{2 \cdot M_{B.pl.gr.2.Rd} + n_B \cdot 2 \cdot F_{T.Rd}}{m_B + n_B} \quad F_{T.Rd.2.B.gr} = 278.0651 \text{ kN}$$

Mode 3:
$$F_{T.Rd.3} = 448.938 \text{ kN}$$

$$F_{T.Rd.B.gr} := \min(F_{T.Rd.1.B.gr} \quad F_{T.Rd.2.B.gr} \quad F_{T.Rd.3}) \quad F_{T.Rd.B.gr} = 210.4799 \text{ kN}$$

$$F_{T.Rd.B} := \min(F_{T.Rd.B.ind} \quad F_{T.Rd.B.gr}) \quad F_{T.Rd.B} = 210.4799 \text{ kN}$$

Calculation of the effective lengths

bolt-row C:

$$l_{\text{eff.C.ind.1.1}} := 2 \cdot \Pi \cdot m_{C2}$$

$$l_{\text{eff.C.ind.1.1}} = 156.507 \text{ mm}$$

$$l_{\text{eff.C.ind.1.2}} := \Pi \cdot m_{C2} + 2 \cdot e_C$$

$$l_{\text{eff.C.ind.1.2}} = 358.2535 \text{ mm}$$

$$\lambda_1 := \frac{m_C}{m_C + e_C} \quad \lambda_1 = 0.1808$$

$$\lambda_2 := \frac{m_{C2}}{m_C + e_C} \quad \lambda_2 = 0.1457$$

$$\alpha := 8.0 \quad (\text{from EC3 1-8, Fig. 6.11})$$

$$l_{\text{eff.C.ind.2.1}} := \alpha \cdot m_C$$

$$l_{\text{eff.C.ind.2.1}} = 247.2706 \text{ mm}$$

$$l_{\text{eff.C.ind.2.2}} := 4 \cdot m_C + 1.25 \cdot e_C$$

$$l_{\text{eff.C.ind.2.2}} = 298.6353 \text{ mm}$$

$$l_{\text{eff.C.gr.1.1}} := \Pi \cdot m_{C2} + p_{CD}$$

$$l_{\text{eff.C.gr.1.1}} = 158.2535 \text{ mm}$$

$$l_{\text{eff.C.gr.1.2}} := \Pi \cdot \frac{m_C}{2} + e_C + \frac{p_{CD}}{2}$$

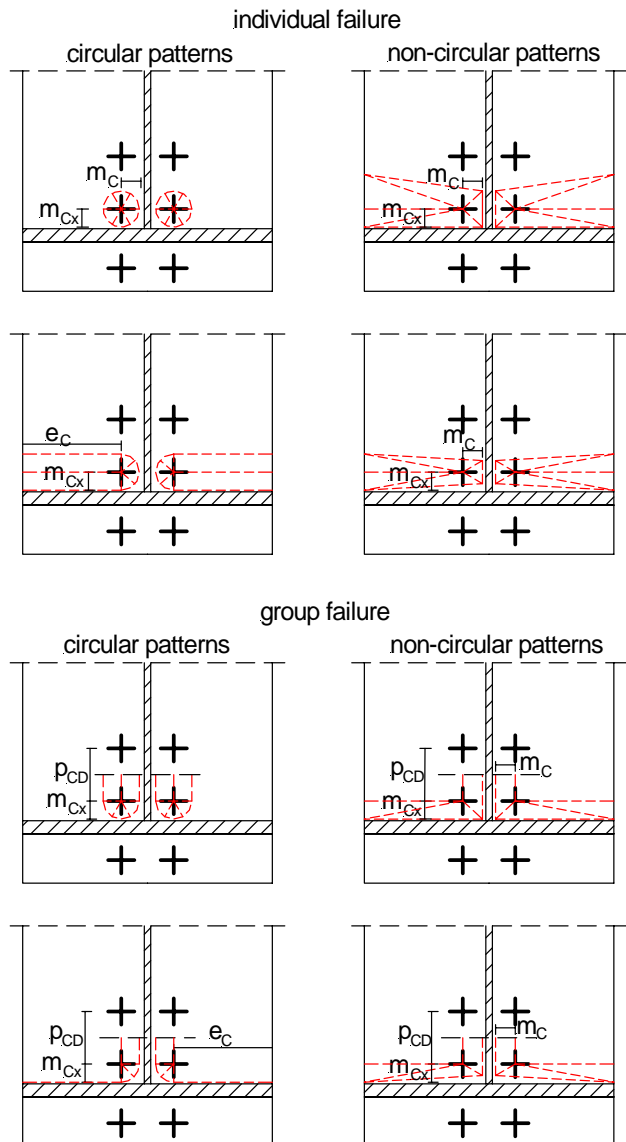
$$l_{\text{eff.C.gr.1.2}} = 228.5515 \text{ mm}$$

$$l_{\text{eff.C.gr.2.1}} := \alpha \cdot m_C + \frac{p_{CD}}{2} - (2 \cdot m_C + 0.625 \cdot e_C)$$

$$l_{\text{eff.C.gr.2.1}} = 137.953 \text{ mm}$$

$$l_{\text{eff.C.gr.2.2}} := 2 \cdot m_C + 0.625 \cdot e_C + \frac{p_{CD}}{2}$$

$$l_{\text{eff.C.gr.2.2}} = 189.3177 \text{ mm}$$



$$l_{\text{eff.C.ind.2}} := \min(l_{\text{eff.C.ind.2.1}}, l_{\text{eff.C.ind.2.2}}) \quad l_{\text{eff.C.ind.2}} = 247.2706 \text{ mm}$$

$$l_{\text{eff.C.ind.1}} := \min(l_{\text{eff.C.ind.1.1}}, l_{\text{eff.C.ind.1.2}}, l_{\text{eff.C.ind.2}}) \quad l_{\text{eff.C.ind.1}} = 156.507 \text{ mm}$$

$$l_{\text{eff.C.gr.2}} := \min(l_{\text{eff.C.gr.2.1}}, l_{\text{eff.C.gr.2.2}}) \quad l_{\text{eff.C.gr.2}} = 137.953 \text{ mm}$$

$$l_{\text{eff.C.gr.1}} := \min(l_{\text{eff.C.gr.1.1}}, l_{\text{eff.C.gr.1.2}}, l_{\text{eff.C.gr.2}}) \quad l_{\text{eff.C.gr.1}} = 137.953 \text{ mm}$$

$$M_{\text{C.pl.ind.1.Rd}} := \frac{1}{4} \cdot l_{\text{eff.C.ind.1}} \cdot t_{\text{ep}}^2 \cdot \frac{f_y}{\gamma_{\text{M.0}}} \quad M_{\text{C.pl.ind.1.Rd}} = 2.2143 \text{ kN}\cdot\text{m}$$

$$M_{\text{C.pl.ind.2.Rd}} := \frac{1}{4} \cdot l_{\text{eff.C.ind.2}} \cdot t_{\text{ep}}^2 \cdot \frac{f_y}{\gamma_{\text{M.0}}} \quad M_{\text{C.pl.ind.2.Rd}} = 3.4984 \text{ kN}\cdot\text{m}$$

$$M_{\text{C.pl.gr.1.Rd}} := \frac{1}{4} \cdot l_{\text{eff.C.gr.1}} \cdot t_{\text{ep}}^2 \cdot \frac{f_y}{\gamma_{\text{M.0}}} \quad M_{\text{C.pl.gr.1.Rd}} = 1.9518 \text{ kN}\cdot\text{m}$$

$$M_{\text{C.pl.gr.2.Rd}} := \frac{1}{4} \cdot l_{\text{eff.C.gr.2}} \cdot t_{\text{ep}}^2 \cdot \frac{f_y}{\gamma_{\text{M.0}}} \quad M_{\text{C.pl.gr.2.Rd}} = 1.9518 \text{ kN}\cdot\text{m}$$

Design resistance of the T-stub

Bolt-row considered individually:

$$\text{Mode 1:} \quad F_{\text{T.Rd.1.C.ind}} := \frac{4 \cdot M_{\text{C.pl.ind.1.Rd}}}{m_{\text{C2}}} \quad F_{\text{T.Rd.1.C.ind}} = 355.5784 \text{ kN}$$

$$\text{Mode 2:} \quad F_{\text{T.Rd.2.C.ind}} := \frac{2 \cdot M_{\text{C.pl.ind.2.Rd}} + n_{\text{C}} \cdot 2 \cdot F_{\text{T.Rd}}}{m_{\text{C}} + n_{\text{C}}} \quad F_{\text{T.Rd.2.C.ind}} = 350.018 \text{ kN}$$

$$\text{Mode 3:} \quad F_{\text{T.Rd.3}} = 448.938 \text{ kN}$$

$$F_{\text{T.Rd.C.ind}} := \min(F_{\text{T.Rd.1.C.ind}}, F_{\text{T.Rd.2.C.ind}}, F_{\text{T.Rd.3}}) \quad F_{\text{T.Rd.C.ind}} = 350.018 \text{ kN}$$

Bolt-row considered as "horizontal" group:

$$\text{Mode 1:} \quad F_{\text{T.Rd.1.C.gr}} := \frac{4 \cdot M_{\text{C.pl.gr.1.Rd}}}{m_{\text{C2}}} \quad F_{\text{T.Rd.1.C.gr}} = 313.4244 \text{ kN}$$

$$\text{Mode 2:} \quad F_{\text{T.Rd.2.C.gr}} := \frac{2 \cdot M_{\text{C.pl.gr.2.Rd}} + n_{\text{C}} \cdot 2 \cdot F_{\text{T.Rd}}}{m_{\text{C}} + n_{\text{C}}} \quad F_{\text{T.Rd.2.C.gr}} = 305.5395 \text{ kN}$$

$$\text{Mode 3:} \quad F_{\text{T.Rd.3}} = 448.938 \text{ kN}$$

$$F_{\text{T.Rd.C.gr}} := \min(F_{\text{T.Rd.1.C.gr}}, F_{\text{T.Rd.2.C.gr}}, F_{\text{T.Rd.3}}) \quad F_{\text{T.Rd.C.gr}} = 305.5395 \text{ kN}$$

$$F_{\text{T.Rd.C}} := \min(F_{\text{T.Rd.C.ind}}, F_{\text{T.Rd.C.gr}}) \quad F_{\text{T.Rd.C}} = 305.5395 \text{ kN}$$

Calculation of the effective lengths

bolt-row D:

individual failure

$$l_{\text{eff.D.ind.1.1}} := 2 \cdot \Pi \cdot m_D$$

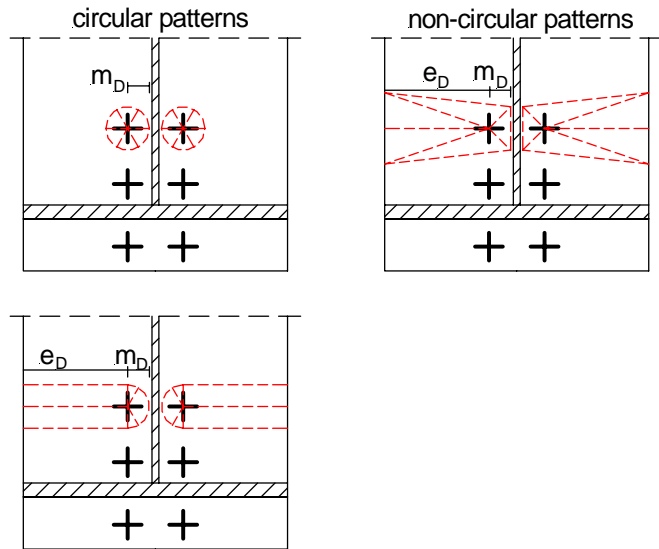
$$l_{\text{eff.D.ind.1.1}} = 194.2061 \text{ mm}$$

$$l_{\text{eff.D.ind.1.2}} := \Pi \cdot m_D + 2 \cdot e_D$$

$$l_{\text{eff.C.ind.1.2}} = 358.2535 \text{ mm}$$

$$l_{\text{eff.D.ind.2.1}} := 4 \cdot m_D + 1.25 \cdot e_D$$

$$l_{\text{eff.D.ind.2.1}} = 298.6353 \text{ mm}$$



group failure

$$l_{\text{eff.D.gr.1.1}} := \Pi \cdot m_D + p_{CD}$$

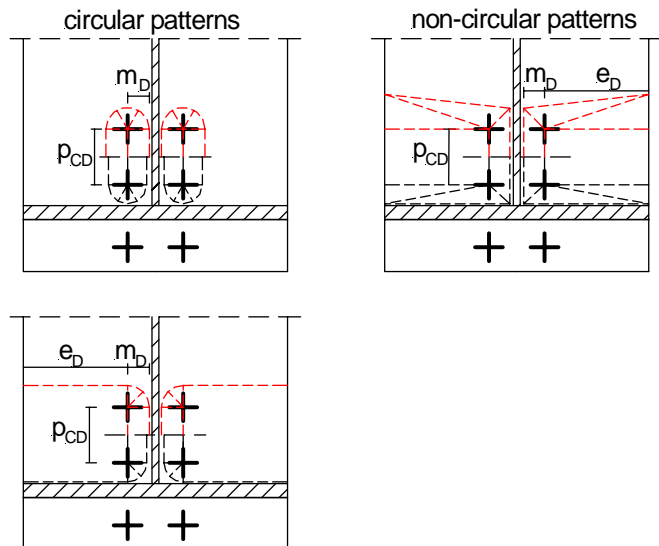
$$l_{\text{eff.D.gr.1.1}} = 177.1031 \text{ mm}$$

$$l_{\text{eff.D.gr.1.2}} := \Pi \cdot \frac{m_D}{2} + e_D + \frac{p_{CD}}{2}$$

$$l_{\text{eff.D.gr.1.2}} = 228.5515 \text{ mm}$$

$$l_{\text{eff.D.gr.2.1}} := 2 \cdot m_D + 0.625 \cdot e_D + \frac{p_{CD}}{2}$$

$$l_{\text{eff.D.gr.2.1}} = 189.3177 \text{ mm}$$



$$l_{\text{eff.D.ind.2}} := l_{\text{eff.D.ind.2.1}}$$

$$l_{\text{eff.D.ind.2}} = 298.6353 \text{ mm}$$

$$l_{\text{eff.D.ind.1}} := \min(l_{\text{eff.D.ind.1.1}}, l_{\text{eff.D.ind.1.2}}, l_{\text{eff.D.ind.2}})$$

$$l_{\text{eff.D.ind.1}} = 194.2061 \text{ mm}$$

$$l_{\text{eff.D.gr.2}} := l_{\text{eff.D.gr.2.1}}$$

$$l_{\text{eff.D.gr.2}} = 189.3177 \text{ mm}$$

$$l_{\text{eff.D.gr.1}} := \min(l_{\text{eff.D.gr.1.1}}, l_{\text{eff.D.gr.1.2}}, l_{\text{eff.D.gr.2}})$$

$$l_{\text{eff.D.gr.1}} = 177.1031 \text{ mm}$$

$$M_{D,pl.ind.1.Rd} = \frac{1}{4} \cdot l_{eff.D.ind.1} \cdot t_{ep}^2 \cdot \frac{f_y}{\gamma_{M,0}}$$

$$M_{D,pl.ind.1.Rd} = 2.7476 \text{ kN} \cdot \text{m}$$

$$M_{D,pl.ind.2.Rd} = \frac{1}{4} \cdot l_{eff.D.ind.2} \cdot t_{ep}^2 \cdot \frac{f_y}{\gamma_{M,0}}$$

$$M_{D,pl.ind.2.Rd} = 4.2251 \text{ kN} \cdot \text{m}$$

$$M_{D,pl.gr.1.Rd} = \frac{1}{4} \cdot l_{eff.D.gr.1} \cdot t_{ep}^2 \cdot \frac{f_y}{\gamma_{M,0}}$$

$$M_{D,pl.gr.1.Rd} = 2.5057 \text{ kN} \cdot \text{m}$$

$$M_{D,pl.gr.2.Rd} = \frac{1}{4} \cdot l_{eff.D.gr.2} \cdot t_{ep}^2 \cdot \frac{f_y}{\gamma_{M,0}}$$

$$M_{D,pl.gr.2.Rd} = 2.6785 \text{ kN} \cdot \text{m}$$

Design resistance of the T-stub

Bolt-row considered individually:

$$\text{Mode 1: } F_{T,Rd.1.D.ind} = \frac{4 \cdot M_{D,pl.ind.1.Rd}}{m_D}$$

$$F_{T,Rd.1.D.ind} = 355.5784 \text{ kN}$$

$$\text{Mode 2: } F_{T,Rd.2.D.ind} = \frac{2 \cdot M_{D,pl.ind.2.Rd} + n_D \cdot 2 \cdot F_{T,Rd}}{m_D + n_D}$$

$$F_{T,Rd.2.D.ind} = 370.917 \text{ kN}$$

Mode 3:

$$F_{T,Rd.3} = 448.938 \text{ kN}$$

$$F_{T,Rd.D.ind} = \min(F_{T,Rd.1.D.ind} \quad F_{T,Rd.2.D.ind} \quad F_{T,Rd.3})$$

$$F_{T,Rd.D.ind} = 355.5784 \text{ kN}$$

Bolt-row considered as "horizontal" group:

$$\text{Mode 1: } F_{T,Rd.1.D.gr} = \frac{4 \cdot M_{D,pl.gr.1.Rd}}{m_D}$$

$$F_{T,Rd.1.D.gr} = 324.2638 \text{ kN}$$

$$\text{Mode 2: } F_{T,Rd.2.D.gr} = \frac{2 \cdot M_{D,pl.gr.2.Rd} + n_D \cdot 2 \cdot F_{T,Rd}}{m_D + n_D}$$

$$F_{T,Rd.2.D.gr} = 326.4384 \text{ kN}$$

Mode 3:

$$F_{T,Rd.3} = 448.938 \text{ kN}$$

$$F_{T,Rd.CD.gr} = \min(F_{T,Rd.1.C.gr} + F_{T,Rd.1.D.gr} \quad F_{T,Rd.2.C.gr} + F_{T,Rd.2.D.gr} \quad 2 \cdot F_{T,Rd.3})$$

$$F_{T,Rd.CD.gr} = 631.9779 \text{ kN}$$

$$F_{T,Rd.2.C.gr} + F_{T,Rd.2.D.gr} = 631.9779 \text{ kN}$$

$$F_{T,Rd.D.gr} = F_{T,Rd.2.D.gr}$$

$$F_{T,Rd.D.gr} = 326.4384 \text{ kN}$$

$$F_{T,Rd.D} = \min(F_{T,Rd.D.ind} \quad F_{T,Rd.D.gr})$$

$$F_{T,Rd.D} = 326.4384 \text{ kN}$$

T-stub forces

$F_{T.Rd.B} = 210.4799 \text{ kN}$	Mode 1, horizontal group failure
$F_{T.Rd.C} = 305.5395 \text{ kN}$	Mode 2, group failure
$F_{T.Rd.D} = 326.4384 \text{ kN}$	Mode 2, group failure

Beam flange and web in compression

$$M_{c.Rd} := 2755 \cdot \text{kN} \cdot \text{m} \quad h := 900 \cdot \text{mm} \quad t_{fb} := 20 \cdot \text{mm}$$

$$F_{c.fb.Rd} := \frac{M_{c.Rd}}{h - t_{fb}} \quad F_{c.fb.Rd} = 3130.6818 \text{ kN}$$

Web in transverse tension

$$t_{wb} := 8 \cdot \text{mm} \quad F_{t.wb.Rd.B} := I_{\text{eff.B.gr.1}} \cdot t_{wb} \cdot \frac{f_y}{\gamma_{M.0}} \quad F_{t.wb.Rd.B} = 408.2004 \text{ kN}$$

$$F_{t.wb.Rd.C} := I_{\text{eff.C.gr.2}} \cdot t_{wb} \cdot \frac{f_y}{\gamma_{M.0}} \quad F_{t.wb.Rd.C} = 433.7242 \text{ kN}$$

$$F_{t.wb.Rd.D} := I_{\text{eff.D.gr.2}} \cdot t_{wb} \cdot \frac{f_y}{\gamma_{M.0}} \quad F_{t.wb.Rd.D} = 595.2147 \text{ kN}$$

The effective design tension resistance of the bolt-rows B, C and D

$$F_{t.wb.Rd.B} = 408.2004 \text{ kN} > F_{T.Rd.B} = 210.4799 \text{ kN} \quad F_{tr.Rd.B} := F_{T.Rd.B}$$

$$F_{t.wb.Rd.C} = 433.7242 \text{ kN} > F_{T.Rd.C} = 305.5395 \text{ kN} \quad F_{tr.Rd.C} := F_{T.Rd.C}$$

$$F_{t.wb.Rd.D} = 595.2147 \text{ kN} > F_{T.Rd.D} = 326.4384 \text{ kN} \quad F_{tr.Rd.D} := F_{T.Rd.D}$$

and

$$F_{tr.Rd.B} + F_{tr.Rd.C} + F_{tr.Rd.D} = 842.4578 \text{ kN} > F_{c.fb.Rd} = 3130.6818 \text{ kN}$$

The design moment resistance of the joint

because of the symmetry of the bolt arrangement

$$F_{tr.Rd.E} := F_{tr.Rd.D} \quad F_{tr.Rd.E} = 326.4384 \text{ kN} \quad \text{Mode 2, group failure}$$

$$F_{tr.Rd.F} := F_{tr.Rd.C} \quad F_{tr.Rd.F} = 305.5395 \text{ kN} \quad \text{Mode 2, group failure}$$

$$h_B := 930 \cdot \text{mm} \quad h_C := 840 \cdot \text{mm} \quad h_D := 760 \cdot \text{mm} \quad h_E := 120 \cdot \text{mm} \quad h_F := 40 \cdot \text{mm}$$

$$M_{j.Rd} := F_{tr.Rd.B} \cdot h_B + F_{tr.Rd.C} \cdot h_C + F_{tr.Rd.D} \cdot h_D + F_{tr.Rd.E} \cdot h_E + F_{tr.Rd.F} \cdot h_F$$

$$M_{j.Rd} = 751.8869 \text{ kN} \cdot \text{m}$$